Title
Signaling by postsynaptic AMPA receptors in glutamatergic synapse maturation

Author
Tracy, Tara Elizabeth

Publication Date
2010

Peer reviewed|Thesis/dissertation

Signaling by postsynaptic AMPA receptors in glutamatergic synapse maturation

by

Tara Elizabeth Tracy

A dissertation submitted in partial satisfaction of the

requirements for the degree of

Doctor of Philosophy in

Neuroscience

In the

Graduate Division

of the

University of California, Berkeley

Committee in charge:
Professor Lu Chen, Chair
Professor Richard Kramer
Professor Mu-Ming Poo
Professor Matthew Welch

Fall 2010

Signaling by postsynaptic AMPA receptors in glutamatergic synapse maturation

Abstract

Signaling by postsynaptic AMPA receptors in glutamatergic synapse maturation
by
Tara Elizabeth Tracy
Doctor of Philosophy in Neuroscience
University of California, Berkeley
Professor Lu Chen, Chair

Excitatory transmission in the brain is largely mediated by synapses containing the neurotransmitter glutamate. Neuronal circuitry is first established early in brain development requiring the formation of vast numbers of glutamatergic synapses at individual sites of contact made between presynaptic axons and postsynaptic dendrites. Despite mounting efforts in the last decade to identify the complex molecular mechanisms underlying initial synaptogenesis and the subsequent steps of synapse maturation and stabilization, this complex process is still not well understood. Interestingly newly formed glutamatergic synapses in the young brain often lack postsynaptic AMPA-type glutamate receptors (AMPARs). As development progresses, AMPARs are trafficked into synaptic sites but the significance of this event to the functional maturation of synapses remains unclear.

To investigate the role of postsynaptic AMPAR insertion in synapse maturation we used RNA interference (RNAi) to knockdown AMPARs in young cultured hippocampal neurons. Surprisingly, loss of postsynaptic AMPARs caused a concurrent reduction in synaptic responses mediated by NMDA-type glutamate receptors (NMDARs), without an apparent change in their synaptic expression. Strikingly, heterologous synapses formed between axons and co-cultured non-neuronal cells expressing AMPARs develop significantly fewer inactive presynaptic terminals, suggesting that AMPARs mediate a retrograde signal to promote presynaptic function. Indeed, the extracellular domain of the AMPAR subunit GluA2 was sufficient to reproduce this effect at heterologous synapses, indicating that this retrograde signaling is independent of AMPAR channel function. Our findings suggest that postsynaptic AMPARs perform an organizational function at synapses that exceeds their standard role as ionotropic receptors by conveying a retrograde trans-synaptic signal that increases the transmission efficacy at a synapse.

Dedication

To my mom, who is the action potential to my synaptic transmission, and to the memory of my dad, who was the tetanic stimulus to my long-term potentiation.

Table of Contents

Acknowledgements

I would like to give many thanks to Lu for her support during the last six years. I couldn't ask for a better mentor. She has given me a lot of guidance with this project, and I really appreciate all of her help. She has taught me so much about many aspects of neurobiology research and the experiences I have had in her lab are invaluable. From discussing our own experiments to conversations during our lab's weekly journal clubs, she has made an everlasting impact on my approach to research. For this, I am very grateful.

I would like to thank Jenny Yan for all of her hard work on this project. She contributed by doing many experiments using immunocytochemistry, imaging, and immunoblotting. I would also like to thank all of the other members of the Chen lab both past and present. I would like to acknowledge those that I have collaborated with most closely on projects including Bita Magshoodi, Christine Nam and Jason Aoto. I really appreciate all of the advice and assistance that I have gotten from every one of my labmates. They have been a great group of people to work with, and I will miss them all. Finally, I would like to thank my thesis committee members Dr. Richard Kramer, Dr. Mu-Ming Poo, and Dr. Matthew Welch for all of their helpful advice on this project.

I am so lucky that I have the best family. I would like to thank my mom who is a driving force in my life and she always encourages me to do the best that I can. Her love and support have been essential for me during my graduate work. I would like to thank Michael for always looking out for me. Hey brother, you're the best. I have the greatest uncles and aunts who have always been there for me. Uncle Bing, AJ, Uncle Al and Aunt Julie, you are so important to me and I appreciate your love and support. I would also like to acknowledge my grandma Tracy and my adopted grandmother Rina for their love and support. Navigating graduate school would have been very difficult without the incredible support from my family. Last but not least, I would like to thank Grant for his love and support.

Chapter 1

Overview of synapse development

Molecular signaling during excitatory synaptogenesis in the hippocampus

In the developing brain, glutamatergic synapses are formed at individual contact sites between an axon and a dendrite. The establishment of a synaptic connection can be initiated either by projections from an elongating axon, guided by the motile growth cone, or by dynamic filipodia extended from growing dendrites (Figure1.1A) (Ziv & Garner, 2001; Ziv & Garner, 2004). Axodendritic contact is followed by a series of signaling events leading to the differentiation of pre- and postsynaptic compartments (Figure 1.1B). After the initial assembly of synaptic components important for early synaptogenesis, subsequent molecular signaling leads to functional and morphological modifications culminating in the maturation and stabilization of the synaptic connections (Figure 1.1C).

A number of synaptic proteins have been identified that participate in signaling during synapse development by promoting the accumulation of both pre- and postsynaptic specializations (Dalva et al, 2007; Washbourne et al, 2004). The calcium-dependent signaling by multimeric complexes of postsynaptic neuroligins and their trans-synaptic binding partner neurexins seems to play a key organizational role at the synapse. Neuroligin1 (NL1) binds directly to PSD-95 (postsynaptic density protein-95), a postsynaptic PDZ domain containing scaffold protein, through its C-terminal PDZ-binding motif (Meyer et al, 2004). Indeed, the expression of β-neurexin, in non-neuronal cells is sufficient to recruit PSD-95 and NMDARs to contacting postsynaptic sites on cultured neurons(Graf et al, 2004; Nam & Chen, 2005). Presynaptic neurexin has a C-terminal PDZ-binding motif that mediates its interaction with CASK (calcium/calmodulin-dependent serine protein kinase) and Mint (Munc 18 interacting protein) forming a structural complex that supports synaptic vesicle accumulation and release (Biederer & Sudhof, 2000; Butz et al, 1998; Hata et al, 1996). Strikingly, axon terminal differentiation and recruitment of synaptic vesicles is induced onto non-neuronal cells expressing NL1 that are co-cultured with hippocampal neurons (Dean et al, 2003; Fu et al, 2003; Scheiffele et al, 2000). An increase or decrease of postsynaptic NL1 expression in dissociated hippocampal neurons has been shown to change the density of inhibitory and excitatory synaptic contacts suggesting that neuroligin/neurexin trans-synaptic signaling regulates synaptogenesis (Chih et al, 2005; Prange et al, 2004). However, the generation of a NL 1-3 triple knockout mouse did not alter the number of synapses formed in the brain. Instead, the observed impairment in synaptic function of neurons from the NL 1-3 knockout mice was attributed to a defect in synapse maturation (Varoqueaux et al, 2006).

SynCAM 1 is a cell adhesion molecule that can be involved in homophilic binding or heterophilic interactions with SynCAM2 and mediates trans-synaptic signaling during synapse development (Biederer et al, 2002; Fogel et al, 2007). SynCAM 1 or 2 expressed in non-neuronal cells and co-cultured with neurons is sufficient to induce presynaptic differentiation in contacting axons (Biederer et al, 2002; Fogel et al, 2007; Sara et al, 2005). Several reports on the Eph receptor tyrosine kinases and their transmembrane ephrin ligands have provided evidence for their role in signaling to promote synapse formation. Forward signaling by presynaptic ephrinB binding to

postsynaptic EphB receptors contributes to the regulation of dendritic spines, NMDAR clustering, and the number of excitatory synapse (Dalva et al, 2000; Ethell et al, 2001; Henkemeyer et al, 2003; Kayser et al, 2006; Penzes et al, 2003). In addition, reverse signaling by presynaptic EphB receptor interacting with postsynaptic ephrinB is required for excitatory synapse formation specifically on the shaft of dendrites (Aoto et al, 2007). Other synaptic proteins reported to engage in signaling to promote glutamatergic synaptogenesis include Neuregulin-1 and its postsynaptic receptor erbB4 (Li et al, 2007), astrocyte-derived thrombospondin that binds to postsynaptic alpha2delta-1 (Eroglu et al, 2009), postsynaptic Synaptic adhesion-like molecules, SALM3 and SALM5 (Mah et al), SynDIG1 (Kalashnikova et al), trans-synaptic signaling by netrin-G ligand-3 (NGL-3) and leukocyte common antigen-related (LAR) (Woo et al, 2009), and the postsynaptic leucine-rich repeat transmembrane protein, LRRTM2, binding to presynaptic neurexin (de Wit et al, 2009; Ko et al, 2009).

Maturation of the glutamatergic presynaptic terminal

Among the first steps of presynaptic differentiation is the recruitment of active zone components and synaptic vesicles to the presynaptic terminal (Ahmari et al, 2000; Friedman et al, 2000). The presynaptic active zone is recognized in ultrastructural morphological analysis as the electron-dense structure directly opposed to the postsynaptic membrane and it is the site from which neurotransmitter-containing vesicles are released into the synaptic cleft. A current model for the delivery of active zone proteins, including Bassoon and Piccolo, to newly formed synapses entails the packaging of these components into dense core vesicles at the cell body for transport down the axon to the presynaptic terminals (Dresbach et al, 2006; Zhai et al, 2001).

Although detection of neurotransmitter release from growing axons of young neurons suggests that much of the exocytic machinery may be present before synapse formation occurs (Krueger et al, 2003; Matteoli et al, 1992; Young & Poo, 1983), the molecular machinery involved in synaptic vesicle release and recycling is further modified upon axodendritic contact (Coco et al, 1998; Kraszewski et al, 1995; Verderio et al, 1999). The functional significance of glutamate release prior to synapse assembly remains unclear. Is neurotransmitter release in fact required for the initial construction of synapses? Interestingly, a deficiency of Munc18-1 in the mouse brain which results in a striking loss of vesicle release from glutamatergic terminals does not impair the initial formation of morphologically-defined synapses (Verhage et al, 2000). Moreover, chronic treatment of cultured hippocampal neurons with tetanus toxin to inhibit presynaptic vesicle release does not affect synapse development (Harms & Craig, 2005). These results argue that glutamate release from the presynaptic terminal is in fact not required for synapse formation but could instead be important for the maintenance of synaptic connections.

At mature presynaptic terminals there are multiple mechanisms that regulate synaptic vesicle availability which are critical for enabling action potential evoked synaptic transmission (Sudhof, 2000; Sudhof, 2004). First synaptic vesicles must be

localized at the active zone and docked at the presynaptic membrane. In addition, specific molecular mechanisms prime synaptic vesicles to make them competent for release upon stimulation. Vesicles that have been docked and primed constitute the readily releasable pool of synaptic vesicles (RRP). Upon depolarization of the presynaptic terminal, calcium influx from voltage-gated calcium channels triggers the synchronous exocytosis of fusion competent synaptic vesicles at the active zone. Exocytosis is closely followed by endocytic mechanisms that recycle synaptic vesicles making them available for reuse in neurotransmission (Kavalali, 2007). During sustained high frequency synaptic transmission, the depleted RRP can be refilled by synaptic vesicles recruited from a reserve pool of vesicles (Rosenmund & Stevens, 1996; Wu & Borst, 1999). The RRP and the reserve pool together constitute the recycling pool of synaptic vesicles at a presynaptic terminal.

After initial presynaptic differentiation, the next stage in the functional maturation of an axon terminal requires the formation of both the RRP through docking and priming of synaptic vesicles at the presynaptic membrane, and recruitment of the reserve pool through additional vesicle accumulation adjacent to the active zone (Mozhayeva et al, 2002; Renger et al, 2001). Several presynaptic components have been identified that regulate the priming of synaptic vesicles within the RRP. The absolute failure of evoked neurotransmitter release in Munc13 deficient neurons revealed that the function of Munc13s is to establish the pool of fusion competent vesicles at the presynaptic membrane (Augustin et al, 1999; Varoqueaux et al, 2002). The α-RIMs, including RIM1α and RIM2α, were also discovered as essential regulators of vesicle priming (Koushika et al, 2001; Schoch et al, 2002). Indeed, a complex formed by the interaction between α-RIMs and Munc13s is likely fundamental to vesicle availability in the RRP (Betz et al, 2001; Dulubova et al, 2005). Exocytic machinery at the active zone consists of SNARE proteins that assemble into a structurally conserved complex essential for action potential evoked synaptic vesicle release (Rizo & Rosenmund, 2008). The SNARE complex is composed of SNAP-25 and syntaxin-1, bound to the presynaptic membrane, and synaptobrevin, a vesicle associated protein. While recent evidence suggests that Munc13-1 interacts with the SNARE complex to allow vesicle priming (Guan et al, 2008; Richmond et al, 2001) another protein, Munc18-1, directly binds syntaxin-1 and is similarly required for fusion competent vesicles at the active zone (Hata et al, 1993; Verhage et al, 2000).

Throughout development, presynaptic function is continuously adjusted by changes in active zone molecular composition and vesicle release probability (Jin & Garner, 2008; Ziv & Garner, 2004). Even though presynaptic function is heterogeneous among glutamatergic synapses, there is a general decline in vesicle release probability at synapses as neurons mature (Bolshakov & Siegelbaum, 1995; Wasling et al, 2004). In hippocampal neurons, there is a developmental switch in the type of calcium channel responsible for triggering vesicle release from the active zone (Pravettoni et al, 2000; Scholz & Miller, 1995; Verderio et al, 1995). Treatment of young hippocampal neurons with lantrunculin A, a drug that depolymerizes actin, disrupts vesicle clustering and release at immature presynaptic terminals. Interestingly, the same treatment does not affect mature synapses suggesting that the actin cytoskeleton plays a significant

functional role during presynaptic assembly early in development (Zhang & Benson, 2001).

Developmental events in postsynaptic assembly

Dendritic growth and postsynaptic differentiation are highly regulated processes during neuronal development (Biederer, 2005; Carrel et al, 2009; Chen & Firestein, 2007). Postsynaptic events at nascent synapses include the recruitment of scaffolding proteins and the clustering of neurotransmitter receptors juxtaposed to the presynaptic terminal. The protein localized to the postsynaptic membrane form an intricate structure called the postsynaptic density (PSD). Many components of the PSD have been well characterized individually. However interactions within protein complexes at the postsynaptic membrane and how these complexes assemble to mediate the formation of functional synapses are still largely unknown.

PSD-95 belongs to a family of membrane-associated guanylate kinases (MAGUKs), which includes several PDZ domain-containing proteins that are localized to excitatory synapses (Kim & Sheng, 2004). Overexpression of PSD-95 in dissociated hippocampal neurons enhances synapse maturation and increases localization of postsynaptic AMPARs (El-Husseini et al, 2000). The loss of N-terminal palmitoylation excludes PSD-95from synapses and results in the removal of postsynaptic AMPARs (Craven et al, 1999; El-Husseini Ael et al, 2002). Furthermore, PSD-95 is rapidly recruited to nascent axodendritic contact sites, which suggests that it plays a role in the early assembly of glutamatergic synapses (Bresler et al, 2001). PSD-95 directs the synaptic localization of AMPARs through its interaction with stargazin, a transmembrane auxiliary subunit of AMPARs (Schnell et al, 2002). Stargazin has a PDZ binding motif at the end of its intracellular C-terminal domain, which interacts with one of the two PDZ domains of PSD-95. Stargazin, along with other members of the TARP family, enhances the trafficking of AMPARs to the plasma membrane, and the interaction between stargazin and PSD-95 regulates the targeting of AMPARs to synaptic sites (Chen et al, 2000; Ziff, 2007).

Another well-studied postsynaptic MAGUK family member is synapse-associated protein-97 (SAP97). Overexpression of SAP97 in dissociated hippocampal neurons increases surface expression of AMPARs and significantly enhances assembly of presynaptic proteins (Regalado et al, 2006; Rumbaugh et al, 2003). Interestingly, SAP97 can directly interact with PSD-95, and overexpression of PSD-95 in neurons increases synaptic localization of SAP97 and AMPARs (Cai et al, 2006). This work suggests that both SAP97 and PSD-95 may coordinate to promote the synaptic targeting of AMPARs during development.

The Shank proteins are postsynaptic scaffolding components that are enriched in the PSD of glutamatergic synapses (Kim & Sheng, 2004). Shank proteins contain a PDZ domain that binds indirectly to PSD-95 via the guanylate-kinase associated protein (GKAP), and these three proteins co-cluster in heterologous cells (Naisbitt et al, 1999). In neurons, the interaction between Shank and GKAP is required for the synaptic

localization of Shank (Naisbitt et al, 1999; Sala et al, 2001). Interestingly, overexpression of Shank3 in cerebellar granule cells promotes the induction and maturation of dendritic spines and enhances the recruitment of functional glutamate receptors to synaptic sites (Roussignol et al, 2005). The SAM domain of Shank enables its multimerization and consequently Shank assembles into large sheets of proteins, which could act as a platform for the PSD (Baron et al, 2006). This evidence suggests that Shank likely plays a prominent role in organizing the structure of developing excitatory synapses.

Functionally mature glutamatergic synapses require the recruitment of releasable glutamate-containing synaptic vesicles to the axon terminal and the insertion of postsynaptic neurotransmitter receptors including both NMDARs and AMPARs. In the hippocampus, both NMDARs and AMPARs are present at mature glutamatergic synapses. However experiments using immunocytochemistry have revealed that a high proportion of morphologically-defined synapses on young hippocampal neurons contain postsynaptic NMDARs but not AMPARs (Gomperts et al, 1998; Petralia et al, 1999; Pickard et al, 2000) suggesting that synaptic AMPARs are not present until a later stage of synapse maturation. Furthermore, electrophysiological studies on the developing hippocampus have identified "silent synapses" between pyramidal neurons which exhibit NMDAR-mediated but not AMPAR-mediated synaptic responses (Durand et al, 1996; Isaac et al, 1995; Liao et al, 1995). These postsynaptically "silent synapses" indicate that recruitment of AMPARs to synapses is a discrete step during synapse maturation that is regulated by specific mechanisms. Does synapse maturation end with functionally turning on postsynaptically silent synapses by AMPAR insertion? Alternatively, is there additional development of synaptic function following AMPAR insertion? Interestingly some reports have proposed a different interpretation of the mechanism underlying the "silent synapses" recorded from young hippocampal neurons. These studies provide evidence suggesting that the observed "silent synapses" are in fact attributed to either immature presynaptic terminals with very low vesicle release probability or to the spill-over of glutamate from neighboring active synapses (Gasparini et al, 2000; Kullmann & Asztely, 1998; Kullmann et al, 1996; Voronin & Cherubini, 2003). The seemingly conflicting views supporting either a postsynaptic or presynaptic mechanism that gives rise to "silent synapses" underscores the importance of determining whether or not the addition of postsynaptic AMPARs is in fact a critical event during synapse maturation that establishes synapse strength.

AMPARs in synaptic transmission

In the hippocampus, fast excitatory neurotransmission is predominantly mediated by AMPARs comprised of four possible subunits, GluA1-4, which assemble into the tetrameric complex required to make the functional ionotropic receptor. The subunit composition of an AMPAR determines the ion permeability and the channel current kinetics of the receptor (Bredt & Nicoll, 2003; Dingledine et al, 1999). The structure of an AMPAR subunit consists of an ectodomain containing the extended N-terminal

domain and the glutamate-binding domains, a membrane-enclosed loop that forms the ion channel pore, three transmembrane domains, and an intracellular C-terminal domain. The majority of AMPARs in pyramidal neurons of the hippocampus exist as heterotetramers that contain a combination of either the GluR1 and GluR2 subunits or the GluR2 and GluR3 subunits (Wenthold et al., 1996; Lu et al, 2009). It has been well established that modulation of AMPAR cycling into and out of synapses underlies various forms of synaptic plasticity (Bredt & Nicoll, 2003; Song & Huganir, 2002). Despite the apparent central role for AMPARs in regulating synaptic function, it remains unclear as to how they may influence the development of synapses.

Thesis summary

Here we provide evidence that postsynaptic AMPARs influence the maturation of excitatory synapses in developing hippocampal neurons. We found that a deficiency in postsynaptic AMPARs weakens presynaptic function by reducing the total RRP size among synapses. The diminished availability of fusion-competent synaptic vesicles is reminiscent of young presynaptic terminals that are not yet functionally mature. Moreover, at heterologous synapses formed onto postsynaptic non-neuronal cells (i.e. HEK293 cells) expressing neuroligin1 (NL1), we show that co-expression of AMPARs is needed to induce presynaptic vesicle release at a subset of glutamatergic synapses. Finally we provide evidence that the extracellular domain of AMPARs mediates this trans-synaptic effect on presynaptic function. Together, our results suggest that during synaptogenesis, postsynaptic AMPARs provide an additional trans-synaptic instructive signal that directly influences the competency for glutamate release at a subset of presynaptic terminals. The insertion of postsynaptic AMPARs therefore represents a significant step in development that can establish the functional maturity of a synapse.

Figure 1.1

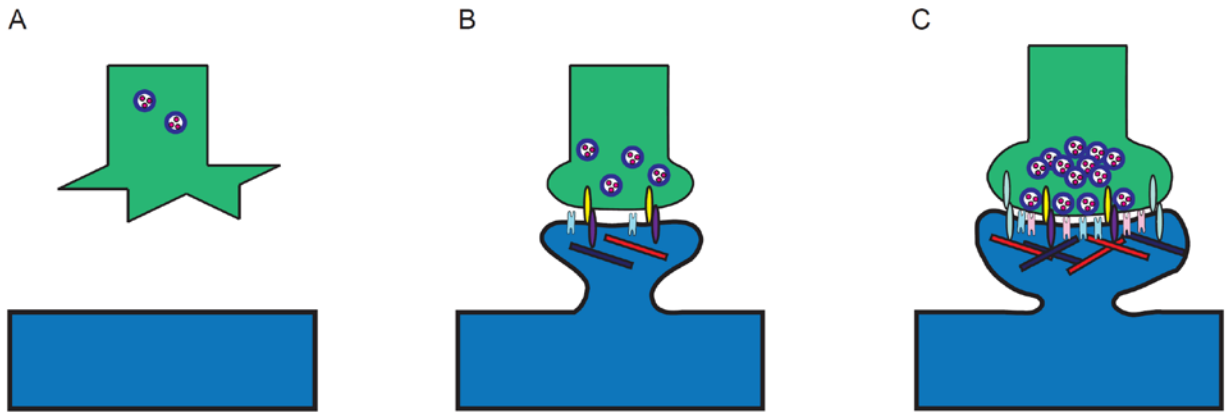

Figure 1.1: Events during synapse development. (**A**) An axon growth cone (green) contacts a dendrite (blue). (**B**) Synapse assembly proceeds with presynaptic and postsynaptic differentiation. (**C**) Ultimately the synapse undergoes a process of stabilization and maturation.

Chapter 2

Knockdown of AMPARs in developing hippocampal neurons

Introduction

Dissociated hippocampal neurons grown *in vitro* are widely used to study molecular mechanisms in synapse development. Hippocampi are dissected from embryonic rats and trypsinized before plating individual cells onto coverslips. Within 5 days *in vitro* the dissociated hippocampal neurons exhibit outgrowth of processes that eventually become dendrites and axons whereas at about 7 days *in vitro*, the first synapses begin to form (Grabrucker et al, 2009; Matteoli et al, 1995). By 14 days *in vitro* dendritic spines are abundant and there are many mature synapses on pyramidal neurons. There are several advantages to using dissociated hippocampal neurons for studies on synaptogenesis. First, the expression of synaptic proteins can be easily manipulated by transfection at specific stages in neuronal development. Secondly, there are many approaches using electrophysiological techniques and immunocytochemistry that one can take to assess synaptic function of hippocampal neurons. Lastly, all synapses in the cultures are formed *de novo* starting at a predictable time, about one week after plating. For these reasons we chose to use cultured hippocampal neurons to examine the role of AMPARs in synapse development.

If the functional significance of a candidate synaptic protein is unknown, useful insight can often be gained by preventing the expression of the protein and observing the consequent changes in synaptic transmission. One approach is to generate a genetic knockout mouse, and another is to make use of RNA interference (RNAi) to specifically stop translation of the candidate protein. Several groups have generated knockout mice deficient in AMPARs including mice lacking the GluA1 subunit (Zamanillo et al, 1999), the GluA2 subunit (Jia et al, 1996), or both the GluA2 and GluA3 subunits (Meng et al, 2003). More recently, a conditional knockout of the GluA1-3 subunits of AMPARs was made (Lu et al, 2009). The main disadvantage of this genetic knockout approach for investigating the role of AMPARs in synapse development involves the likely homeostatic functional compensation resulting from the prolonged decrease in AMPAR number. Alternatively, here we use RNAi-mediated knockdown of AMPAR subunits during synapse development to bring about an acute deficiency in receptor expression thereby avoiding potential long-term homeostatic mechanisms.

Results and Discussion

AMPAR knockdown efficiency with GluA RNAi

In order to determine whether the loss of postsynaptic AMPARs affects synapse maturation, we used plasmid-based RNAi to knock down the expression of the GluA1, GluA2, and GluA3 AMPAR subunits in young cultured hippocampal neurons that exhibit ongoing synaptogenesis. Given that the majority of AMPARs expressed in hippocampal pyramidal neurons are GluA1/2 or GluA2/3 heteromers (Lu et al, 2009; Wenthold et al, 1996), we did not include a shRNA for the GluA4 subunit in these experiments. We first established the knockdown efficiency of each GluA-shRNA in HEK293 cells (Figures 2.1A-C), and then confirmed the knockdown efficiency of the GluA-shRNAs in hippocampal neurons. When all three GluA-shRNAs were co-expressed in hippocampal neurons for five days, the total AMPAR immunostaining in the soma of transfected neurons was dramatically reduced (Figures 2.2A-D). Consistent with this observation, AMPA-evoked currents from somatic outside-out patches, which reflects extrasynaptic AMPAR density on the somatic surface, were diminished by >75% (Figures 2.2E and F). Thus, these shRNAs effectively suppress AMPAR expression.

GluA RNAi weakens AMPAR-mediated synaptic transmission

In dendrites, AMPAR RNAi depleted intracellular and extrasynaptic pools of AMPARs to below detection. Interestingly, we still observed residual AMPARs clustered at synaptic sites as identified by labeling of VGluT1, a marker for glutamatergic presynaptic terminals (Figure 2.3A). Quantification of AMPAR immunofluorescence co-localized with VGluT1 puncta revealed a reduction in the number of synaptic AMPARs to approximately 40% of control neurons (Figure 2.3B). Moreover, GluA RNAi significantly increased the proportion of glutamatergic synapses lacking AMPARs (Figure 2.3C).

To investigate the impact of the AMPAR RNAi on synaptic function, we performed whole-cell patch-clamp recordings of miniature EPSCs (mEPSCs) on neurons expressing GluA-shRNAs (Figure 2.4B). We found a reduction in the average mEPSC amplitude, indicative of the removal of postsynaptic AMPARs as a result of AMPAR knockdown (Figure 2.4C). We also observed a significant decrease in the frequency of mEPSCs (Figure 2.4D). These impairments could be reversed to the level of control neurons with the co-expression of either a GluA1 or GluA2 rescue construct insensitive to the GluA-shRNAs (Figure 2.4A), indicating that our results are not due to an off target effect of GluA RNAi. Sucrose (0.2 M) was then applied to enhance the number of mEPSCs that were sampled during recordings (Figure 2.5A) (Rosenmund & Stevens, 1996; Zhou et al, 2000). A reduction in sucrose-evoked mEPSC amplitude and frequency was also observed with AMPAR knockdown (Figures 2.5B and C). The decrease in mEPSC frequency could be primarily due to an increase in miniature events that are below detection threshold, alternatively it could represent a decline in

presynaptic function or in the number of functional synapses. To more closely examine these possibilities we applied a low concentration of CNQX, a competitive antagonist of AMPARs and recorded sucrose-evoked mEPSCs (Figures 2.5D and E). If the GluA RNAi induced decrease in mEPSC frequency was entirely due to the increased prevalence of mEPSCs below detection threshold, we would expect to see a comparable decrease in mEPSC frequency following CNQX application. Indeed we did find a marginal decrease in mEPSC frequency in 250nM CNQX, however compared to control neurons the decline in frequency of events was not as robust as GluA RNAi neurons (Figure 2.5E). This suggests that the decrease in mEPSC frequency with GluA RNAi is partially caused by a change in presynaptic function or in the number of functional synapses.

Having established the functional effect of AMPAR knockdown on mEPSCs, we next evaluated synaptic transmission by recording postsynaptic responses to action potential-evoked presynaptic vesicle release elicited by extracellular local field stimulation (Maximov et al, 2007). We first established the input-output curve of the evoked responses by applying an increment of extracellular stimulation. The evoked response amplitude increased with the strength of the stimulus intensity and plateaued at a stimulus higher than 4 mA (Figure 2.6A). We observed a significant reduction in the amplitude of evoked EPSCs (eEPSCs) mediated by AMPARs at all stimulus intensities (Figure 2.6A). For subsequent experiments, we used a 6mA stimulus to excite all presynaptic axons thereby eliciting the maximum synaptic response in neurons. When all active synapses are engaged, the degree of reduction in the synaptic AMPAR response (Figure 2.6B) corresponds well to the magnitude of synaptic AMPAR depletion assessed by immunocytochemistry (Figures 2.3B and C). Co-expression of either the GluA-shRNA insensitive GluA1 or GluA2 rescue construct restored the AMPAR eEPSC amplitude to a level comparable to that found in untransfected neurons (Figure 2.6B). In addition we designed a GluA3 rescue construct that is insensitive to GluA3 RNAi when expressed in HEK293 cells (Figure 2.6D). When the GluA3 rescue construct was co-expressed in neurons with GluA RNAi we did not get any appreciable restoration of AMPAR eEPSCs suggesting that homomeric GluA3 receptors are not sufficient to re-establish synaptic function (Figure 2.6C). For this reason, we used only the GluA1 or GluA2 rescue construct in further experiments.

NMDAR-mediated synaptic transmission is impaired

We next wondered whether a deficiency in AMPARs influences any other property of synaptic function that is fundamental to synapse maturation. Since mature glutamatergic synapses contain both AMPA- and NMDA-type glutamate receptors, we examined NMDAR-mediated evoked synaptic responses in AMPAR knockdown neurons. Surprisingly, loss of AMPARs caused a significant decrease in the amplitude of NMDAR eEPSCs (Figure 2.7A). This decrease was almost as large as the reduction in AMPAR-mediated eEPSCs, and could also be restored by co-expression of either the GluA1 or GluA2 rescue construct (Figure 2.7A). Thus, knockdown of AMPARs in cultured neurons leads to an unexpected concomitant decrease of NMDAR-mediated

synaptic responses, suggesting that the insertion of postsynaptic AMPARs is important for establishing functionally mature excitatory synapses beyond the role of AMPARs in sensing glutamate.

Synaptic NMDAR composition is unaltered by GluA RNAi

The subunit composition of NMDARs is developmentally regulated and establishes the NMDAR channel properties, which in turn influences the observed NMDAR-mediated synaptic current (Erreger et al, 2005; Flint et al, 1997; Hestrin, 1992; Monyer et al, 1994). We examined the decay kinetics of the NMDAR eEPSCs as a method of testing whether the AMPAR knockdown caused a shift in the incorporation of different GluN2 subunit types into synaptic NMDARs. The decay phase of the NMDAR eEPSCs was best fit with a double exponential function, corresponding to a fast and slow decay component. AMPAR knockdown had no affect on either kinetic component (Figure 2.7B), indicating that the synaptic NMDAR subunit composition was not significantly altered.

Alternatively, the decline in NMDAR-mediated synaptic transmission could occur if AMPAR knockdown leads to an equivalent loss of synaptic NMDARs. To address this possibility, we assayed the totality of functional receptors, including both synaptic and extrasynaptic, that were expressed on the neuronal surface by whole-cell patch-clamp recordings of agonist-evoked currents. Unlike AMPA-evoked whole-cell currents, which were greatly reduced upon AMPAR knockdown (Figure 2.8A), NMDA-evoked whole-cell currents were not altered (Figure 2.8B). Thus, the overall expression of functional NMDARs on the plasma membrane was unaffected by the loss of AMPARs. Since both published works (Rosenmund et al, 1995; Thomas et al, 2006) and our results after the blockade of synaptic NMDARs with the irreversible open channel blocker MK-801 (Figures 2.8C and D) indicate that a large proportion (roughly 80%) of surface NMDARs are located at synapses, the sustained NMDA-evoked surface response suggests that most likely, synaptic NMDAR abundance is unaltered by AMPAR knockdown.

To address this question more directly, we next examined the number of NMDARs at synapses. We immunolabeled neurons with antibodies to GluN1, the essential subunit for all NMDARs, and to VGluT1, and quantified the amount of GluN1 that co-localized with VGlut1 puncta (Figure 2.9A). The intensity of synaptic GluN1 puncta was comparable between control and AMPAR RNAi neurons, and nearly all of the glutamatergic synapses contained NMDARs with no apparent difference between control and AMPAR knockdown neurons in the amount of synaptic NMDARs (Figures 2.9B and C). Next, we determined the average amplitude of NMDAR-mediated mEPSCs from recordings of both dual component and AMPAR-mediated miniature events (Gomperts et al, 2000; Gomperts et al, 1998). Importantly, despite a significant decrease in AMPAR mEPSC amplitude, there was no difference in NMDAR mEPSC amplitude with GluA RNAi compared to control neurons (Figures 2.9D-F). Collectively, these results suggest that an alteration in NMDAR expression is not responsible for the reduction in NMDAR-mediated synaptic transmission.

Figure 2.1

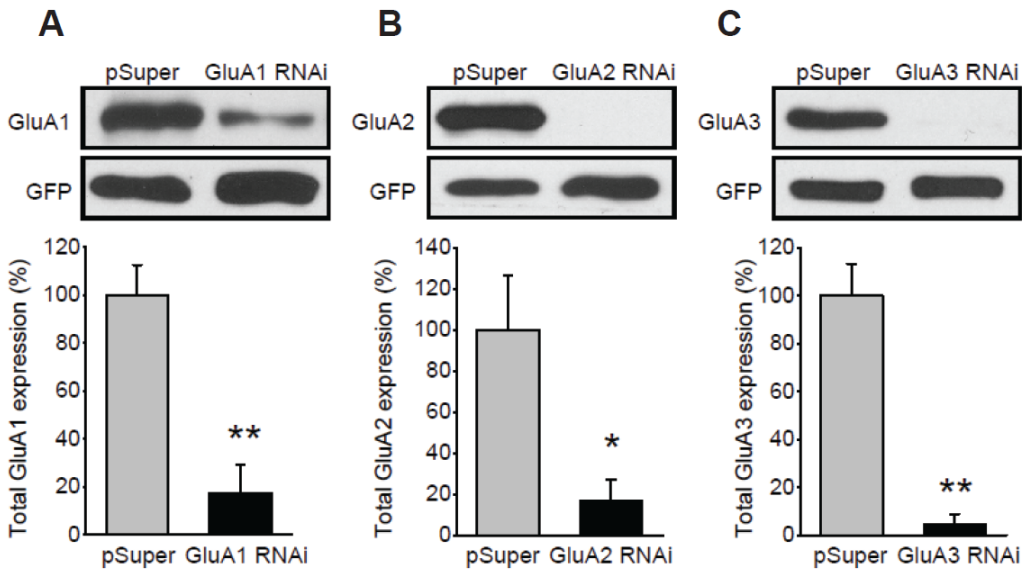

Figure 2.1: Assessment of knockdown by RNAi of the three individual AMPAR subunits in HEK293 cells. **(A-C)** AMPAR knockdown efficiencies of GluA1 **(A)**, GluA2 **(B)** , and GluA3 **(C)** shRNA were determined by co-expression with GFP-tagged GluA1, GluA2 or GluA3, respectively, in HEK293 cells. Quantifications were made by measuring the integrated intensity of each GluA band and normalizing it to GFP expression and GluA expression in the pSuper empty-vector control (n = 3 experiments/group; *, $p < 0.05$; **, $p < 0.005$).

Figure 2.2

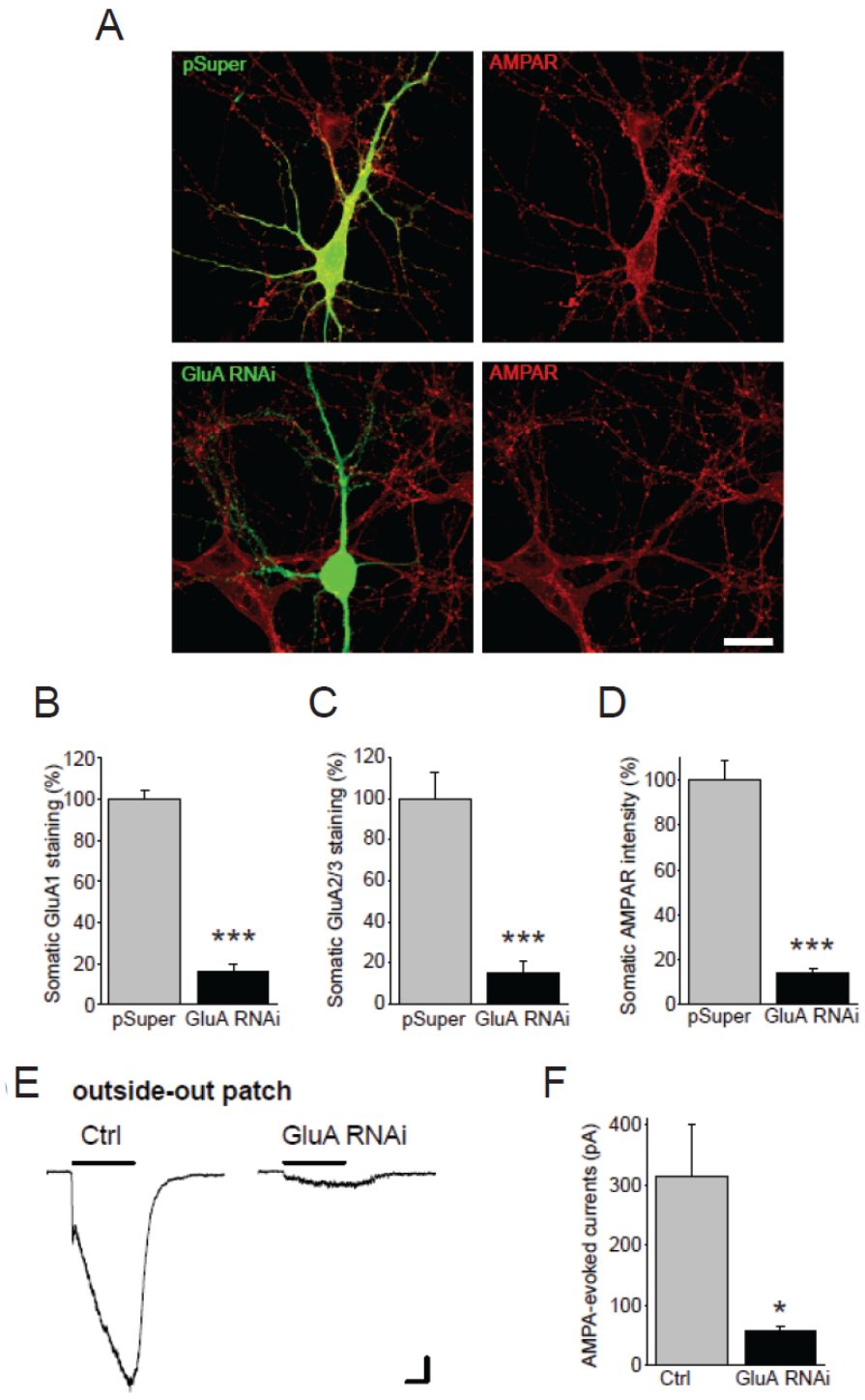
A
pSuper
AMPAR
GluA RNAi
AMPAR
B
Somatic GluA1 staining (%)
120
100
80
60
40
20
0
***
pSuper
GluA RNAi
C
Somatic GluA2/3 staining (%)
120
100
80
60
40
20
0
***
pSuper
GluA RNAi
D
Somatic AMPAR intensity (%)
100
80
60
40
20
0
***
pSuper
GluA RNAi
E
outside-out patch
Ctrl
GluA RNAi
F
AMPA-evoked currents (pA)
400
300
200
100
0
*
Ctrl
GluA RNAi

Figure 2.2: Decrease in AMPAR expression with GluA RNAi in hippocampal neurons **(A)** Neurons were transfected with either the pSuper empty-vector control (upper panels) or GluA1, GluA2 and GluA3 shRNA constructs (lower panels) and immunostained 5 days later for all three AMPAR subunits (red). Scale bar, 20 µm. **(B-D)** Depletion of AMPARs from the somatic region confirms the effectiveness of GluA RNAi in neurons. Graph showing the average intensity of GluA1 **(B)**, GluA2/3 **(C)**, and all three subunits GluA1, GluA2, and GluA3 together **(D)** in the soma of GluA RNAi neurons compared to control (n = 8-10; ***, $p < 1 \times 10^{-4}$). The average intensity of the immunofluorescence in the soma of each neuron was normalized to neighboring untransfected neurons. (**E-F**) Example traces and quantification of somatic outside-out patch recordings from control and GluA RNAi neurons. AMPAR currents were evoked with a 3 second application of AMPA (100 µm) in the presence of cyclothiazide (100 µm). Scale bars: 50 pA, 1 s. (n = 11 neurons/group; *, $p < 1 \times 10^{-5}$).

Figure 2.3

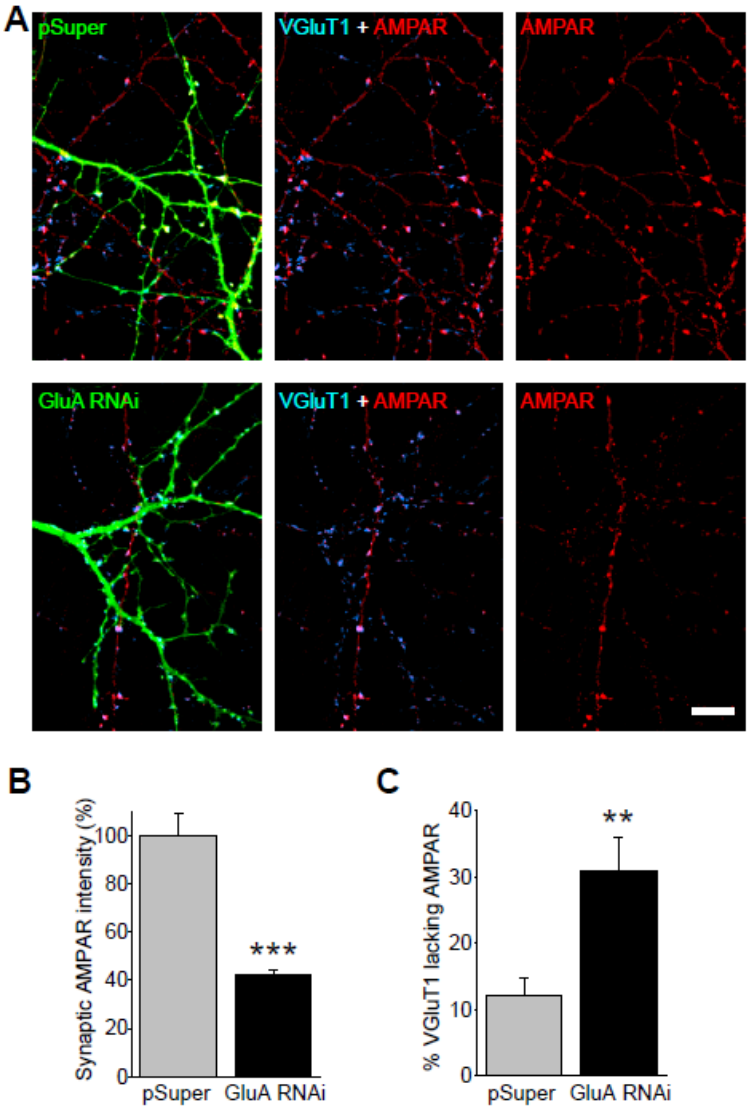

Figure 2.3: The number of synaptic AMPARs is reduced with GluA RNAi. (**A**) Synaptic AMPARs in neurons expressing pSuper (upper panels) or GluA-shRNAs (lower panels) were identified by co-localization of AMPAR puncta, comprised of total GluA1, GluA2 and GluA3 immunostaining (red), with VGluT1 (blue). Scale bar, 10 µm. (**B**) Quantification of the average AMPAR immunoreactivity at synapses was normalized to control pSuper-expressing neurons. (n = 9-10 cells/group; ***, $p < 1 \times 10^{-5}$). (**C**) Quantification of the percentage of AMPAR-lacking synapses identified by VGluT1 puncta devoid of AMPAR immunostaining (n = 9-10 cells/group; **, $p < 0.005$).

Figure 2.4

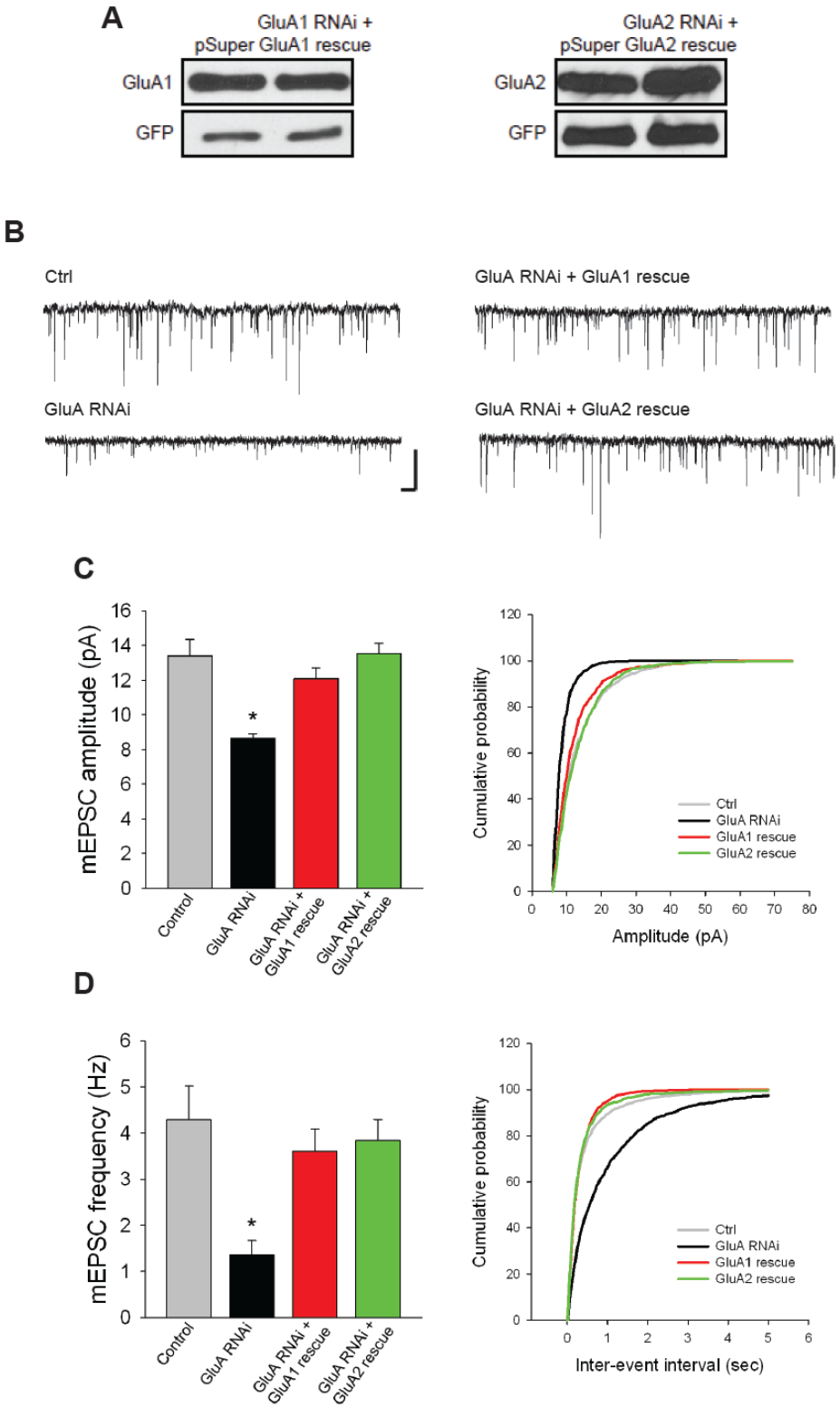
A
GluA1 RNAi +
pSuper GluA1 rescue
GluA1
GFP
GluA2 RNAi +
pSuper GluA2 rescue
GluA2
GFP
B
Ctrl
GluA RNAi
GluA RNAi + GluA1 rescue
GluA RNAi + GluA2 rescue
C
mEPSC amplitude (pA)
Control
GluA RNAi
GluA RNAi +
GluA1 rescue
GluA RNAi +
GluA2 rescue
Cumulative probability
Amplitude (pA)
Ctrl
GluA RNAi
GluA1 rescue
GluA2 rescue
D
mEPSC frequency (Hz)
Control
GluA RNAi
GluA RNAi +
GluA1 rescue
GluA RNAi +
GluA2 rescue
Cumulative probability
Inter-event interval (sec)
Ctrl
GluA RNAi
GluA1 rescue
GluA2 rescue

Figure 2.4: Both the amplitude and frequency of miniature synaptic transmission are decreased by AMPAR knockdown. (**A**) The expression levels of GFP-tagged GluA1 and GluA2 rescue constructs were unaffected by the corresponding GluA-shRNAs in HEK293 cells. (**B**) Example traces of mEPSCs recorded in the presence of tetrodotoxin (1 µM) at from dissociated neurons at 12 DIV. Scale bars: 20 pA, 200ms. (**C-D**) Quantification of the average mEPSC amplitude (**C**) and average mEPSC frequency (**D**) with corresponding cumulative probability plots. (n = 13-16 cells/group; *, $p < 1 \times 10^{-3}$).

Figure 2.5

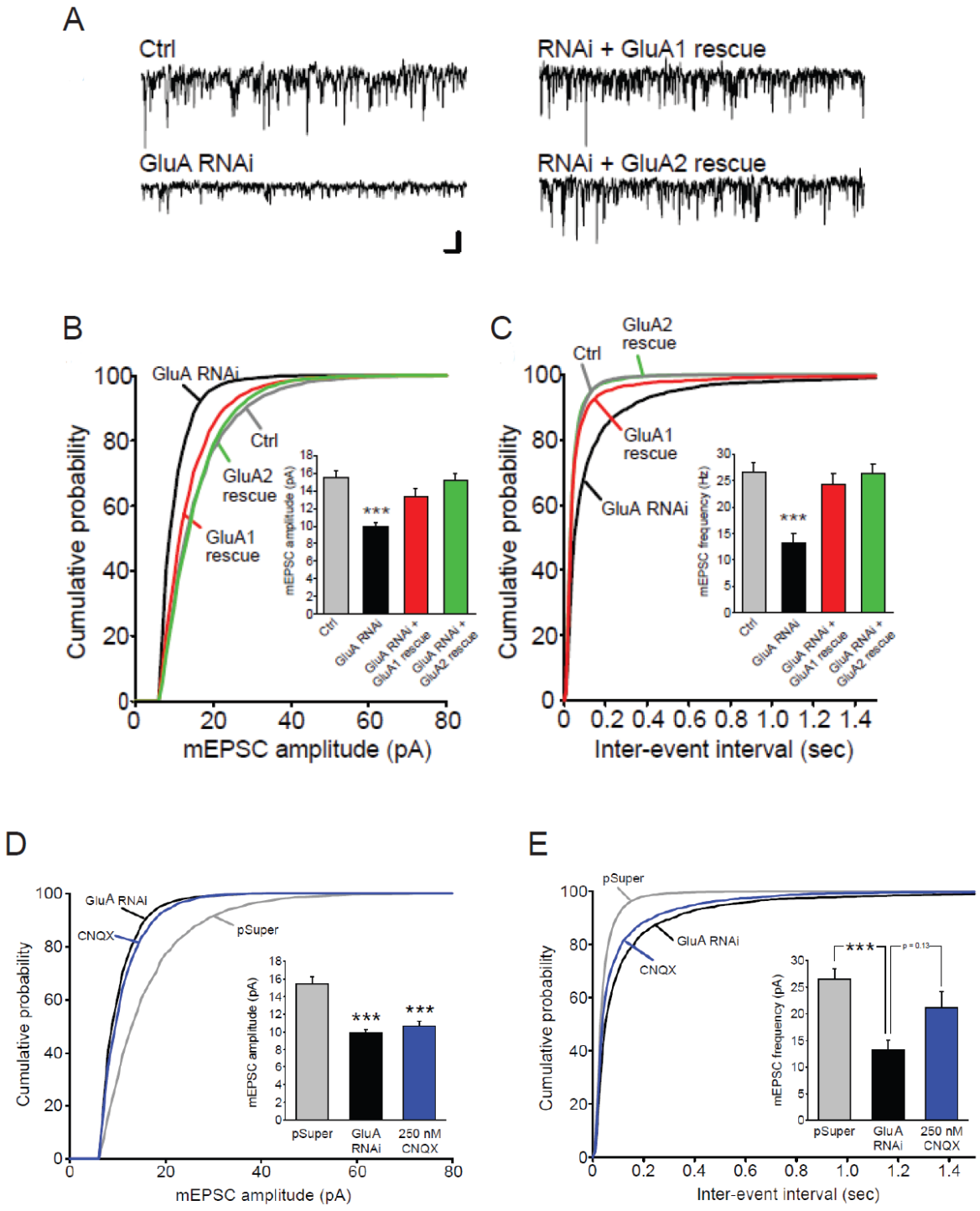
A
Ctrl
GluA RNAi
RNAi + GluA1 rescue
RNAi + GluA2 rescue
B
Cumulative probability
mEPSC amplitude (pA)
GluA RNAi
Ctrl
GluA2 rescue
GluA1 rescue
mEPSC amplitude (pA)
***
Ctrl
GluA RNAi
GluA RNAi + GluA1 rescue
GluA RNAi + GluA2 rescue
C
Cumulative probability
Inter-event interval (sec)
Ctrl
GluA2 rescue
GluA1 rescue
GluA RNAi
mEPSC frequency (Hz)
***
Ctrl
GluA RNAi
GluA RNAi + GluA1 rescue
GluA RNAi + GluA2 rescue
D
Cumulative probability
mEPSC amplitude (pA)
GluA RNAi
CNQX
pSuper
mEPSC amplitude (pA)
***
***
pSuper
GluA RNAi
250 nM CNQX
E
Cumulative probability
Inter-event interval (sec)
pSuper
GluA RNAi
CNQX
mEPSC frequency (pA)
***
p = 0.13
pSuper
GluA RNAi
250 nM CNQX

Figure 2.5: Sucrose-evoked mEPSCs are reduced with AMPAR knockdown. (**A**) Example traces of mEPSCs evoked with 0.2 M sucrose from dissociated cultured hippocampal neurons at 10 DIV. Scale bars: 10 pA, 200 ms. (**B,C**) Cumulative probability plot of mEPSC event amplitude and frequency. Inset: average mEPSC amplitude and frequency for each group (n = 26-39 cells/group; ***, $p < 1 \times 10^{-5}$). (**D**,**E**) A low concentration of CNQX (250 nM) was applied during sucrose-evoked mEPSC recordings. Cumulative probability plot of mEPSC event amplitude and frequency. Inset: average mEPSC amplitude and frequency for each group (n = 14-17 cells/group; ***, $p < 0.005$).

Figure 2.6

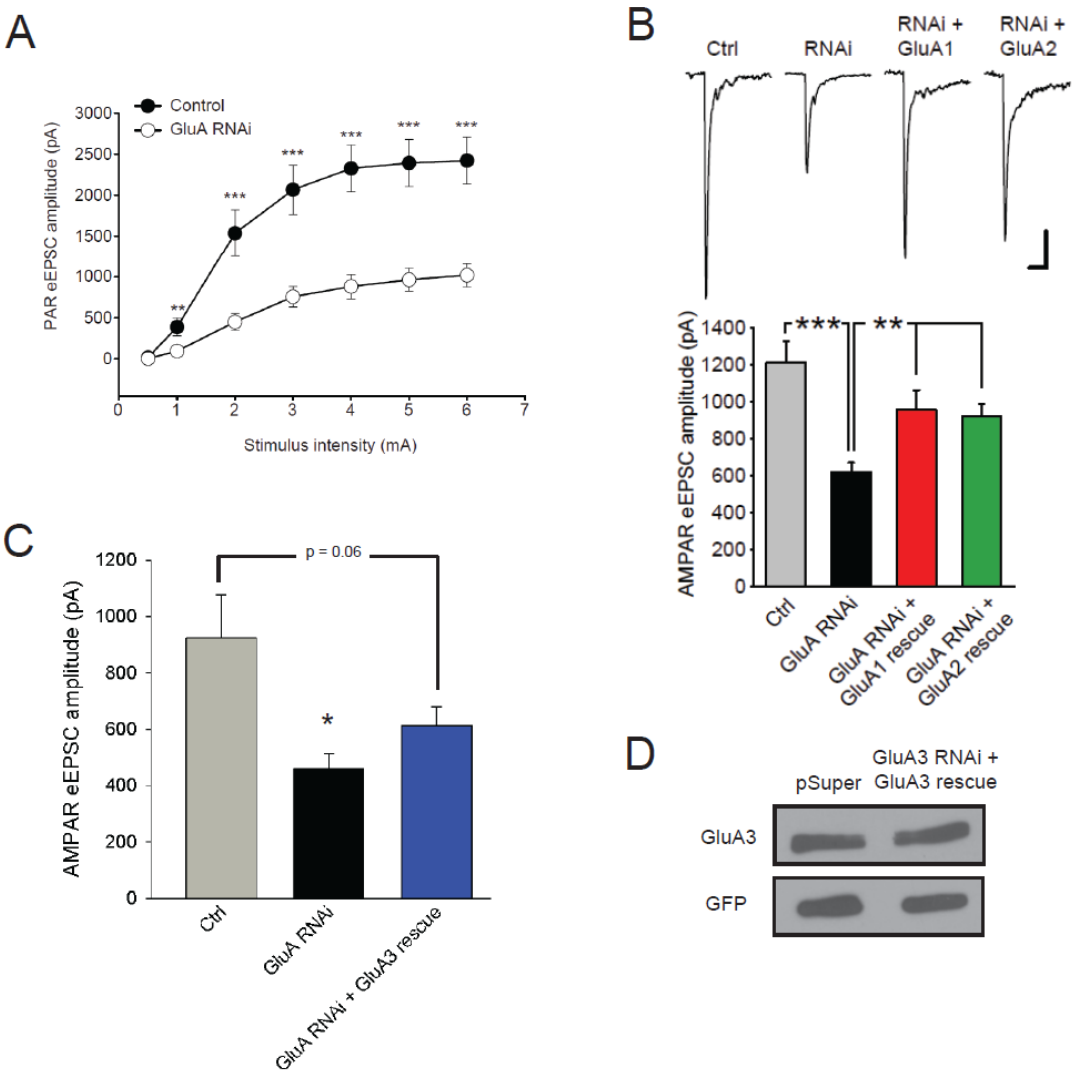
A
Control
GluA RNAi
PAR eEPSC amplitude (pA)
Stimulus intensity (mA)
B
Ctrl
RNAi
RNAi + GluA1
RNAi + GluA2
AMPAR eEPSC amplitude (pA)
Ctrl
GluA RNAi
GluA RNAi + GluA1 rescue
GluA RNAi + GluA2 rescue
C
p = 0.06
AMPAR eEPSC amplitude (pA)
Ctrl
GluA RNAi
GluA RNAi + GluA3 rescue
D
pSuper
GluA3 RNAi + GluA3 rescue
GluA3
GFP

Figure 2.6: Reduced NMDAR-mediated synaptic responses in neurons after AMPAR knockdown. **(A)** Graph depicting the mean AMPAR eEPSC amplitude recorded from neurons in response to increasing extracellular stimulus strength. For each neuron the average amplitude of five responses was calculated at every specified stimulus intensity. The stimulus duration was kept constant at 1ms. (n=18-21 cells/group; **, $p < 0.001$; ***, $p < 0.0001$). (**B**) Representative traces and quantification of AMPAR-mediated eEPSCs in cultured hippocampal neurons elicited by extracellular local field stimulation. Each trace is an average of five eEPSCs recorded from one neuron (n = 12-28 cells/group; **, $p<0.005$; ***, $p < 1 \times 10^{-4}$). Scale bars: 200 pA, 50 ms. (**C**) Quantification of AMPAR eEPSCs (n = 19 cells/group; *, $p < 0.006$). (**D**) The expression level of a GFP-tagged GluA3 rescue construct was unaffected by the GluA3 shRNA in HEK293 cells.

Figure 2.7

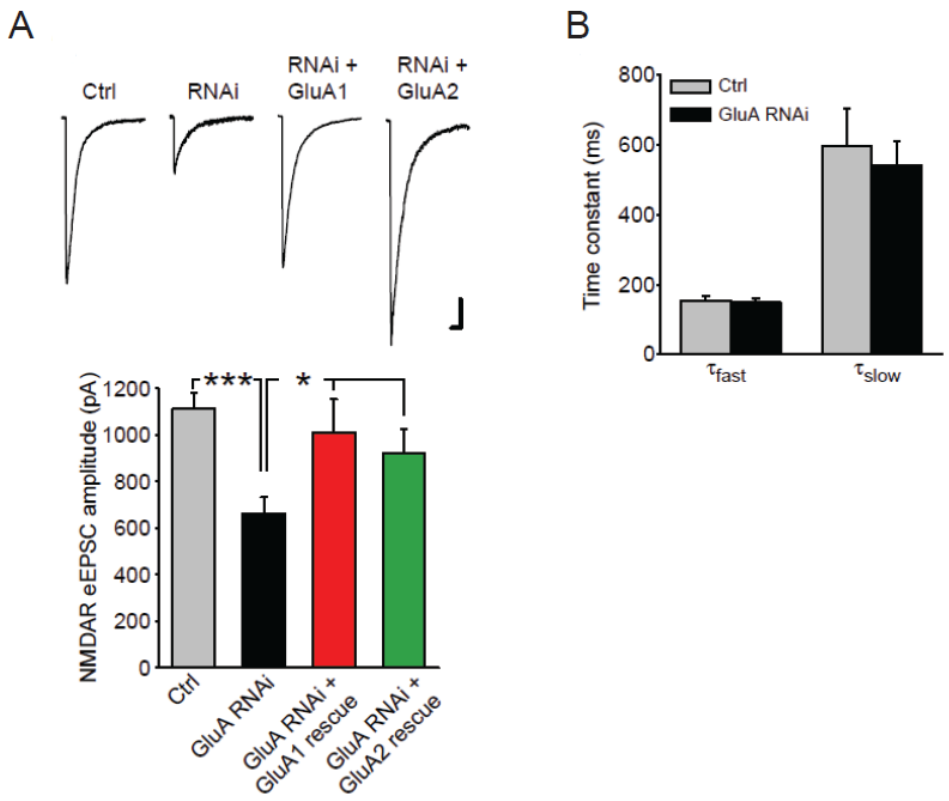

Figure 2.7: NMDAR-mediated synaptic transmission is impaired by GluA RNAi. (**A**) Representative traces and quantification of evoked NMDAR-mediated eEPSCs recorded at -60mV in external solution with CNQX (10 µM) and glycine (20 µm) and without magnesium. Each trace is the average of five eEPSCs recorded from one neuron (n = 11-25 cells/group; *, $p<0.05$; ***, $p < 1 \times 10^{-4}$). Scale bars: 200 pA, 200 ms. (**B**) The decay kinetics of NMDAR eEPSCs in control and AMPAR knockdown neurons. A double exponential fit was applied to the decay of NMDAR eEPSCs (n = 24-25 cells/group, $p > 0.6$).

Figure 2.8

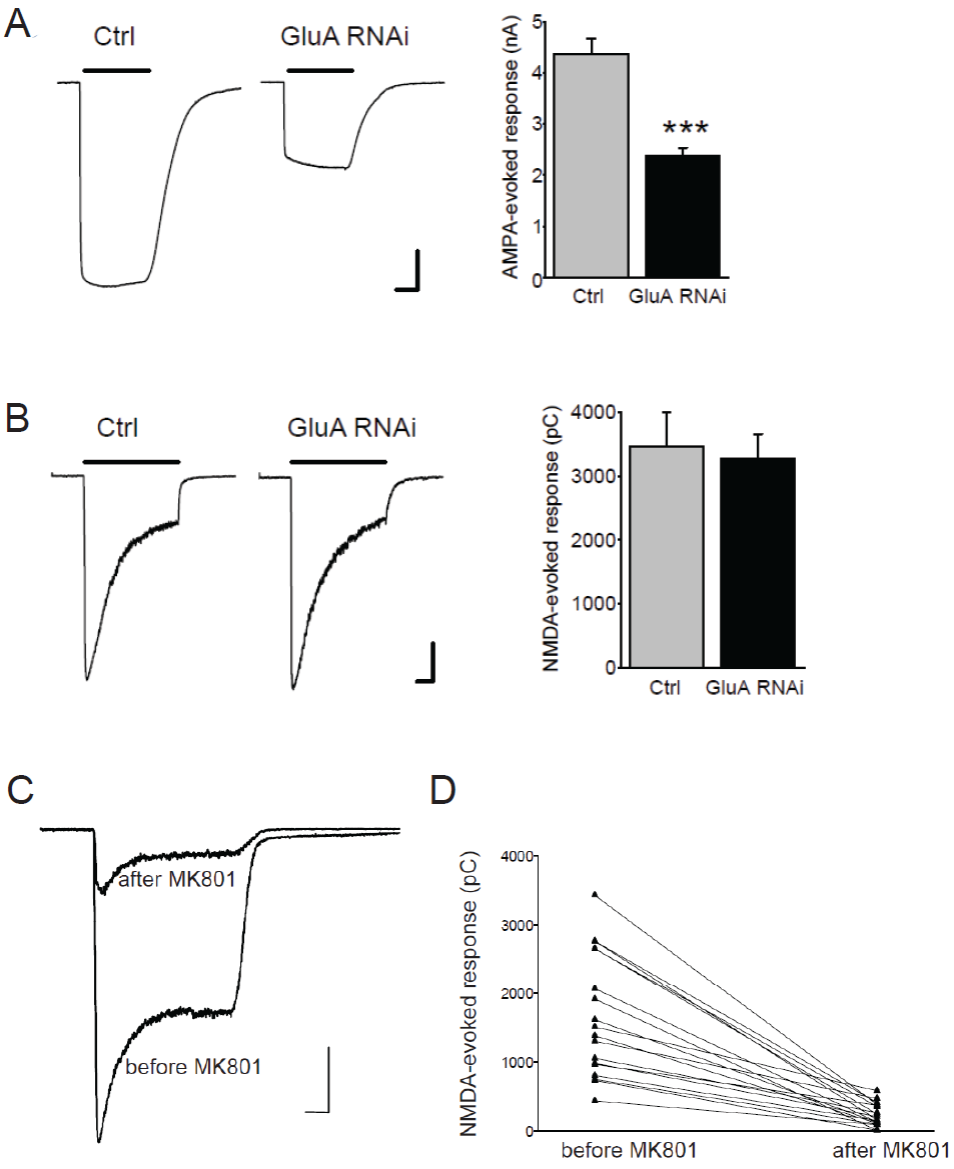
A
Ctrl
GluA RNAi
AMPA-evoked response (nA)
***
Ctrl
GluA RNAi
B
Ctrl
GluA RNAi
NMDA-evoked response (pC)
Ctrl
GluA RNAi
C
after MK801
before MK801
D
NMDA-evoked response (pC)
before MK801
after MK801

Figure 2.8: AMPAR knockdown does not affect the functional NMDARs on the cell surface. (**A**) Representative traces and quantification of whole-cell currents from cultured hippocampal neurons evoked by local application of a 3-second AMPA (100 µm) pulse in the presence of cyclothiazide (100 µm) (n = 11 cells/group; ***, $p < 1 \times 10^{-5}$). Scale bars: 1 nA, 1 s. (**B**) Representative traces and quantification of whole cell currents from cultured hippocampal neurons evoked by local application of a 3-second NMDA (1 mM) pulse (n = 16 cells/group; p > 0.7). Scale bars: 0.5 nA, 0.5 s. (**C**) Example traces of whole-cell currents in response to a 3-second local application of NMDA (1mM). The NMDA-evoked response was recorded from the neuron followed by MK-801 (10 µM) bath perfusion and 50 stimuli administered at 0.5Hz. Having thus blocked synaptic NMDARs, the remaining NMDA-evoked response of the neuron was measured. Scale bars: 0.5 nA, 0.5 s. (**D**) Graph of the NMDA-evoked response size recorded from each neuron before and after the MK-801 blockade of synaptic NMDARs (n = 18 cells/group).

Figure 2.9

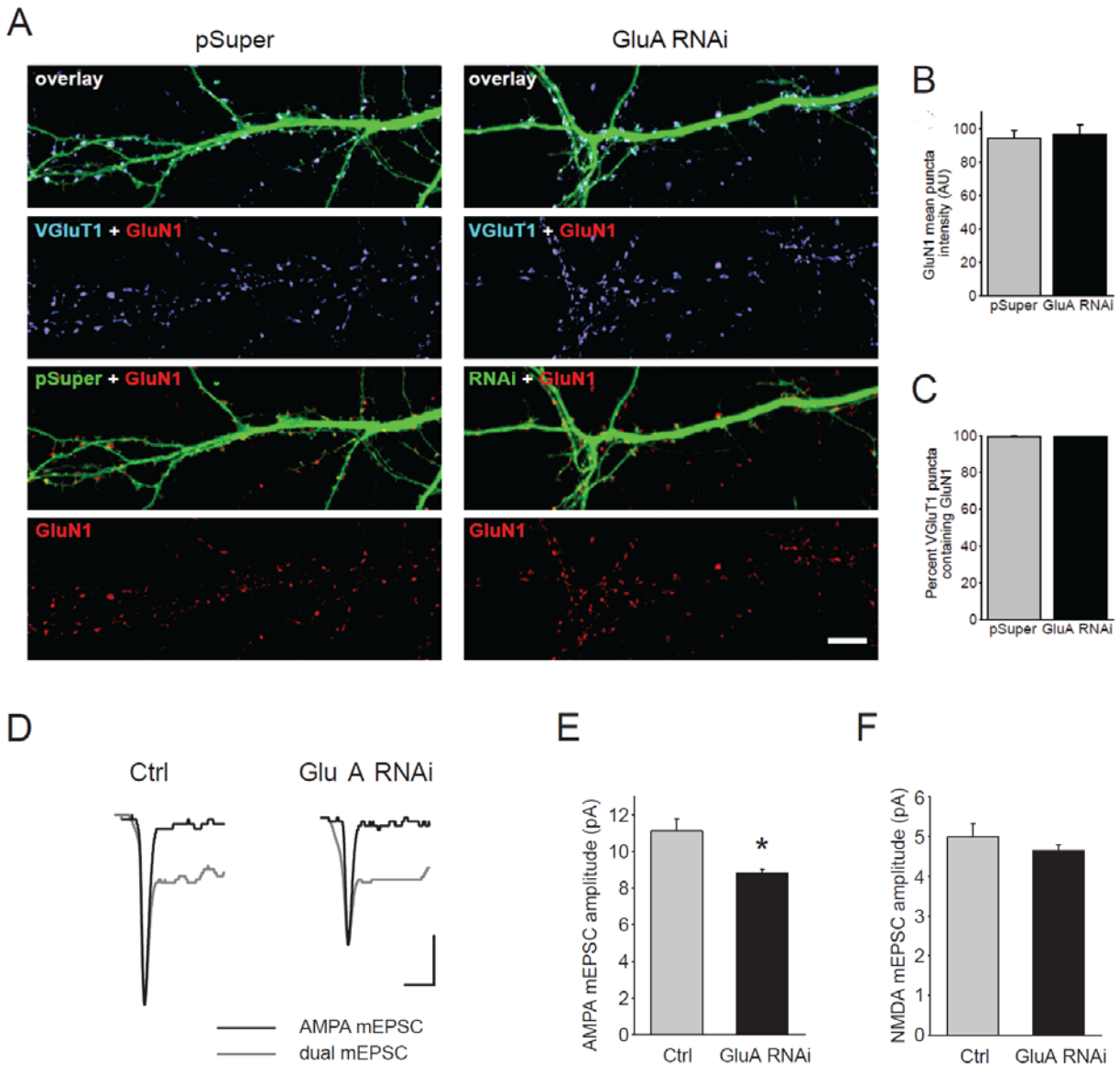
A
pSuper
GluA RNAi
overlay
overlay
VGluT1 + GluN1
VGluT1 + GluN1
pSuper + GluN1
RNAi + GluN1
GluN1
GluN1
B
GluN1 mean puncta intensity (AU)
100
80
60
40
20
0
pSuper GluA RNAi
C
Percent VGluT1 puncta containing GluN1
100
80
60
40
20
0
pSuper GluA RNAi
D
Ctrl
Glu A RNAi
AMPA mEPSC
dual mEPSC
E
AMPA mEPSC amplitude (pA)
12
10
8
6
4
2
0
*
Ctrl
GluA RNAi
F
NMDA mEPSC amplitude (pA)
6
5
4
3
2
1
0
Ctrl
GluA RNAi

Figure 2.9: NMDARs remain at synapses following AMPAR knockdown. (**A**) Immunolabeling of the NMDAR subunit GluN1 (red) and VGluT1 (blue) on dendrites of neurons expressing either pSuper or GluA RNAi. Scale bar, 10 µm. (**B,C**) Quantification of synaptic GluN1 expression identified as GluN1 puncta that co-localized with VGluT1. (**B**) The mean intensity of synaptic GluN1 immunoreactivity. (**C**) The percentage of NMDAR-containing glutamatergic synapses (n = 10 cells/group; $p > 0.6$). (**D**) The average dual component mEPSC, including both AMPAR- and NMDAR-mediated currents, and the average AMPAR-mediated mEPSC recorded after APV perfusion from a control neuron and a neuron with GluA RNAi. The average AMPA mEPSC is shown scaled to the peak of the dual component mEPSC. The mEPSC traces represent the average of at least 50 events recorded from each cell. Scale bars: 4 pA. 20 ms. (**E**) Quantification of the mean AMPAR-mediated mEPSC amplitude (n = 18 cells/group; *, $p < 0.002$). (**F**) Quantification of the mean NMDAR-mediated mEPSC amplitude from the same neurons quantified in **E**. The average NMDA mEPSC amplitude for each cell was determined by subtraction of the scaled average of the AMPAR mEPSCs, recorded in the presence of APV, from the average dual component mEPSC (n = 18 cells/group; $p > 0.3$).

Chapter 3

Loss of postsynaptic AMPARs increases the prevalence of functionally inactive presynaptic terminals

Introduction

Neuronal activity in the brain is regulated by a vast number of complex molecular signaling pathways, including numerous mechanisms that can modulate the efficacy of synaptic transmission. For this reason, the identification and characterization of specific mechanisms underlying synapse development is a challenging task. Moreover, distinct signaling pathways are likely important for each stage of synaptogenesis from axodendritic contact to initial assembly of pre- and postsynaptic components culminating in the functional maturation and stabilization.

During a period of ongoing synaptogenesis in dissociated hippocampal neurons, we have found that postsynaptic AMPARs are important for establishing glutamatergic synaptic transmission; however AMPARs are not required for NMDAR expression at the PSD. Alternatively, we reasoned that postsynaptic AMPAR insertion may modulate another aspect of synaptic transmission during development, namely one of the following processes: the morphological development of excitatory synapses, the number of synaptic connections formed, or the capacity for glutamate release from presynaptic terminals. Here we systematically explored these potential mechanisms by which AMPARs may affect synaptic function. Our goal was to delineate the specific deficit in synaptic function associated with the observed decrease in synaptic transmission by GluA RNAi.

Results and Discussion

Analysis dendrite morphology and excitatory synapse density

The decrease in NMDAR-mediated synaptic transmission induced by AMPAR RNAi without a change in postsynaptic NMDARs prompted us to consider another explanation: could the development of dendrites be hindered by AMPAR knockdown? Both Sholl analysis and a quantification of the total length of dendrites for each neuron revealed no significant differences between control and GluA RNAi neurons (Figures 3.1A-C). Alternatively, could the weakened synaptic strength by the loss of AMPARs lead to structural instability and the eventual retraction of synaptic connections? The growth and stability of dendritic spines is a structural hallmark of excitatory synapse maturation in hippocampal pyramidal neurons (Yoshihara et al, 2009). To determine whether the AMPAR knockdown affects structural postsynaptic development, we measured the density of spines in control and AMPAR RNAi neurons, but found no difference (Figures 3.1D and E).

Next, we evaluated the glutamatergic synapse density by counting the number of VGluT1 puncta per unit dendrite. However, reduced postsynaptic AMPAR expression did not alter the density of glutamatergic presynaptic terminals on dendrites of pyramidal neurons (Figures 3.2A and B). Moreover, immunostaining for PSD-95, a postsynaptic scaffold protein at glutamatergic synapses, revealed that AMPAR knockdown had no effect on the number of PSD-95 puncta co-localized with VGluT1 puncta (Figures 3.2A and C). This confirms that postsynaptic AMPARs do not play a major role in determining how many excitatory synapses are formed, and rules out a reduction in synapse density as an explanation for the reduction in NMDAR-mediated synaptic transmission. Lastly, the mean puncta intensity as well as the integrated puncta intensity of both the VGluT1 and PSD-95 immunostaining remain unaffected by GluA-shRNA expression similar to that of GluN1 (Figures 3.2B and C), demonstrating that the expression and localization of synaptic proteins are not generally perturbed by loss of AMPARs.

Measurements of presynaptic release probability

We next wondered whether the knockdown of postsynaptic AMPARs at developing synapses might weaken presynaptic function by decreasing the probability of vesicle release. Changes in vesicle release probability often lead to altered paired-pulse ratio (PPR) of evoked synaptic responses (Katz & Miledi, 1968; Zucker & Regehr, 2002). We recorded pairs of evoked AMPAR eEPSCs, and calculated the PPR at various inter-stimulus intervals (Figure 3.3A). Reducing the external Ca^{2+} concentration from 2.5 mM to 1 mM decreases the synaptic release probability, and this manipulation significantly increased PPR. However, there was no detectable difference between the PPR measured from control and GluA RNAi neurons (Figures 3.3A and B). We repeated this experiment with paired recordings of two connected neurons, in which current is directly injected into a presynaptic neuron and the evoked AMPAR-mediated

response is recorded from its target postsynaptic neuron, either untransfected or expressing GluA shRNAs (Figure 3.3C). In accordance with our results using extracellular stimulation, AMPAR knockdown did not alter PPR measured from paired recordings (Figure 3.3C and D).

In addition to PPR, changes in synaptic release probability can be evaluated by analyzing the progressive block of synaptic NMDAR responses with the irreversible open channel blocker MK-801 (Hessler et al, 1993; Rosenmund et al, 1993). We recorded NMDAR eEPSCs in the presence of bath applied MK-801. Extracellular stimulation was applied at a 0.5 Hz frequency, and the amplitude of 50 postsynaptic responses from successive stimuli was measured. The rate of the decline in eEPSC amplitude represents the progressive block of synaptic NMDARs by MK-801, which is dependent on the release probability of synapses. Indeed, decreasing the external Ca^{2+} from 2 mM to 1 mM to reduce the release probability dramatically slowed the rate of eEPSC blockade, thereby validating this approach (Figures 3.4A and B). If AMPAR knockdown causes a decrease in synaptic release probability, we would expect to see a comparable slowing of the MK-801-mediated blockade. However, the rate of NMDAR eEPSC decline in GluA RNAi neurons was not significantly different from control neurons (Figures 3.4C and D), arguing against the possibility that a lower release probability at synapses underlies the reduced synaptic NMDAR responses following AMPAR knockdown.

Finally, we monitored the rate of vesicle depletion from synapses during high frequency stimulation (Dobrunz & Stevens, 1997). We applied a train of 60 pulses at 20 Hz, and recorded AMPAR eEPSCs. At the train onset, eEPSCs exhibited a rapid depression, which was followed by a slower decay of the responses. The knockdown of AMPARs did not alter the rate of eEPSC depression during the high frequency stimulus train (Figures 3.5A and B). Consistent with our previous results, this suggests that the synaptic release probability is unchanged, and in addition, that the loss of postsynaptic AMPARs does not dramatically alter the rate of vesicle depletion from presynaptic terminals.

Reduction in the readily releasable pool of synaptic vesicles with postsynaptic AMPAR knockdown

Our results thus far show that the reduction of NMDAR eEPSCs following AMPAR RNAi is not due to a loss of postsynaptic NMDARs or a lower synaptic release probability. Instead, the decreased transmission could be the consequence of a decline in the number of presynaptic terminals that contain vesicles available for release (i.e., an increase in presynaptically inactive synapses). To examine this possibility, we applied hypertonic sucrose (0.5 M for 3 sec) to neurons to estimate the size of the RRP in the totality of synapses on a neuron (Rosenmund & Stevens, 1996). Because postsynaptic NMDARs were unaltered by AMPAR knockdown, we performed whole-cell patch-clamp recordings of NMDAR-mediated responses. Before applying the hypertonic solution to assay the RRP, the average NMDAR eEPSC was measured for each cell (Figures 3.5C and D). Indeed, AMPAR knockdown significantly reduced the

charge transfer of the sucrose-evoked NMDAR current (Figures 3.5C and E). Given that the charge of the NMDAR eEPSC represents the amount of vesicle release at presynaptic terminals in response to a single action potential, we divided it by the RRP charge to estimate the probability of release per vesicle (Fernandez-Chacon et al, 2001). Loss of AMPARs had no effect on the vesicular release probability at presynaptic terminals (Figure 3.5F).

We did not observe a change in the probability of vesicle release with AMPAR knockdown, so we next wondered whether the impairment in synaptic transmission is instead due to a reduction in the amount of glutamate released per vesicle. With the application of the low-affinity NMDAR competitive antagonist L-APV during recordings of NMDAR eEPSCs one can effectively monitor changes in glutamate concentration in the synaptic cleft (Choi et al, 2000). If the vesicular glutamate concentration was decreased by GluA RNAi, in the presence of L-APV we would expect to see a more efficient blockade of NMDAR eEPSCs compared to control neurons. In fact, at two concentrations of L-APV, we did not observe a difference in the amount of the NMDAR eEPSC blocked by L-APV suggesting that AMPAR knockdown does not alter the concentration of glutamate released from presynaptic terminals (Figures 3.6A and B). Together, these results are consistent with the notion that the AMPAR knockdown lowers the total number of fusion-competent vesicles among all synapses, but leaves the responsiveness, namely release probability and glutamate content, of the remaining releasable vesicles unaffected. Accordingly, it is conceivable that the loss of AMPARs increases the number of immature presynaptic terminals that are deficient in fusion-competent vesicles, whereas other synapses maintain presynaptic terminals that are functionally normal.

GluA RNAi increases number of inactive glutamatergic terminals

To visualize whether AMPAR knockdown affects the number of presynaptic terminals that participate in vesicle release, we used an antibody that recognizes the intraluminal domain of synaptotagmin 1 (Syt1) to directly monitored presynaptic vesicle cycling at individual synapses (Malgaroli et al, 1995; Matteoli et al, 1992). The Syt1 antibody was applied to live neurons in the culture media and the differential uptake of the antibody driven by endogenous network activity enabled us to assess vesicle fusion at individual synapses. Post-fixation immunostaining for VGluT1 and GAD-65 revealed that Syt1 antibody uptake occurred at both glutamate and GABA releasing synapses with roughly 65% excitatory release sites and 35% inhibitory release sites (Figures 3.7A and B). Therefore a combination of Syt1 antibody uptake and VGluT1 immunostaining allows us to specifically monitor vesicle release from glutamatergic terminals. VGluT1-positive puncta containing Syt1 labeling indicates active glutamate release sites and VGluT1-positive puncta lacking Syt1 labeling indicates inactive glutamate release sites.

Using this approach, we first monitored the amount of vesicle release that occurred during either 5 or 20 minutes of antibody incubation compared to Syt1 post-fixation immunolabeling (Figure 3.7C). There was a notable increase in the Syt1 immunolabeling intensity co-localized with VGluT1 puncta with longer antibody

incubation reflecting a greater number of vesicles recycled over time (Figure 3.7D). The intensity of Syt1 immunofluorescence following permeabilization was far greater suggesting that many vesicles at the presynaptic terminal do not routinely participate in synaptic transmission (Figure 3.7D). Next we measured the proportion of glutamatergic synapses that were inactive. We found a modest reduction in synapses lacking Syt1 antibody uptake with the longer 20 minute antibody incubation, but most importantly, with post-fixation immunostaining almost all glutamatergic synapses displayed Syt1 immunofluorescence (Figure 3.7E). Thus we confirmed the effectiveness of the Syt1 antibody uptake assay and we continued to use it to faithfully measure vesicle cycling at presynaptic terminals.

Interestingly, we found that a loss of postsynaptic AMPARs increased the number of glutamatergic presynaptic terminals that did not release any synaptic vesicles during the 20 minute period of Syt1 labeling (Figures 3.8A and B) suggesting that a subset of terminals became functionally inactive. This effect is specifically due to the loss of AMPARs because the number of inactive presynaptic terminals could be reduced to control levels with the co-expression of either the GluA1 or GluA2 rescue mutant (Figures 3.8A and B). In agreement with our assessment of presynaptic release probability, the average intensity of Syt1 antibody uptake at VGlut1-positive puncta was not changed, suggesting that the amount of vesicle release at active glutamatergic presynaptic terminals was unaltered by AMPAR knockdown (Figure 3.8C).

Since we used basal network activity to drive uptake of the Syt1 antibody, one concern was that knocking down AMPA receptors in a neuron might reduce the overall network activity of the area surrounding the GluA-shRNA transfected neuron and this could account for observed increase in functionally inactive presynaptic terminals following AMPAR knockdown. To address this issue we measured the number of inactive presynaptic terminals of neighboring untransfected neurons adjacent to the transfected neuron for each of the groups. There was no difference in either the percent of inactive presynaptic terminals or the average intensity of Syt1 antibody uptake between the untransfected neurons of each group (Figures 3.8D and E), confirming that the global network activity was unaffected by AMPAR knockdown. Finally, the neurons were immunostained with the Syt1 antibody after fixation and permeabilization and we found that almost all glutamatergic terminals contained Syt1 (pSuper: 97.11 +/- 0.63%; GluA RNAi: 96.56 +/- 0.56%; n = 10 for each group) and the mean Syt1 puncta intensity was no different between control and GluA-shRNA expressing neurons (pSuper: 100.61 +/- 5.63 A.U.; GluA RNAi: 110.87 +/- 5.94 A.U.; n = 10 for each group).

At mature glutamatergic synapses, postsynaptic AMPARs and NMDARs respond to glutamate released from cycling synaptic vesicles at the presynaptic active zone (Figure 3.9A). With the knockdown of AMPARs during development we observed a decrease in the RRP at presynaptic terminals along with an increase in the number of functionally inactive presynaptic terminals. These results are most consistent with an increased prevalence of immature glutamatergic synapses lacking fusion-competent vesicles when postsynaptic AMPAR expression is decreased during synaptogenesis (Figure 3.9B).

Figure 3.1

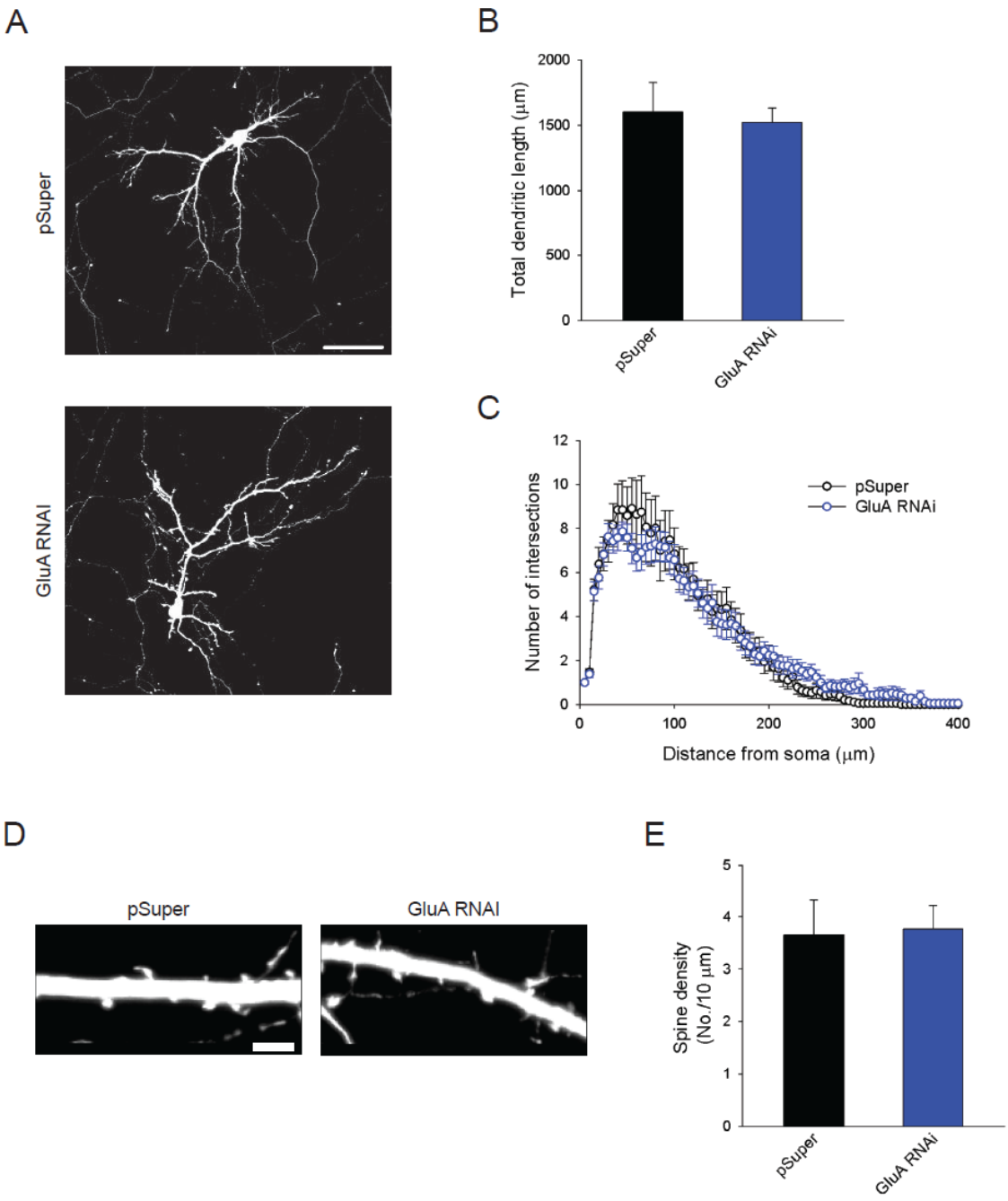
A
pSuper
GluA RNAI
B
Total dendritic length (μm)
2000
1500
1000
500
0
pSuper
GluA RNAi
C
Number of intersections
12
10
8
6
4
2
0
0
100
200
300
400
Distance from soma (μm)
pSuper
GluA RNAi
D
pSuper
GluA RNAI
E
Spine density (No./10 μm)
5
4
3
2
1
0
pSuper
GluA RNAi

Figure 3.1: AMPAR knockdown does not alter dendrite morphology or the number of postsynaptic spines. (**A**) Neurons transfected with pSuper or GluA RNAi at 7 DIV and fixed at 12 DIV. Dendrite morphology was visualized by the fluorescence of GFP expressed in transfected cells. Scale bar, 80 µm. (**B**) Quantification of the mean total length of dendrites (n = 19-21 neurons/group; $p > 0.7$). (**C**) Sholl's analysis was performed to investigate the complexity of dendritic branches after AMPAR knockdown (n = 19-21 neurons/group). (**D**) The spines of neurons transfected with pSuper or GluA RNAi were visualized by GFP fluorescence. Scale bar, 3 µm (**E**) The mean number of spines per length dendrite was quantified for each group (n = 15 neurons/group; $p > 0.8$).

Figure 3.2

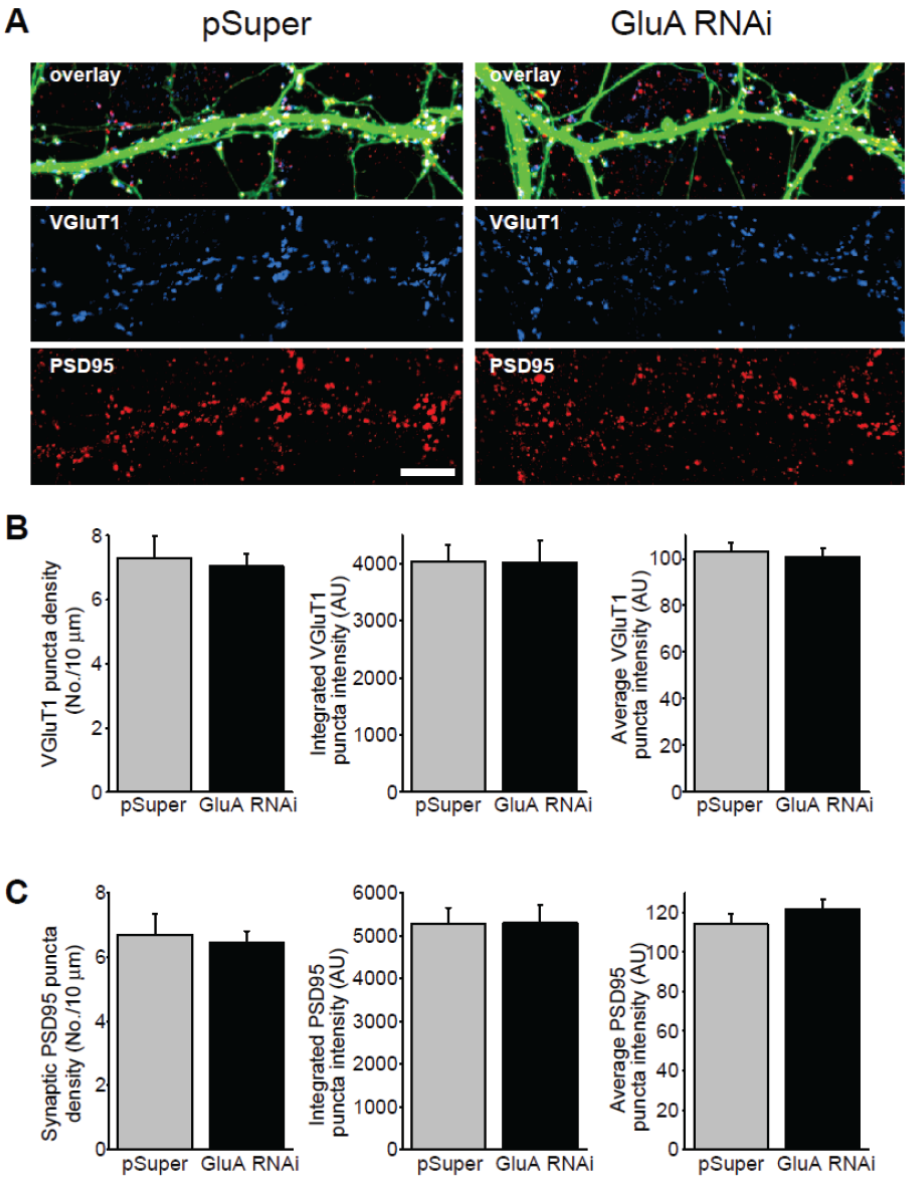

Figure 3.2: Reduction in postsynaptic AMPARs does not alter synapse density. (**A**) Immunostaining for synaptic markers used to detect glutamatergic contacts, namely VGluT1 (blue) to label presynaptic terminals and PSD-95 (red) to label postsynaptic sites. Neurons were transfected with either pSuper or the GluA-shRNAs at 7 DIV, and fixed for immunocytochemistry at 12 DIV. Scale bar, 10 µm. (**B**, **C**) Quantification of the density of glutamatergic synapses formed onto neurons expressing pSuper or GluA-shRNAs. Signals from both the presynaptic marker VGluT1, **B**, and the postsynaptic marker PSD-95, **C**, were analyzed (n =12-15 cells/group; $p > 0.6$).

Figure 3.3

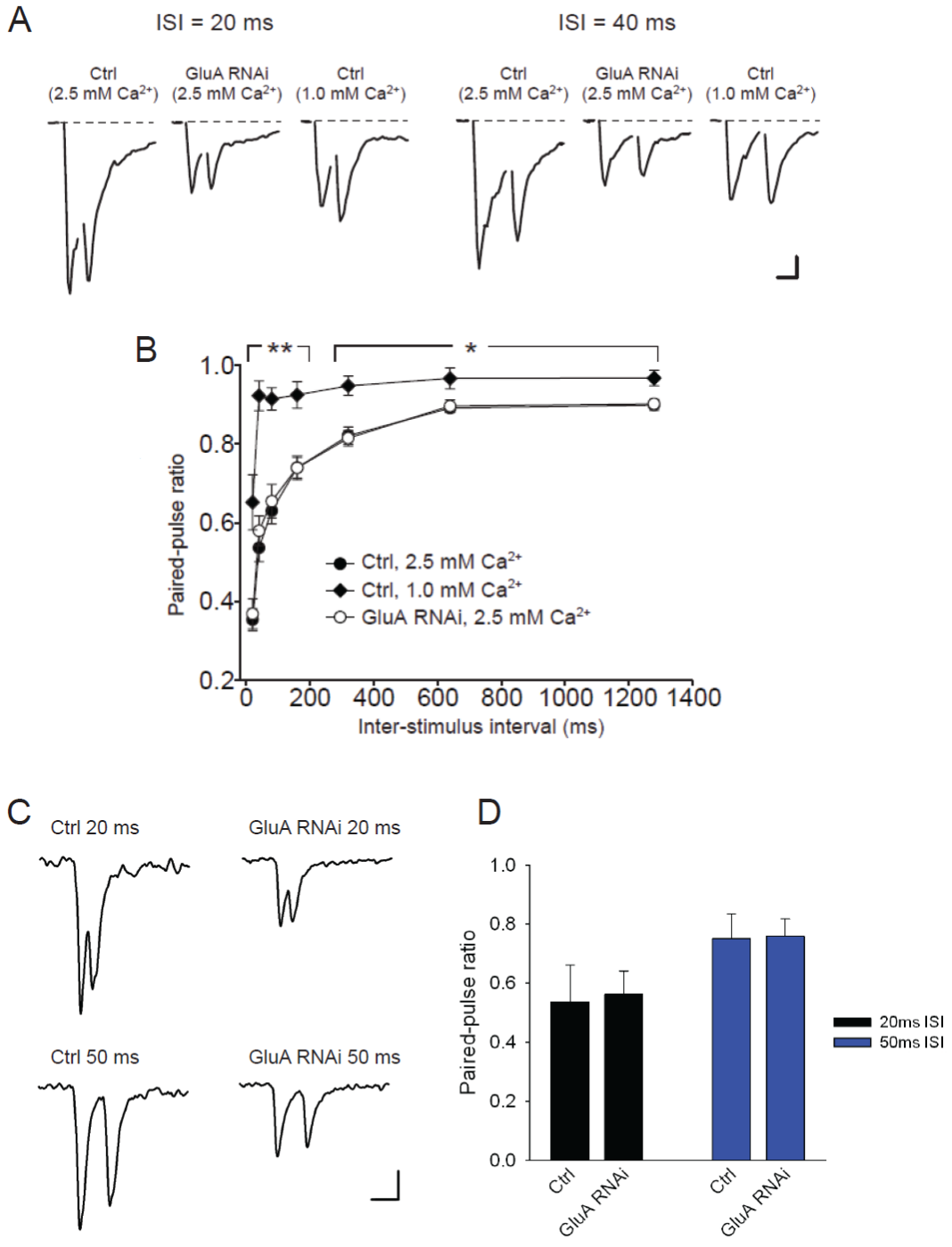
A
ISI = 20 ms
ISI = 40 ms
Ctrl (2.5 mM Ca2+)
GluA RNAi (2.5 mM Ca2+)
Ctrl (1.0 mM Ca2+)
B
**
*
Paired-pulse ratio
Inter-stimulus interval (ms)
Ctrl, 2.5 mM Ca2+
Ctrl, 1.0 mM Ca2+
GluA RNAi, 2.5 mM Ca2+
C
Ctrl 20 ms
GluA RNAi 20 ms
Ctrl 50 ms
GluA RNAi 50 ms
D
Paired-pulse ratio
20ms ISI
50ms ISI
Ctrl
GluA RNAi

Figure 3.3: Loss of postsynaptic AMPARs does not alter the release probability at synapses measured by paired-pulse ratio. (**A**) Paired-pulse ratio (PPR) of AMPAR eEPSCs. Representative traces of AMPAR eEPSCs elicited by extracellular local field stimulation at a 20 ms and 40 ms inter-stimulus interval (ISI). Each trace is an average of five individual responses recorded from one neuron. Scale bars: 200 pA, 20 ms. (**B**) Quantification of PPR for each group over a range of ISI (n = 11-14 cells/group; *, $p < 0.01$; **, $p < 0.001$). (**C**) PPR of AMPAR EPSCs recorded from synaptically connected neurons. Representative traces of AMPAR EPSCs elicited by current injection to a connected presynaptic neuron in whole cell current clamp recording mode. Each trace is an average of at least five individual responses recorded from one neuron. Scale bars: 20 pA, 50 ms. (**D**) Quantification of PPR for control and GluA RNAi neurons at a 20ms and 50 ms ISI (n = 10-14 cells/group; $p > 0.8$).

Figure 3.4

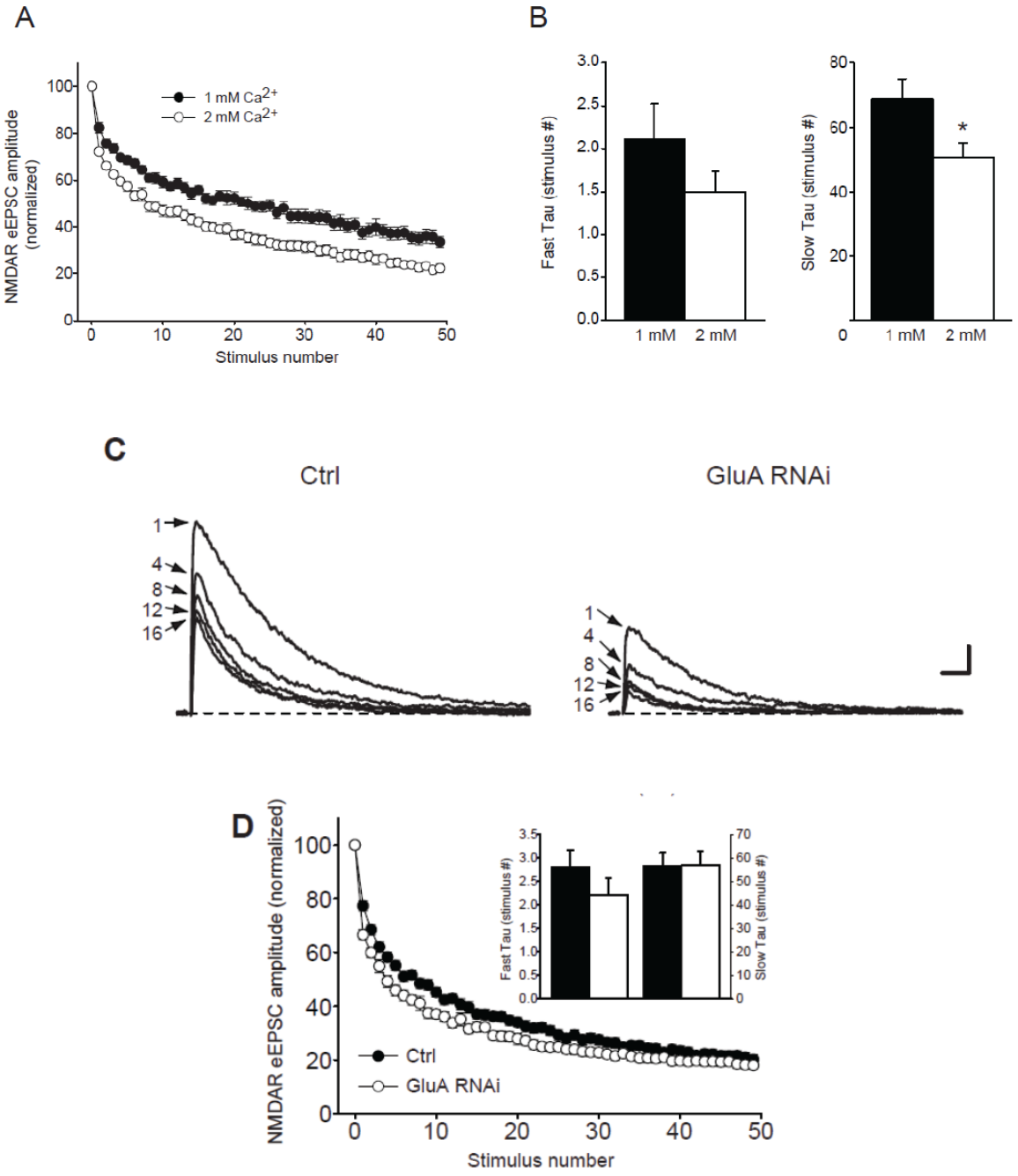
A
NMDAR eEPSC amplitude (normalized)
1 mM Ca2+
2 mM Ca2+
Stimulus number
B
Fast Tau (stimulus #)
Slow Tau (stimulus #)
1 mM
2 mM
*
C
Ctrl
GluA RNAi
1
4
8
12
16
D
NMDAR eEPSC amplitude (normalized)
Ctrl
GluA RNAi
Stimulus number

Figure 3.4 Activity-dependent blockade of NMDAR eEPSCs with MK-801 confirms that the presynaptic release probability is unaltered by AMPAR knockdown. (**A**) A decrease in synaptic release probability slows the rate of NMDAR eEPSC blockade by MK-801. The progressive block of NMDAR EPSCs recorded from untransfected neurons in 10 μM MK-801 at two concentrations of external calcium, 1 mM (black) and 2 mM (white). The amplitudes at consecutive stimuli were normalized to the first response (n = 13-14 cells/group). (**B**) The rate of NMDAR eEPSC blockade was fitted with a double exponential equation (*, $p < 0.05$). (**C**) Example traces of NMDAR eEPSCs recorded at +40 mV in the presence of 10 μM MK-801 showing the progressive block of the postsynaptic responses at each designated stimulus number. Scale bars: 200 pA, 100 ms. (**D**) Quantification of the NMDAR eEPSC amplitude in the presence of MK-801 at consecutive stimuli normalized to the amplitude of the first response. Inset: Rate of response decay fitted with a double exponential equation (n = 22-24 cells/group; $p > 0.2$).

Figure 3.5

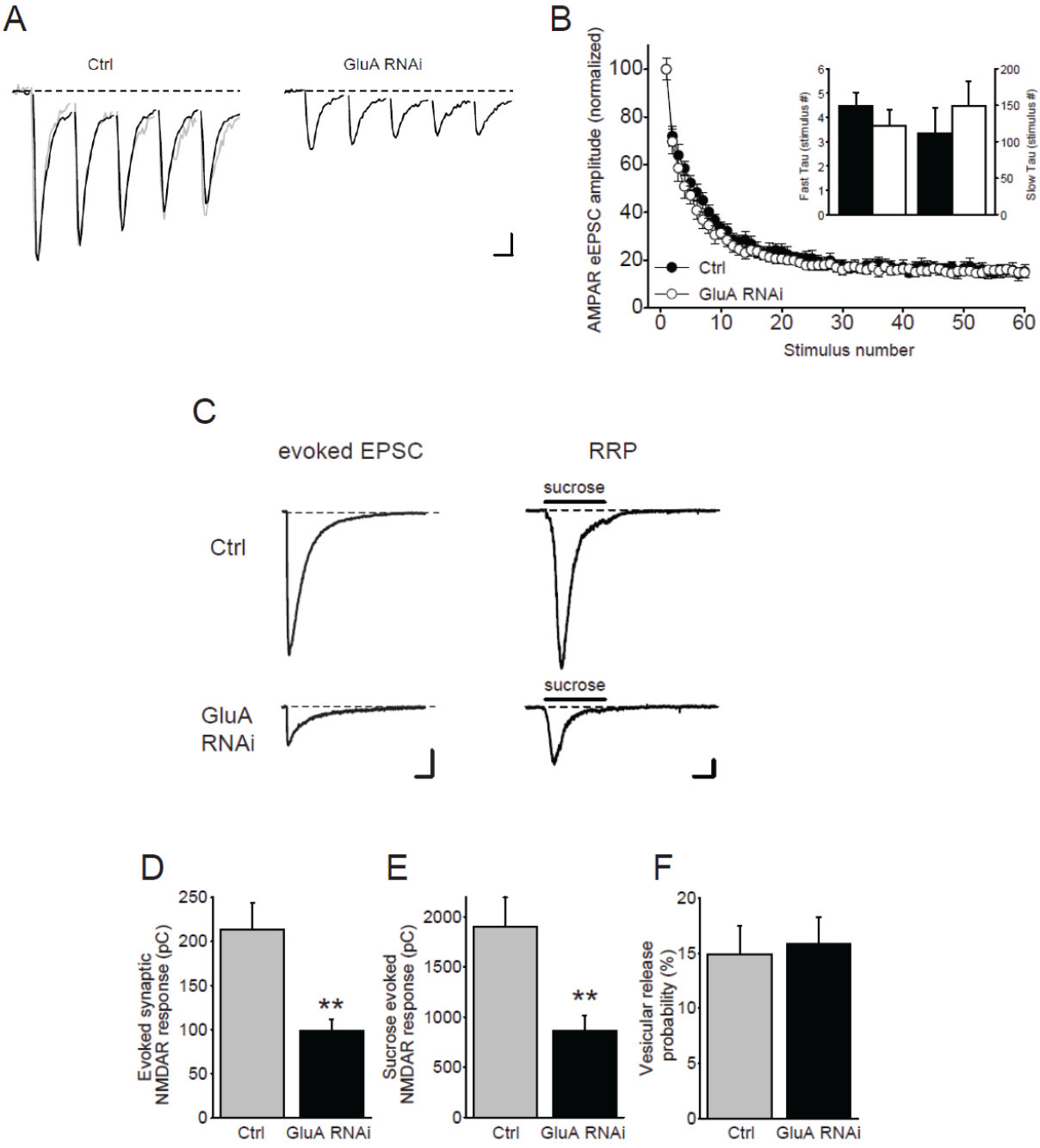
A
Ctrl
GluA RNAi
B
AMPAR eEPSC amplitude (normalized)
Stimulus number
Ctrl
GluA RNAi
Fast Tau (stimulus #)
Slow Tau (stimulus #)
C
evoked EPSC
RRP
sucrose
Ctrl
GluA RNAi
D
Evoked synaptic NMDAR response (pC)
**
E
Sucrose evoked NMDAR response (pC)
**
F
Vesicular release probability (%)

Figure 3.5: AMPAR knockdown decreases the total size of the readily-releasable vesicle pool at excitatory synapses. (**A**) Example traces of the first five AMPAR eEPSCs in response to a 20 Hz stimulation from an untransfected neuron and a GluA RNAi neuron (black traces). The response from the GluA RNAi neuron was scaled and superimposed onto the control response (gray trace). Each trace is an average of three individual 20Hz trains of eEPSCs recorded from one neuron. Scale bars: 200 pA, 20 ms. (**B**) The amplitude of each successive response was normalized to the size of the first AMPAR eEPSC. Inset: Time constants of the response decay fitted with a double exponential equation (n = 13 cells/group; $p > 0.3$). (**C**) Representative traces of NMDAR eEPSCs (left) and NMDAR-mediated responses evoked by 3 seconds of 0.5 M sucrose (right). For each neuron, five NMDAR eEPSCs were recorded to generate an average response to extracellular stimulation, which was followed by a single application of 0.5M sucrose to estimate the size of the RRP. (**D**) Average charge transfer of NMDAR eEPSCs elicited by extracellular field stimulation from control and AMPAR knockdown neurons. (**E**) Average sucrose-evoked NMDAR responses from the same neurons in **D** (n = 22-23 cells; **, $p < 0.005$). (**F**) The vesicular release probability estimated for each neuron by calculating the charge transfer of the average NMDAR eEPSC as a percentage of the total sucrose-evoked current (n = 22-23 cells; $p > 0.7$).

Figure 3.6

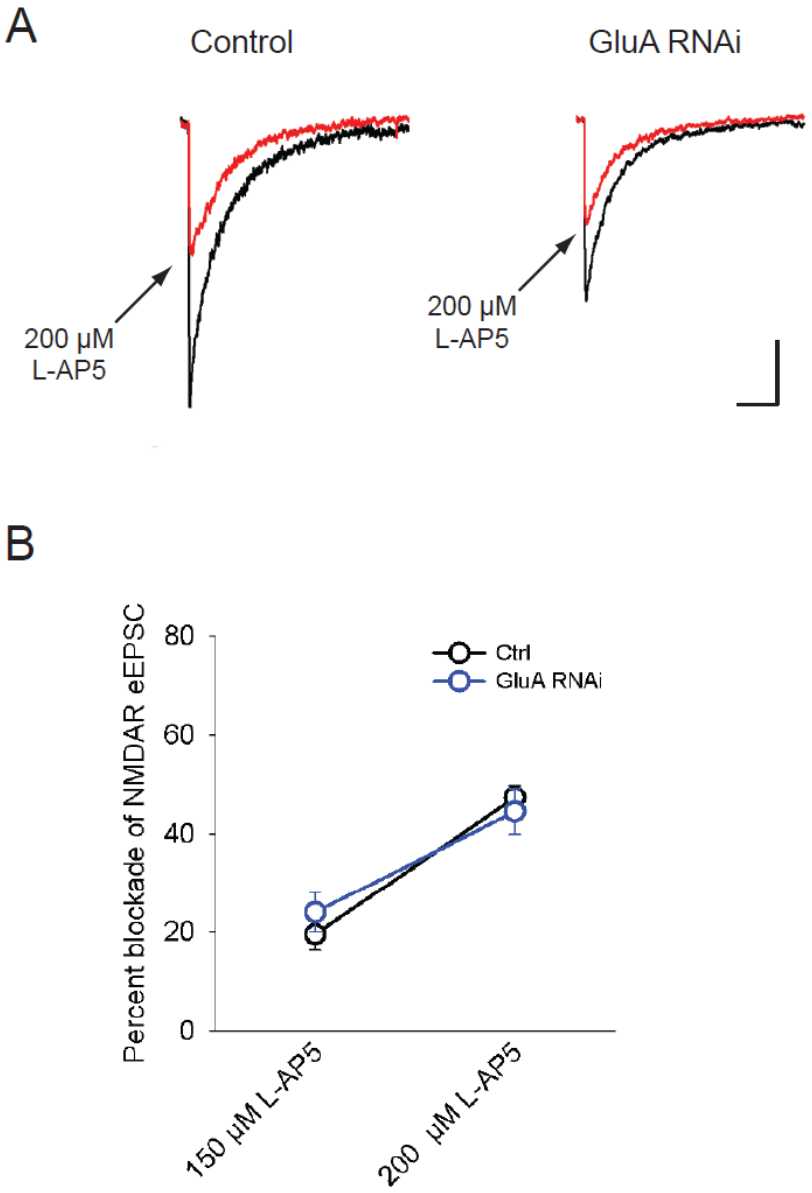

Figure 3.6: Decreased NMDAR-mediated synaptic transmission is not due to a lower concentration of glutamate released into the synaptic cleft upon synaptic vesicle exocytosis. (**A**) Representative traces of NMDAR eEPSCs recorded from a untransfected control neuron and a GluA RNAi neuron before (black trace) and after bath application of 200 μM L-APV (red trace). Each trace is an average of five individual responses recorded from one neuron. Scale bars: 300pA, 500ms. (**B**) Quantification of the mean percent of the NMDAR eEPSC that was effectively blocked by bath application of L-AP5 at two different concentrations (n = 10-12 cells/group; $p > 0.3$).

Figure 3.7

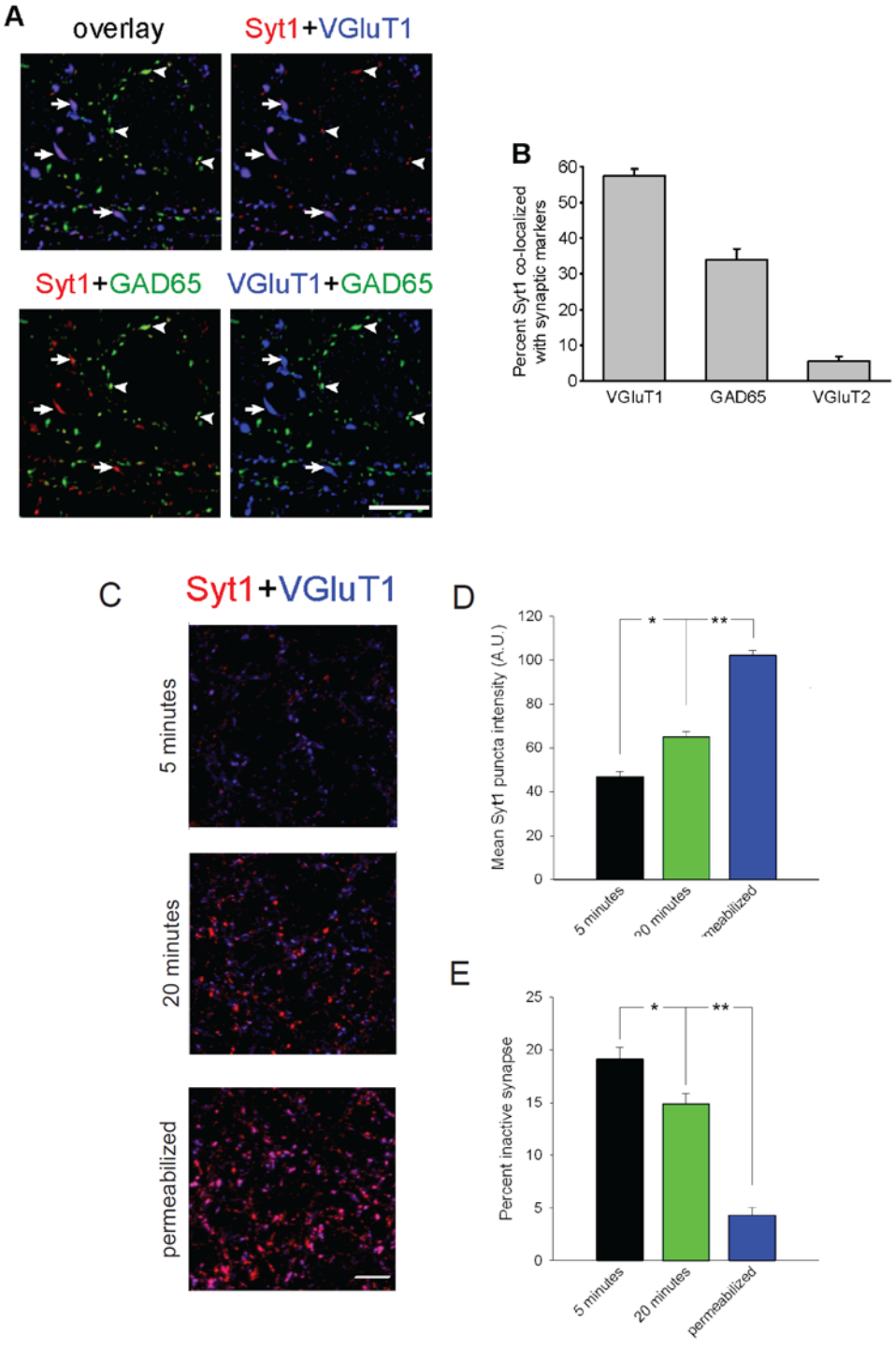
A
overlay
Syt1+VGluT1
Syt1+GAD65
VGluT1+GAD65
B
Percent Syt1 co-localized with synaptic markers
60
50
40
30
20
10
0
VGluT1
GAD65
VGluT2
C
Syt1+VGluT1
5 minutes
20 minutes
permeabilized
D
Mean Syt1 puncta intensity (A.U.)
120
100
80
60
40
20
0
*
**
5 minutes
20 minutes
E
Percent inactive synapse
25
20
15
10
5
0
*
**
5 minutes
20 minutes
permeabilized

Figure 3.7: Syt1 antibody uptake occurs at both glutamate and GABA releasing terminals. (**A**) Syt1 antibody uptake (red) was co-localized predominantly with either VGluT1 (blue) or GAD65 (green) immunolabeling. Synaptic vesicle release is evident at both excitatory synapses (arrows) and inhibitory synapses (arrowheads). Scale bar, 10 µm. (**B**) Quantification of the fraction of total Syt1 puncta that co-localize with the excitatory synaptic markers, VGluT1 and VGluT2, and the inhibitory synaptic marker, GAD65. (**C**) Syt1 antibody uptake (red) was performed at two different incubation periods, either 5 or 20 minutes, and compared to Syt1 immunostaining after fixation and permeabilization. VGluT1 immunolabeling (blue) was used to identify glutamatergic terminals. (**D**) Graph showing the mean puncta intensity of Syt1 co-localized with VGluT1 at 5 and 20 minute antibody incubation time or after permeabilization (n = 4-6 images/group; *, $p < 0.001$; **, $p < 1 \times 10^{-5}$). (**E**) Graph showing the percent of the total number of synapses that are functionally inactive. Inactive synapses are identified as VGluT1 puncta lacking Syt1 co-localization (n = 4-6 images/group; *, $p < 0.01$; **, $p < 1 \times 10^{-4}$).

Figure 3.8

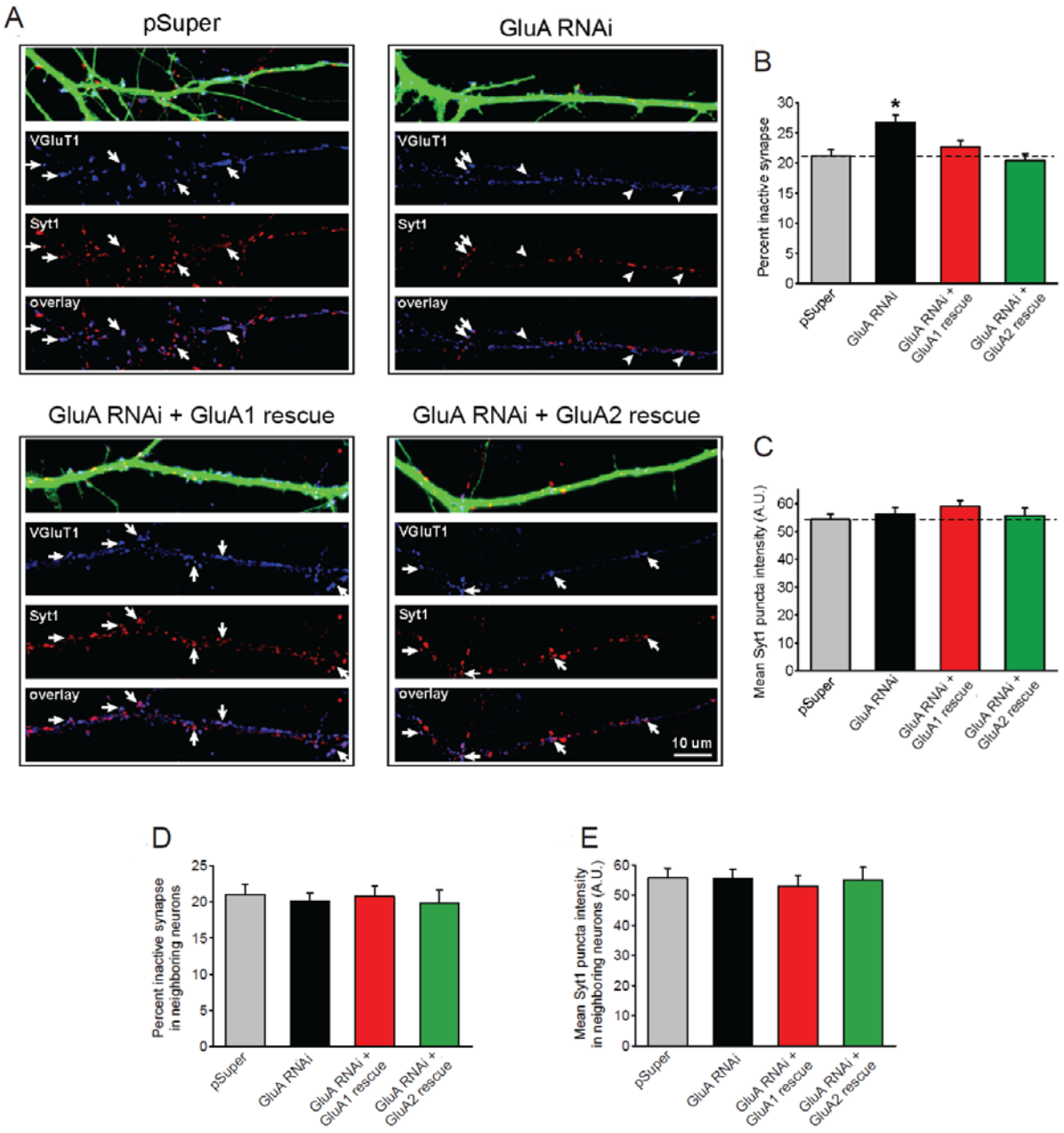
A
pSuper
GluA RNAi
VGluT1
Syt1
overlay
GluA RNAi + GluA1 rescue
GluA RNAi + GluA2 rescue
10 um
B
Percent inactive synapse
pSuper
GluA RNAi
GluA RNAi + GluA1 rescue
GluA RNAi + GluA2 rescue
C
Mean Syt1 puncta intensity (A.U.)
D
Percent inactive synapse in neighboring neurons
E
Mean Syt1 puncta intensity in neighboring neurons (A.U.)

Figure 3.8: GluA RNAi increases the proportion of glutamatergic presynaptic terminals that are functionally inactive. (**A**) The Syt1 antibody uptake (red) method was applied to neurons transfected with pSuper, GluA-shRNAs, or GluA-shRNAs with one of the shRNA-insensitive GluA constructs. Post-fixation immunostaining of VGluT1 was used to identify glutamatergic synapses (blue). Active glutamatergic presynaptic terminals exhibit Syt1 immunostaininig (arrows), whereas inactive terminals do not (arrowheads). (**B**) Graph of the proportion of functionally inactive glutamatergic synapses on transfected neurons (n = 18-30 neurons/group; *, $p < 0.001$). (**C**) Graph of the mean intensity of Syt1 immunostaining at active glutamatergic synapses (n = 18-30 neurons/group; $p > 0.1$). (**D,E**) Graph of the proportion of functionally inactive synapses (**D**) and the mean intensity of Syt1 puncta co-localized with VGluT1 (**E**) on neighboring untransfected neurons (n= 13-15 neurons/group; $p > 0.5$).

Figure 3.9

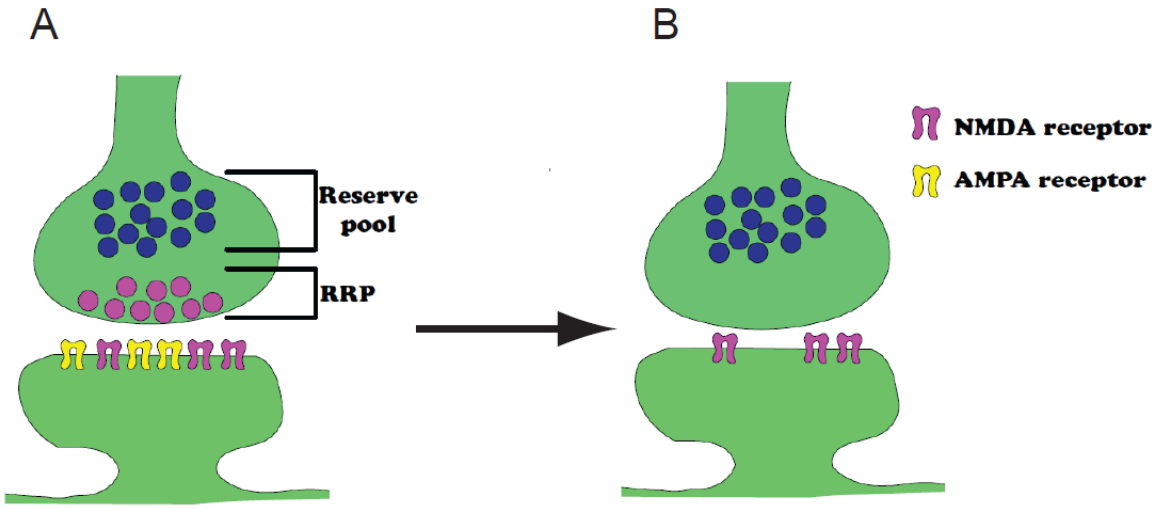

Figure 3.9: GluA RNAi impairs synaptic transmission by making more presynaptic terminals functionally inactive most likely due to a loss of synaptic vesicles in the RRP. (**A**) Mature glutamatergic synapses contain AMPA- and NMDA-type glutamate receptors postsynaptically and they accumulate both a reserve pool and a readily releasable pool of synaptic vesicles at the presynaptic terminal. (**B**) Following AMPAR knockdown during early synapse development we propose that a subset of synapses do not sufficiently recruit a readily releasable pool of vesicles making the presynaptic terminal functionally inactive.

Chapter 4

Trans-synaptic signaling by postsynaptic AMPARs promotes presynaptic terminal maturation

Introduction

Activity-dependent retrograde signaling at hippocampal synapses can promote modifications in synaptic function. A number of retrograde messengers have been identified that are released from a postsynaptic neuron in response to changes in activity. These messengers include neurotrophins, endocannabinoids, and nitric oxide (Feil & Kleppisch, 2008; Lessmann, 1998; Wilson & Nicoll, 2001). We found that the loss of postsynaptic AMPARs during development causes an increase in the number of inactive presynaptic terminals suggesting that a retrograde signal for synapse maturation is triggered by postsynaptic AMPARs. It is possible that an increase in postsynaptic activity from the insertion of AMPARs during synapse maturation promotes the release of a retrograde messenger to enhance presynaptic function.

If the release of a retrograde messenger is triggered by AMPAR activity during development, we would expect to block its effect on presynaptic function by treatment with an AMPAR antagonist. Alternatively, a trans-synaptic interaction between the AMPAR ectodomain and a binding partner expressed at the presynaptic terminal may convey the retrograde signal. The ectodomain of an AMPAR subunit consists of a large N-terminal domain and the ligand binding domains. Members of the neuronal pentraxin family interact with the ectodomain domain of AMPARs and may play a role in synapse development (O'Brien et al, 2002; Sia et al, 2007; Xu et al, 2003). A recent study has identified a specific interaction between N-cadherin and the N-terminal domain of the GluA2 subunit that is important for spine growth (Saglietti et al, 2007).

Here, we investigate the mechanism involved in this retrograde signaling during synapse development. We considered three possible mechanisms for the effect of AMPARs on presynaptic function. First, the enhanced postsynaptic activity following AMPAR insertion could trigger the release of a retrograde messenger promoting the maturation of presynaptic terminals. Second, upon insertion into the postsynaptic membrane, AMPARs indirectly promote vesicle release at presynaptic terminals by interacting with another postsynaptic protein engaged in trans-synaptic signaling. Lastly, the presence of postsynaptic AMPARs could directly influence presynaptic function by interacting with an unknown presynaptic component through binding to the AMPAR ectodomain.

Results and Discussion

AMPAR channel activity is not required for retrograde signaling

To probe the mechanism by which postsynaptic AMPARs affect presynaptic function, we asked whether retrograde signaling mediated by AMPARs is activity-dependent, i.e., whether receptor activation is required for promoting presynaptic function. We investigated this possibility by re-examining the rescue of NMDAR synaptic transmission following GluA RNAi while blocking all AMPAR activity with the selective AMPAR antagonist CNQX. CNQX was added to the culture concurrently with transfection of the GluA-shRNAs and the GluA1 or GluA2 rescue construct, and was maintained in the culture for five days until the time of recording. Evoked synaptic NMDAR responses were used to monitor synaptic function. Blocking AMPAR activity with CNQX for five days did not change NMDAR eEPSCs recorded from untransfected neurons (Figures 4.1C). Surprisingly, the NMDAR eEPSC amplitude that was reduced in neurons with AMPAR knockdown was successfully rescued by GluA1 or GluA2 co-expression despite the complete blockade of AMPAR activity by CNQX (Figures 4.1A and B), suggesting that the activation of AMPARs with subsequent postsynaptic depolarization is not required for presynaptic maturation. Therefore, it is improbable that the activity-dependent release of a retrograde messenger is responsible for AMPAR-mediated signal transduction during synapse development.

Heterologous synapses reveal a distinct role for AMPARs in the induction of synaptic vesicle release at a subset of presynaptic terminals

To investigate the specific role of AMPARs in modifying presynaptic function at newly formed synapses, we took advantage of the heterologous synapse formation assay (Dalva et al, 2007; Washbourne et al, 2004). Expression of the postsynaptic cell adhesion molecule NL1 in heterologous cells has been shown to induce presynaptic differentiation in contacting neuronal axons (Scheiffele et al, 2000). We confirmed that synaptic currents generated at heterologous synapses can be recorded from HEK293 cells expressing NL1 and AMPARs (Figure 4.2A). The amplitude and kinetics of these synaptic currents look similar to mEPSCs recorded from hippocampal neurons (Figure 4.2B).

We expressed NL1 with or without AMPARs in HEK293 cells, and co-plated them with dissociated hippocampal neurons at 9 DIV, a stage of active synaptogenesis. Three days after co-plating, we evaluated presynaptic function at heterologous synapses using an antibody that recognizes the intraluminal domain of synaptotagmin 1 (Syt1) to directly monitor presynaptic vesicle recycling (Malgaroli et al, 1995; Matteoli et al, 1992). The Syt1 antibody was applied to live co-cultures in the culture media, and the differential uptake of the antibody driven by endogenous network activity enabled us to assess vesicle fusion at individual synapses. Syt1 antibody uptake with post-fixation

immunostaining of VGluT1 allowed us to specifically examine vesicle release from glutamatergic terminals at heterologous synapses. VGluT1 puncta co-localized with Syt1 labeling indicate active glutamate release sites, and VGluT1 puncta lacking Syt1 labeling signify functionally inactive glutamatergic terminals that fail to undergo vesicle release.

Consistent with previous reports, the expression of NL1 in HEK293 cells induced glutamatergic presynaptic terminal differentiation, as manifested by the accumulation of VGluT1 puncta above the cells (Figure 4.3A). Due to the strong synaptogenic effect of NL1 expression, some co-cultured HEK293 cells developed significant overlap of synaptic contacts to the extent that individual synapses could not be clearly resolved. These cells were excluded from our analysis. To evaluate presynaptic maturation at heterologous synapses in comparison to neuronal synapses, and to account for variability in culture density and immunostaining, we normalized quantifications of both VGluT1 and Syt1 immunostaining at each HEK293 cell to the corresponding quantifications made from neighboring neuronal synapses.

Intrigued by the effect of AMPAR RNAi on the supply of releasable presynaptic vesicles at neuronal synapses, we first examined the proportion of functionally inactive glutamatergic terminals at heterologous synapses with or without postsynaptic AMPARs. Interestingly, although HEK293 cells expressing either NL1 alone or NL1 together with AMPARs potently induced formation of excitatory synapses from contacting axons, HEK293 cells expressing NL1 alone exhibited a greater proportion of inactive glutamatergic terminals than HEK293 cells expressing both NL1 and AMPARs (Figures 4.3A and B). This effect was specific to AMPARs, because co-expression of the kainate receptor subunit GluK2 with NL1 in HEK293 cells did not reduce the fraction of inactive glutamatergic terminals. Co-expression of AMPARs with NL1 did not alter the size of the HEK293 cells (Figure 4.4C); therefore, the contact area for crossing axons is not influenced by AMPAR expression. The mean intensity of Syt1 antibody uptake at active glutamatergic terminals was similar between heterologous synapses with or without AMPARs (Figure 4.3C). Likewise, the mean VGlut1 puncta intensity (Figure 4.4A) and the density of glutamatergic presynaptic terminals (Figures 4.4B and D) were comparable between HEK293 cells that expressed AMPARs and those that did not. From these results, it is evident that although AMPARs are not required for the recruitment of actively recycling vesicles to all glutamatergic presynaptic terminals, they dramatically decrease the proportion of terminals that are functionally inactive.

A direct trans-synaptic interaction mediates AMPAR-induced presynaptic vesicle release

Given that AMPAR channel activity was not required for the retrograde effect of AMPAR on presynaptic function as demonstrated by rescue of synaptic NMDAR responses in the presence of CNQX (Figure 4.1B), we next tested an alternative signaling mechanism: a direct trans-synaptic interaction between the AMPAR ectodomain and an unidentified component of the presynaptic membrane. We

generated a chimeric AMPAR construct, GluA2 ecto, which consists of the GFP-tagged GluA2 extracellular domain fused to the transmembrane domain of the interleukin-2 receptor (Tac) (Standley et al, 2000), with the intracellular GluA1 C-terminal domain (Figure 4.5A). Although in neurons the GluA2 ecto protein was not efficiently exported from the endoplasmic reticulum (Figure 4.5C), when expressed in HEK293 cells, GluA2 ecto was trafficked robustly to the cell surface (Figure 4.5B). In the co-culture heterologous synapse system, GluA2 ecto behaved similarly to the full-length GluA2 in that when co-expressed with NL1 it greatly reduced the number of inactive presynaptic terminals compared to NL1-alone expression (Figures 4.6A and B).

HEK293 cells are not known to endogenously express synaptic proteins, making it unlikely that another postsynaptic protein is involved as an intermediary between AMPARs and developmental signaling at the presynaptic terminal. Taken together, our results point to a transduction mechanism that involves a direct trans-synaptic interaction between the postsynaptic AMPAR extracellular domain and an unknown presynaptic protein, which ultimately makes a subset of presynaptic terminals functional by recruiting a releasable pool of synaptic vesicles.

Figure 4.1

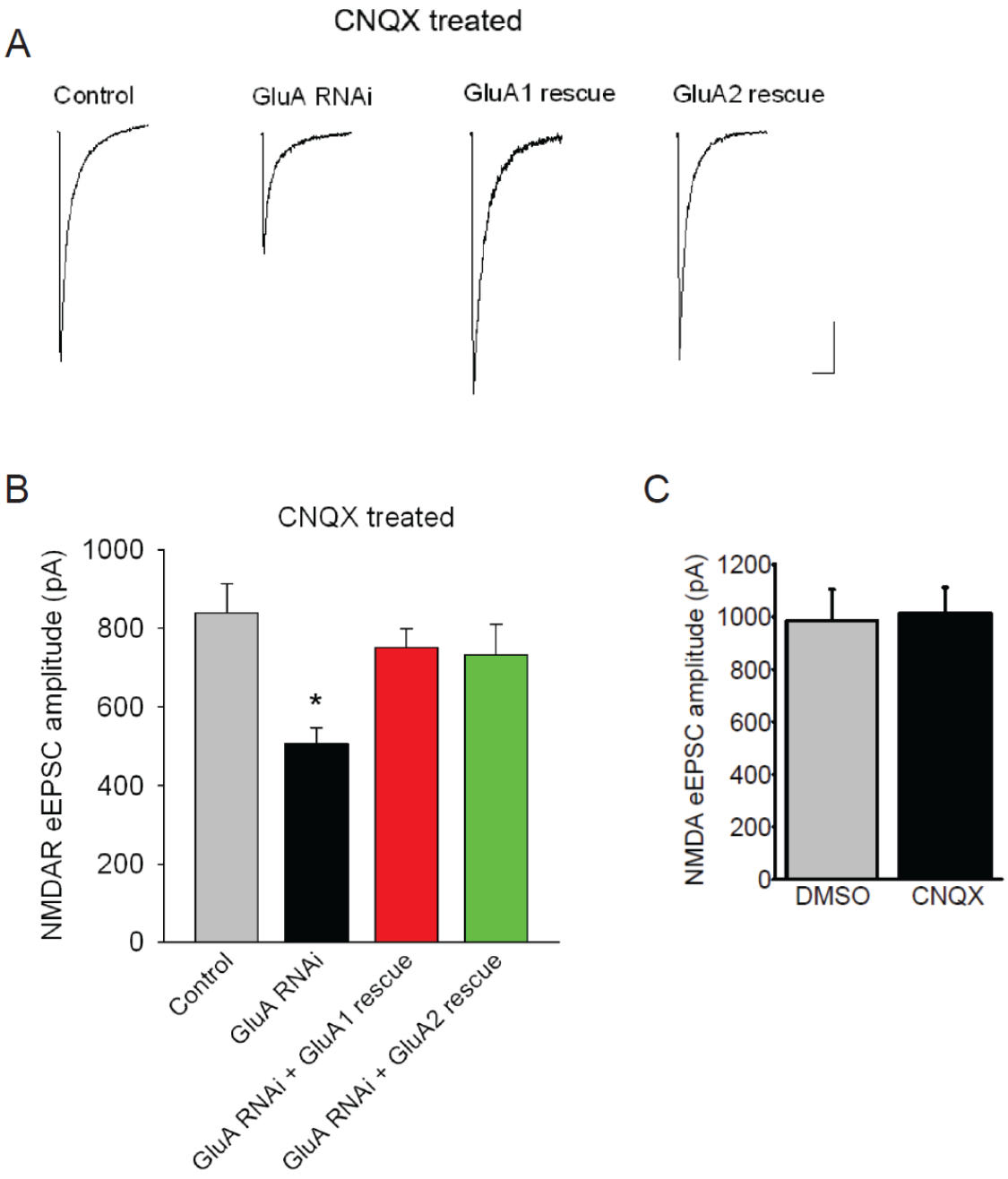
A
CNQX treated
Control
GluA RNAi
GluA1 rescue
GluA2 rescue
B
CNQX treated
NMDAR eEPSC amplitude (pA)
1000
800
600
400
200
0
*
Control
GluA RNAi
GluA RNAi + GluA1 rescue
GluA RNAi + GluA2 rescue
C
NMDA eEPSC amplitude (pA)
1200
1000
800
600
400
200
0
DMSO
CNQX

Figure 4.1: AMPAR channel activity is not required for the retrograde effect on presynaptic vesicle release. (**A**) Representative traces of NMDAR eEPSCs recorded from neurons treated with CNQX (10 μM) throughout the five days of construct expression. Each trace is the average of 5-10 eEPSCs recorded from one neuron. (**B**) Quantification of the mean amplitude of NMDAR eEPSCs recorded after chronic CNQX treatment (n = 32-37 cells/group; **, $p < 0.005$). Scale bars: 200pA, 200 ms. (**C**) Chronic blockade of AMPARs does not alter synaptic NMDAR-mediated responses. The mean amplitude of NMDAR eEPSCs recorded from untransfected neurons that were treated with either DMSO or 10 μM CNQX for 5 days (n = 12 cells/group; $p > 0.8$).

Figure 4.2

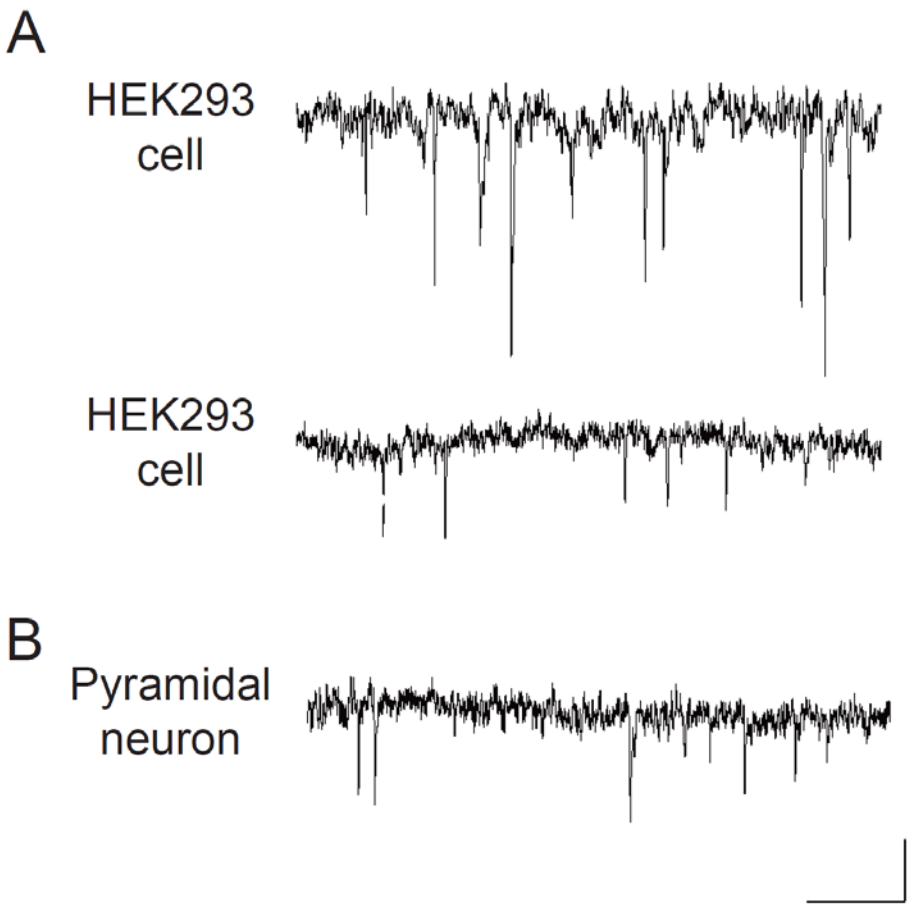

Figure 4.2: Synaptic transmission at heterologous synapses. (**A**) Example traces from whole-cell patch clamp recordings of spontaneous currents from HEK293 cells in co-culture with neurons. HEK293 cells were co-transfected before co-plating with HA-NL1, stargazin, PSD-95 and either the GluA1 subunit (top trace) or the GluA2 subunit (bottom trace). (**B**) Excitatory miniature synaptic transmission recorded from a pyramidal neuron in the presence of TTX. Scale bars: 10 pA, 200ms.

Figure 4.3

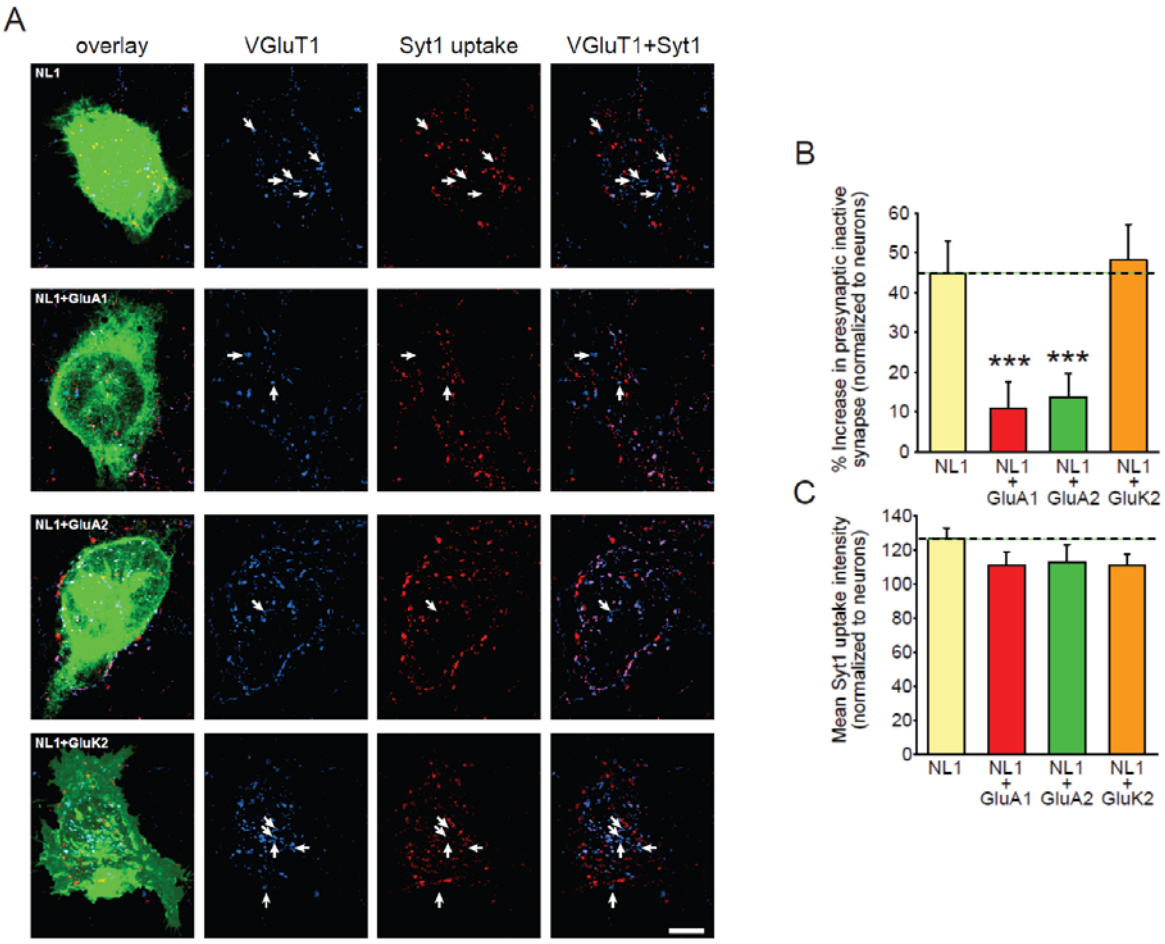
A
overlay
VGluT1
Syt1 uptake
VGluT1+Syt1
NL1
NL1+GluA1
NL1+GluA2
NL1+GluK2
B
% Increase in presynaptic inactive synapse (normalized to neurons)
60
50
40
30
20
10
0
***
***
NL1
NL1 + GluA1
NL1 + GluA2
NL1 + GluK2
C
Mean Syt1 uptake intensity (normalized to neurons)
140
120
100
80
60
40
20
0
NL1
NL1 + GluA1
NL1 + GluA2
NL1 + GluK2

Figure 4.3: Postsynaptic AMPARs at heterologous synapses promote glutamate release at a subset of presynaptic terminals. (**A**) Images of heterologous synapse formation between HEK293 cells and neurons. HEK293 cells were transfected with NL1 alone, or NL1 with either a GFP-tagged AMPAR subunit, GluA1 or GluA2, or a GFP-tagged kainate receptor subunit, GluK2, and co-plated with hippocampal neurons. Glutamatergic presynaptic terminals were identified by VGluT1 puncta (blue). Synaptic vesicle cycling at each terminal was measured by the uptake of an antibody directed against the luminal domain of Syt1 (red). Functionally inactive presynaptic terminals were identified as VGluT1 puncta that lack co-localizing Syt1 immunofluozrescence (arrows). Scale bar, 10 μm. (**B**) Quantification of functionally inactive presyanptic terminals. The fraction of all glutamatergic terminals on each HEK293 cell that were inactive was calculated and normalized to the fraction of inactive presynaptic terminals at neighboring neuronal synapses (n = 24-27 cells; ***, $p < 0.005$). (**C**) Quantification of mean Syt1 uptake intensity at heterologous synapses (value normalized to the mean intensity of Syt1 uptake at neighboring neuronal synapses; n = 24-27 cells/group; $p > 0.05$).

Figure 4.4

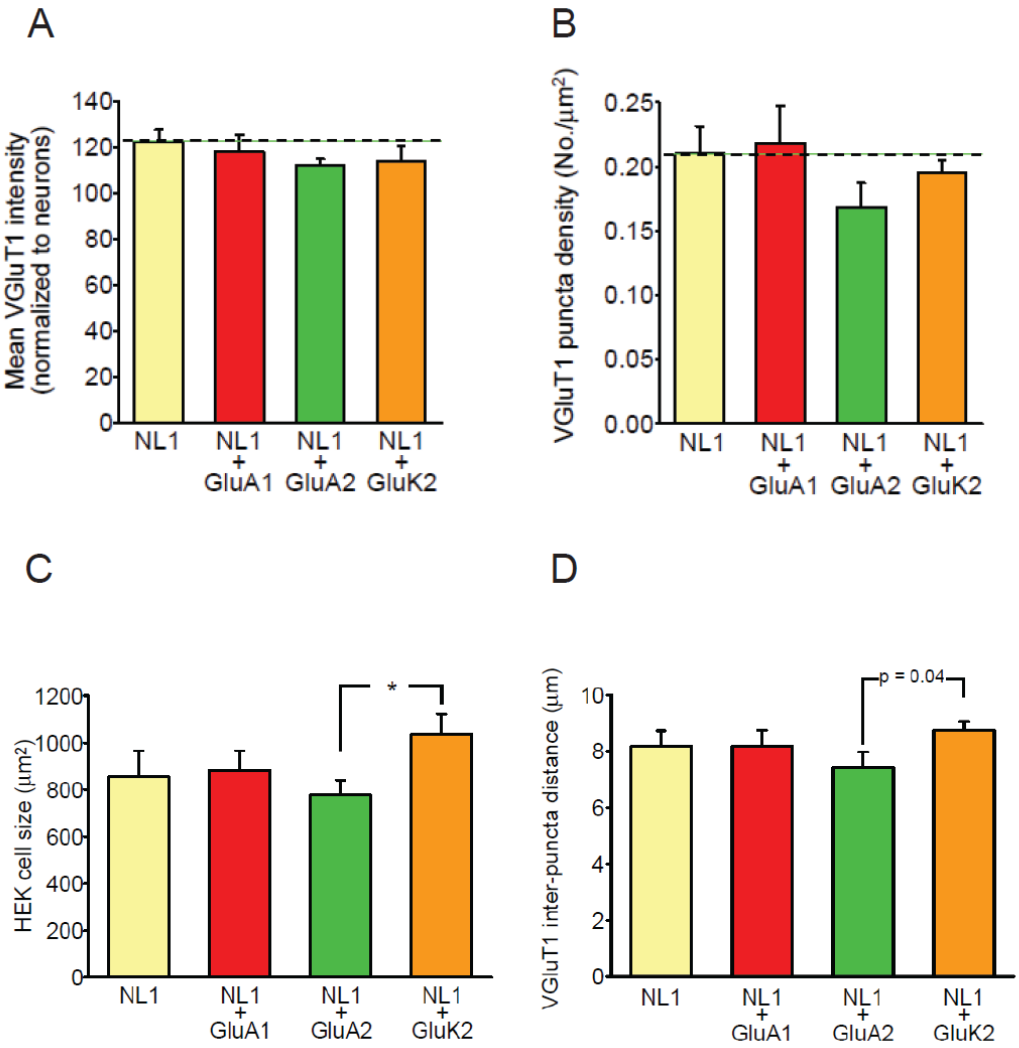

Figure 4.4: HEK293 cell size and the density of synaptic contacts is unaffected by the expression of AMPARs. (**A**) Mean puncta intensity of VGluT1 at heterologous synapses (value normalized to the VGluT1 intensity at neighboring neuronal synapses, n = 24-27 cells/group; $p > 0.05$). (**B**) Density of glutamatergic synaptic contacts made onto HEK293 cells (n = 24-27 cells/group; $p > 0.1$). (**C**) The average size of HEK293 cells from co-culture experiments was estimated by calculating the total area of green fluorescence which delineates the morphology of each cell (n = 24-27 cells/group; $p > 0.15$; *, $p = 0.016$). (**D**) The average distance between glutamatergic synapses on HEK293 cells (n = 24-27 cells/group, $p > 0.3$; *, $p = 0.04$).

Figure 4.5

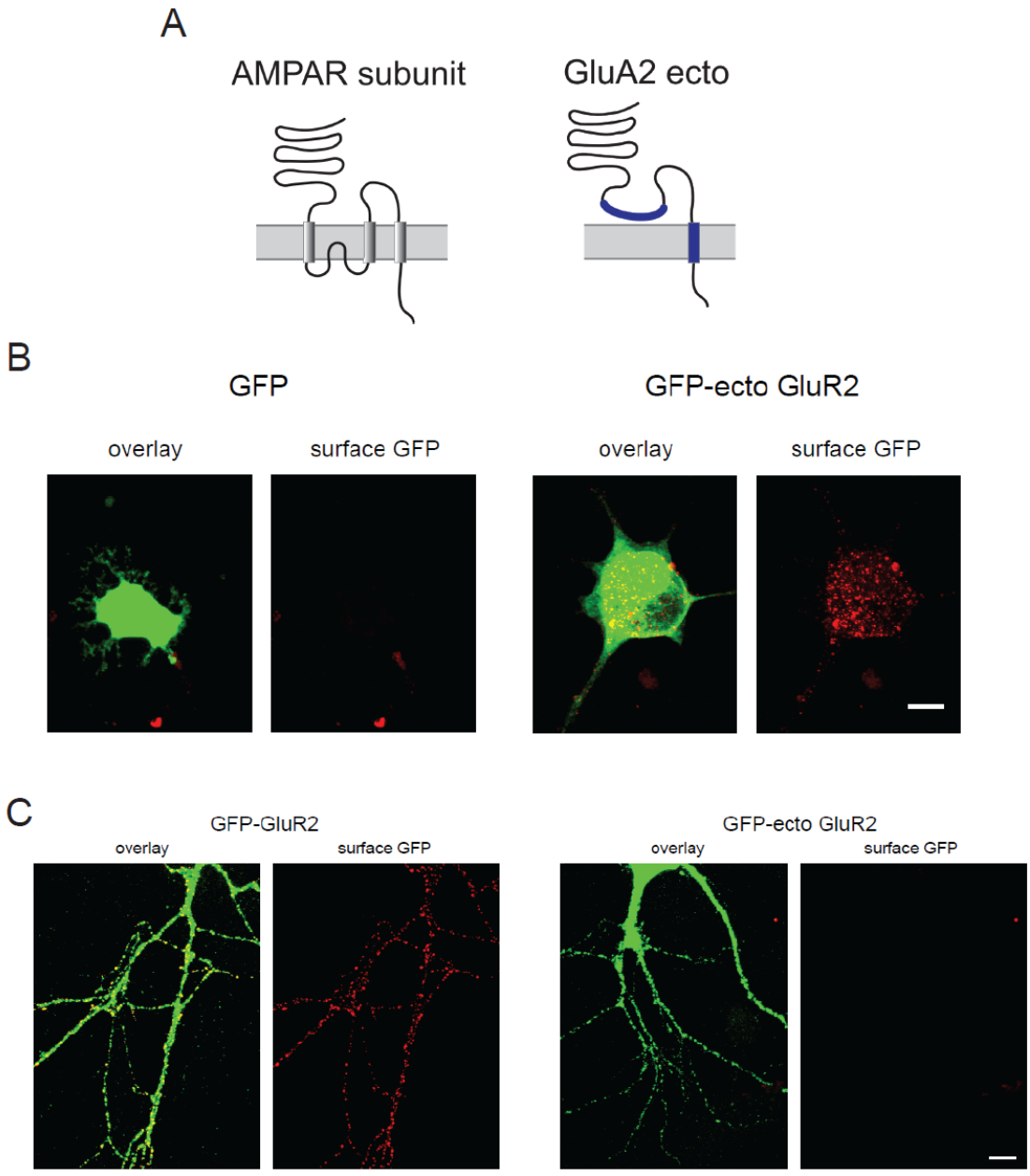
A
AMPAR subunit
GluA2 ecto
B
GFP
GFP-ecto GluR2
overlay
surface GFP
overlay
surface GFP
C
GFP-GluR2
overlay
surface GFP
GFP-ecto GluR2
overlay
surface GFP

Figure 4.5: Validation of chimeric AMPAR expression as a tool to investigate the role of AMPAR channel activity in synapse maturation. (**A**) Schematic showing the strategy used to construct the GluA2 ecto chimera. The endogenous GluA2 subunit (*left*) has three transmembrane domains and a fourth membrane domain that forms the pore of the ion channel. For the GluA2 ecto construct (*right*), all three transmembrane domains were removed along with the channel forming membrane domain. The extracellular ligand binding domains of GluA2 were fused together with a flexible linker region. Then the ectodomain including the GluA2 N-terminal domain and the ligand binding domains were fused to the transmembrane segment from the interleukin-2 receptor (Tac). Finally, the GluA1 C-terminal domain was added. Dr. Christine Nam designed and made this construct and first characterized its expression. (**B**) HEK293 cells expressing GFP alone or GFP-GluA2ecto, which is GFP-tagged on the extracellular domain. The incubation of live cells with media containing a GFP antibody only immunolabeled GFP-GluA2ecto expressed on the cell surface (red). Scale bar, 10 µm. (**C**) Hippocampal neurons expressing GFP-GluA2 or GFP-GluA2 ecto both GFP-tagged on the extracellular domain. The incubation of live cells with media containing a GFP antibody only immunolabeled GFP-GluA2 expressed on the cell surface (red). Although GFP-GluA2ecto was indeed expressed by neurons the lack of surface immunostaining of GFP suggests that this construct is not trafficked properly in neurons. Scale bar, 10 µm.

Figure 4.6

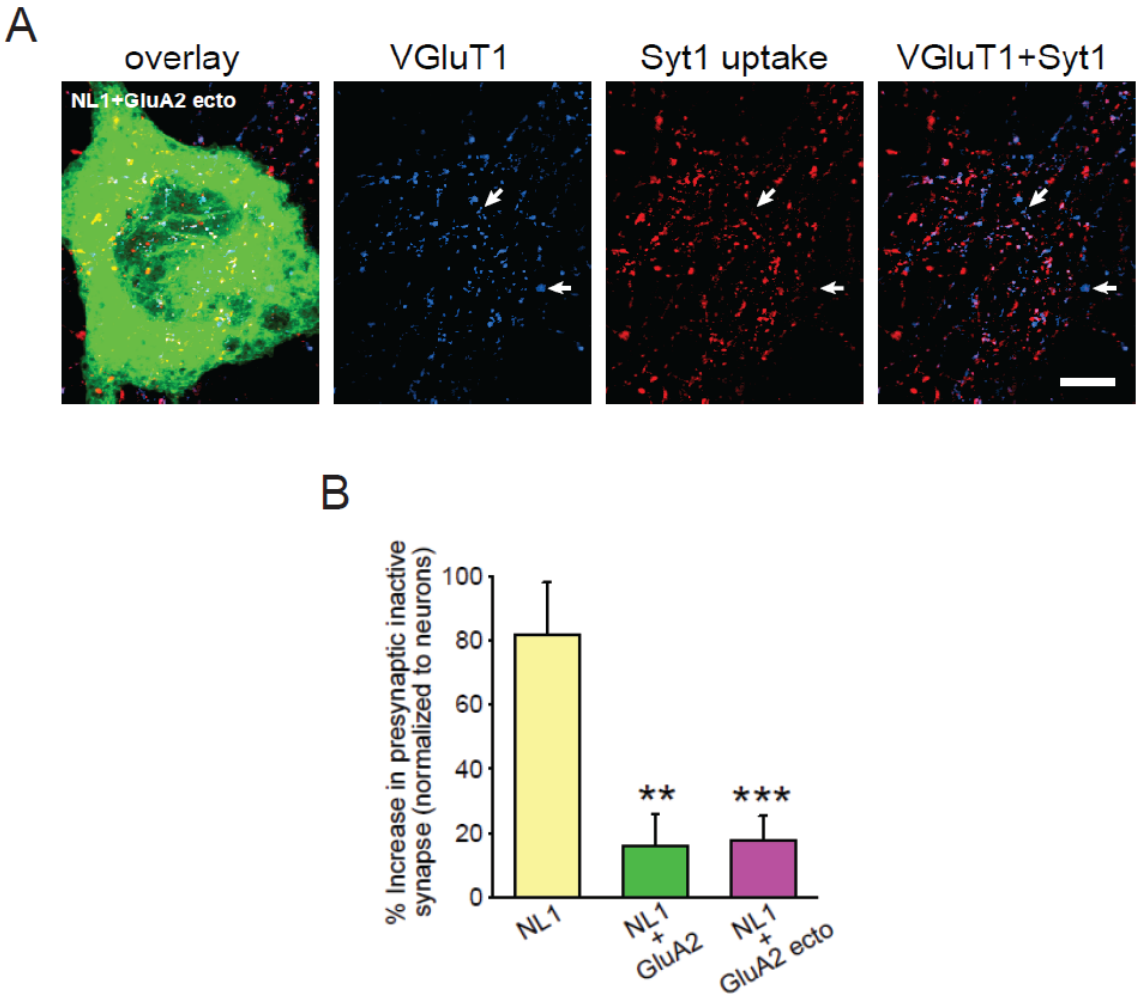

Figure 4.6: Postsynaptic AMPARs participate directly in trans-synaptic retrograde signaling to influence glutamate release at a subset of presynaptic terminals. (**A**) Image of heterologous synapse formation on a HEK293 cell co-expressing NL1 and GluA2 ecto. Arrows indicate functionally inactive presynaptic terminals. Scale bar, 10 µm. (**B**) Quantification of functionally inactive presynaptic terminals formed on HEK293 cells expressing NL1 alone, NL1+GluA2, or NL1+GluA2 ecto (n = 27-31; **, $p < 0.005$; ***, $p < 0.001$).

Chapter 5

Materials and Methods

DNA constructs

Each GluA-shRNA sequence was inserted into pSuper-Retro-GFP (Oligogene) according to the manufacturer's protocol. The GluA1 shRNA targeted nucleotides 2276-2294 in the flop isoform of rat GluA1. The sense sequence was 5'cagtaaacctggcagtgtt3' and the antisense sequence was 5'aacactgccaggtttactg3'. The GluA2 shRNA targeted nucleotides 400-418 of rat GluA2 and was previously used by Passafaro et al. (2003) and Saglietti et al. (2007). The sense sequence was 5'ggagcactccttagcttga3'and the antisense sequence was 5'tcaagctaaggagtgctcc3'. The GluA3 shRNA targets nucleotides 1280-1298 of rat GluA3. The sense sequence was 5'caccatatgtgatgtataa3' and the antisense sequence was 5'ttatacatcacatatggtg3'. To generate the GluA1 rescue construct, a silent point mutation (N761) was introduced to a GFP-GluA1 construct using PCR mutagenesis. The same method was used for the GluA2 rescue construct (L136). GFP-GluA1, GFP-GluA2 and GFP-GluK2 constructs were in pCI-Neo (Promega). HA tagged NL1 was in pNice.

Cell cultures and transfection

Primary hippocampal cultures were prepared from embryonic day 22 rat brains and plated at a density of 100 x 10^3 cells/ml for electrophysiology and 50 x 10^3 cells/ml for immunostaining. The neuronal cultures were maintained in serum-free Neurobasal media with B27-supplement (Life Technologies) and Glutamax (Invitrogen, Grand Island, NY). Neurons were transfected using calcium phosphate at 5-7 DIV. DNA constructs were allowed to express for 5 days before the cultures were used for experiments. HEK293 cells maintained in DMEM (GIBCO) with 10% FBS were transfected using calcium phosphate. After one day of expression, the cells were gently resuspended in neurobasal media and plated at low density onto hippocampal neurons at 9 DIV. Three days later, the co-cultures were used for immunocytochemistry.

Antibodies

The following mouse monoclonal antibodies were used: Syt1 (1:100; Synaptic Systems), GFP (1:500; Millipore), GluN1 (1:200; BD Pharmingen), PSD-95 (1:200; Affinity Bioreagents). The following polyclonal antibodies were used: rabbit anti-GFP (WB, 1:10,000; ICC, 1:800; Abcam), guinea pig anti-VGluT1 (1:500; Millipore), rabbit anit-GluA2/3 (1:200; Millipore), rabbit anti-GluA1C (1:500; Millipore), rabbit anti-HA (1:1000; Abcam).

Immunocytochemistry

Coverslips were fixed in 4% PFA then incubated in blocking solution containing 0.3% Triton X-100 and 2% NGS. The primary antibodies were added to the cells followed by flourophore conjugated secondary antibodies. For the Syt1 antibody uptake assay, live cells were incubated with the Syt1 antibody in neurobasal media for 20-30 minutes, then washed thoroughly and fixed. For immunostaining of the GluN1 subunit, the neurons were fixed in methanol for 10 min at -20^{o}C following the fixation in 4% PFA.

Image acquisition and quantification

For fluorescent image analysis, cells were chosen randomly from three or more cover slips per group. Fluorescent images were acquired with an Olympus (Tokyo, Japan) FV1000 BX61WI laser-scanning confocal microscope, using an Olympus Plan Apochromat 60x oil objective [numerical aperture (NA), 1.42; working distance (WD), 0.15] or an Olympus U-Plan Apochromat 100x oil objective (NA, 1.40; WD, 0.12) with sequential acquisition setting at 1024 x 1024 pixel resolutions. Laser power and photomultipliers were set such that no detectable bleedthrough occurred between different channels. Digital images of the cells were captured with Fluoview Imaging software (Olympus). Eight to 10 sections were taken from top to bottom of the specimen, and brightest point projections were made. Images for the same experiments were taken using identical settings for laser power, photomultiplier gain, and offset. These settings were chosen such that the pixel intensities for the brightest samples were just below saturation, with the exception that when contours of the cell or contours of the neuronal processes had to be clearly determined, signals from certain areas (center of the HEK cell body or soma of the neurons) were saturated to obtain clear signals from the periphery of the cell body or neuronal dendrites. For the analysis of synaptic proteins, images from the same experiment were thresholded identically by intensity to exclude the diffuse/intracellular pool. To reduce the effect of background staining on synaptic co-localization analysis, VGlut1 puncta smaller than 0.4 μm^2 were excluded from analysis. Image quantification was performed by experienced investigators who were blind to the experimental conditions.

Electrophysiological recordings of mEPSCs

Whole-cell patch-clamp recordings were made at room temperature with 3-7 MΩ patch pipettes filled with an internal solution containing (in mM) 140 CsCl, 2 $MgCl_2$, 5 EGTA, 10 HEPES, 0.3 Na_3-GTP, 4 Na_2-ATP, Ph = 7.35. Cultures were continuously superfused with external solution (in mM, 119 NaCl, 26 $NaHCO_3$, 2.5 KCl, 10 glucose, 2.5 $CaCl_2$, 1.3 $MgSO_4$, 1 NaH_2PO_4). Recordings of mEPSCs were done in the presence of tetrodotoxin (1 µM) and picrotoxin (100 µM). Sucrose (0.2 M) was locally applied during the recording to increase the frequency of mEPSCs. Miniature responses were analyzed with the Mini Analysis Program from Synaptosoft.

Electrophysiological recordings of eEPSCs

The recording method for evoked synaptic response using extracellular stimulation in dissociated cultures was adopted from Maximov et al. (2007). AMPAR-mediated eEPSCs were recorded in external solution containing picrotoxin (100 µM). NMDAR-mediated eEPSCs were recorded in external solution containing CNQX (10 µM), picrotoxin (100 µM), and glycine (20 µM) but lacking Mg^{2+}. QX-314 (10 mM) was added to the internal solution used in recordings of all eEPSCs. Cells were held at -60 mV. Local extracellular field stimulation was applied using a concentric bipolar electrode (FHC; Cat#CBAEC75) placed 50 µm from the cell soma. A current injection of 6 mA with 1 ms duration was sufficient to evoke reliable postsynaptic currents, and the stimulus was kept constant during each experiment. The stimulus was controlled by the Model 2100 Isolated Pulse Stimulator (A-M Systems, Inc.). Recordings of NMDAR eEPSCs with MK-801 (10 µM) were done at a +40mV holding potential in external solution containing CNQX (10 µM), picrotoxin (100 µM), and glycine (20 µM).

Electrophysiological recordings of agonist-evoked and sucrose-evoked glutamate receptor currents

Whole-cell AMPAR currents and currents from somatic outside-out patches were recorded in external solution containing picrotoxin (100 µM) and tetrodotoxin (1 µM). AMPAR currents were evoked with a local 3-second application of AMPA (100 µM) with cyclothiazide (100 µM). A local 3 second application of NMDA (1 mM) was used to evoke whole-cell NMDAR currents. To estimate the size of the readily releasable pool of vesicles, a hypertonic solution of sucrose (0.5 M) was locally applied to each neuron for 3 seconds. The NMDA- and sucrose-evoked responses were recorded at -60mV in the presence of CNQX (10 µM), picrotoxin (100 µM), and glycine (20 µM) but lacking Mg^{2+}. The internal solution for NMDA- and sucrose-evoked recordings contained QX-314 (10 mM).

Chapter 6

Conclusions

A novel role for AMPARs in synapse maturation

In this study, we describe an unexpected finding: RNAi-mediated knockdown of postsynaptic AMPAR expression in young neurons not only decreased AMPAR-mediated synaptic currents, but also caused a dramatic, corresponding decrease in NMDAR-mediated currents. This overall weakening of synaptic transmission was accompanied by a reduction in the total pool of presynaptic vesicles available for release among synapses, as defined by the synaptic response to hypertonic sucrose. In a second set of experiments that makes use of the heterologous synapse formation assay, we showed that postsynaptic AMPARs reduce the number of functionally inactive presynaptic terminals via a mechanism that does not require glutamate-activated postsynaptic currents, but is fully mediated by an AMPAR ectodomain. Based on these key observations, supported by ancillary control experiments that validated the specificity of these results, we propose that AMPARs contribute to functional synapse maturation, and that they operate, at least in part, by mediating a retrograde trans-synaptic signal carried out by an interaction between the postsynaptic AMPAR ectodomain and an unknown presynaptic component.

Glutamatergic synapse maturation is marked by discrete events occurring both at pre- and post-synaptic sites; the process entails the organization of the presynaptic active zone, the accumulation of postsynaptic scaffold proteins and receptors, the upregulation of synaptic vesicle cycling, and finally the modification of vesicle release efficacy and postsynaptic sensitivity to glutamate (Ziv & Garner, 2001). Changes in the probability of vesicle release at presynaptic terminals have been documented throughout development at different synapses in the CNS (Bolshakov & Siegelbaum, 1995; Choi & Lovinger, 1997; Iwasaki & Takahashi, 2001; Mori-Kawakami et al, 2003). In our study, however, modulation of presynaptic release probability does not seem to be the step regulated by postsynaptic AMPAR insertion, as we failed to detect a difference in synaptic release probability following AMPAR knockdown. In addition to the calcium-dependency of vesicle release, presynaptic function is also dependent on the number of recycling vesicles at the terminal, including both vesicles capable of immediate exocytosis from the RRP upon excitation and vesicles in the reserve pool, which can be recruited for release only after prolonged stimulation (Sudhof, 2000). Indeed, immature presynaptic terminals that lack an RRP have been reported at newly formed synapses in dissociated hippocampal cultures (Mozhayeva et al, 2002). Thus, our results indicate that developmental restructuring of vesicle pools in presynaptic terminals may be triggered by the insertion of postsynaptic AMPARs, which then trans-synaptically activate presynaptic RRP formation. Previous studies have established the postsynaptic silent synapse as an immature stage in synapse development (Gomperts et al, 1998; Petralia et al, 1999; Pickard et al, 2000). We have shown here that additional presynaptic functional maturation can proceed after postsynaptic silent synapses are switched on.

Influence of AMPARs on functional synapse development

Previous attempts to understand how AMPARs influence synaptic function in the hippocampus entailed the use of knockout mice deficient in either the GluA1 subunit (Zamanillo et al, 1999), the GluA2 subunit (Jia et al, 1996), or both the GluA2 and GluA3 subunits (Meng et al, 2003). Importantly, these studies provided insight into AMPAR subunit-specific effects on synaptic strength, but no changes in synapse maturation were identified. In our study, we observed that simultaneous knockdown of all three AMPAR subunits impairs presynaptic function, and show that either GluA1 or GluA2 expression is sufficient to restore presynaptic function, suggesting that the effect of AMPARs on synapse maturation is not subunit-specific. Compensation by remaining AMPARs in the subunit-specific knockouts could explain why there is no apparent impairment in synapse maturation. In another study, RNAi was used to acutely knockdown GluA2 expression in hippocampal neurons, demonstrating a specific role for this subunit in promoting spine formation (Passafaro et al, 2003; Saglietti et al, 2007). By contrast, we did not observe a change in spine density on pyramidal neurons expressing all three GluA-shRNA during a stage of rapid synaptogenesis. GluA2 may be primarily required for spine stabilization and maintenance after synapse maturation is established, which occurs at a later stage in the lifetime of a synapse that was not addressed in our study.

More recently, a conditional knockout of the GluA1, GluA2, and GluA3 subunits was generated, which resulted in a virtually complete loss of postsynaptic AMPAR-mediated responses recorded from Schaffer collateral synapses in the hippocampus (Lu et al, 2009). This study found no change in NMDAR eEPSCs following the conditional knockout of AMPARs. At present, we have no ready explanation for the discrepancy between our results and those of Lu et al. (2009), although it should be noted that our experiments were performed in very different systems. Specifically, although it seems unlikely that Lu et al. (2009) would not have detected a change in postsynaptic NMDARs, their analysis may not be sensitive enough to detect the observed effect of AMPAR deficiency on presynaptic vesicle release. A decrease in the RRP among a large population of synapses may only be observable if the total pool size is directly tested, which was not done by Lu et al. (2009). Moreover, homeostatic compensation after prolonged loss of AMPARs (up to 3 weeks in the Lu et al., 2009 study) could further mask the direct effect of AMPAR removal observed five days after shRNA-mediated acute knockdown. A fundamental difference in experimental approach could thus underlie this discrepancy in results following the loss of postsynaptic AMPARs.

Mechanism underlying functionally inactive presynaptic terminals

The synaptic phenotype we observe upon AMPAR knockdown consists of a decrease in both AMPAR- and NMDAR-mediated synaptic responses, without a change in postsynaptic NMDAR expression, or in presynaptic release probability. Importantly, the significant decrease in hypertonic sucrose-evoked currents signified a loss of synaptic vesicles from the RRP. The synaptic phenotype is most consistent with the

notion that a subset of synapses lacks a functional presynaptic RRP, as opposed to a gradual decrease of the RRP in all synapses. This is because the size of the RRP influences the synaptic release probability (Dobrunz & Stevens, 1997), which was unchanged in our experiments. Although we do not know how precisely postsynaptic AMPARs influence the presynaptic RRP, e.g. what its presynaptic molecular interaction partners may be, we feel that our results are compelling in delineating this pathway.

Previous studies have implicated several presynaptic candidates that mediate the availability of releasable vesicles at a synapse (referred to as priming factors). These include Munc13-1 and its homologs (Augustin et al, 1999); RIM proteins (Schoch et al., 2002), and SNARE- and SM-proteins (reviewed in (Rizo & Rosenmund, 2008). Interestingly, loss of bassoon, a scaffolding protein in the active zone, at synapses on autaptic neurons only causes a subset of glutamatergic terminals to become functionally inactive (Altrock et al, 2003). Similar to our results from AMPAR knockdown, neurons of the bassoon mutant had a specific deficit in releasable vesicles which underlies the increased prevalence of inactive terminals (Altrock et al, 2003).

Our evaluation of presynaptic function at heterologous synapses revealed that HEK293 cells expressing NL1 alone had more inactive glutamatergic terminals but simultaneously maintained terminals with active vesicle release akin to neighboring neuronal synapses. This suggests that AMPARs are only required for the functional maturation of a subset of presynaptic terminals. Why do postsynaptic AMPARs influence presynaptic function at only a distinct population of synapses? For now, the reason for this disparate effect on synapses remains unclear. At excitatory synapses, significant heterogeneity exists in presynaptic morphology (Schikorski & Stevens, 1997), properties of vesicle release (Hessler et al, 1993; Moulder et al, 2007; Murthy et al, 1997; Rosenmund et al, 1993) and molecular composition (Altrock et al, 2003; Atwood & Karunanithi, 2002; Reid et al, 1997; Rosenmund et al, 2002). Accordingly, it is conceivable that a subset of presynaptic terminals, perhaps with distinct molecular composition, is more susceptible to remain at an immature developmental stage in the absence of postsynaptic AMPARs. A thorough investigation of the molecular and/or structural identity of immature presynaptic terminals may elucidate the selective effect of AMPARs on synapse maturation.

Implications for trans-synaptic signaling by postsynaptic AMPARs

Activity-dependent signaling by BDNF has been reported to rapidly unsilence immature glutamatergic terminals of hippocampal neurons (Cabezas & Buno; Shen et al, 2006). Accordingly, AMPAR-mediated postsynaptic activity could induce release of a retrograde messenger required for presynaptic maturation. However, prolonged CNQX treatment during the rescue of synaptic transmission following AMPAR knockdown showed that postsynaptic excitation by AMPARs was not required for the functional maturation of presynaptic terminals. Instead, additional experiments using heterologous synapses revealed that the ectodomain of the AMPARs was sufficient for promoting vesicle release at glutamatergic terminals. This finding implies that AMPARs

signal trans-synaptically by binding directly to a yet unknown presynaptic protein to enhance synapse maturation. To date only a few proteins have been identified that interact with AMPARs extracellularly, including both Narp and NP1 from the neuronal pentraxin family (O'Brien et al, 2002; Sia et al, 2007; Xu et al, 2003). A trans-synaptic interaction between N-cadherin and AMPARs has been found; however, this interaction appears to be specific to the GluA2 subunit (Saglietti et al, 2007). Ongoing work to elucidate the complexity of signaling events during synapse development may provide insight regarding the AMPAR trans-synaptic binding partner that mediates presynaptic terminal maturation.

References

Ahmari SE, Buchanan J, Smith SJ (2000) Assembly of presynaptic active zones from cytoplasmic transport packets. *Nat Neurosci* 3(5): 445-451

Altrock WD, tom Dieck S, Sokolov M, Meyer AC, Sigler A, Brakebusch C, Fassler R, Richter K, Boeckers TM, Potschka H, Brandt C, Loscher W, Grimberg D, Dresbach T, Hempelmann A, Hassan H, Balschun D, Frey JU, Brandstatter JH, Garner CC, Rosenmund C, Gundelfinger ED (2003) Functional inactivation of a fraction of excitatory synapses in mice deficient for the active zone protein bassoon. *Neuron* 37(5): 787-800

Aoto J, Ting P, Maghsoodi B, Xu N, Henkemeyer M, Chen L (2007) Postsynaptic ephrinB3 promotes shaft glutamatergic synapse formation. *J Neurosci* 27(28): 7508-7519

Atwood HL, Karunanithi S (2002) Diversification of synaptic strength: presynaptic elements. *Nat Rev Neurosci* 3(7): 497-516

Augustin I, Rosenmund C, Sudhof TC, Brose N (1999) Munc13-1 is essential for fusion competence of glutamatergic synaptic vesicles. *Nature* 400(6743): 457-461

Baron MK, Boeckers TM, Vaida B, Faham S, Gingery M, Sawaya MR, Salyer D, Gundelfinger ED, Bowie JU (2006) An architectural framework that may lie at the core of the postsynaptic density. *Science* 311(5760): 531-535

Betz A, Thakur P, Junge HJ, Ashery U, Rhee JS, Scheuss V, Rosenmund C, Rettig J, Brose N (2001) Functional interaction of the active zone proteins Munc13-1 and RIM1 in synaptic vesicle priming. *Neuron* 30(1): 183-196

Biederer T (2005) Progress from the postsynaptic side: signaling in synaptic differentiation. *Sci STKE* 2005(274): pe9

Biederer T, Sara Y, Mozhayeva M, Atasoy D, Liu X, Kavalali ET, Sudhof TC (2002) SynCAM, a synaptic adhesion molecule that drives synapse assembly. *Science* 297(5586): 1525-1531

Biederer T, Sudhof TC (2000) Mints as adaptors. Direct binding to neurexins and recruitment of munc18. *J Biol Chem* 275(51): 39803-39806

Bolshakov VY, Siegelbaum SA (1995) Regulation of hippocampal transmitter release during development and long-term potentiation. *Science* 269(5231): 1730-1734

Bredt DS, Nicoll RA (2003) AMPA receptor trafficking at excitatory synapses. *Neuron* 40(2): 361-379

Bresler T, Ramati Y, Zamorano PL, Zhai R, Garner CC, Ziv NE (2001) The dynamics of SAP90/PSD-95 recruitment to new synaptic junctions. *Mol Cell Neurosci* 18(2): 149-167

Butz S, Okamoto M, Sudhof TC (1998) A tripartite protein complex with the potential to couple synaptic vesicle exocytosis to cell adhesion in brain. *Cell* 94(6): 773-782

Cabezas C, Buno W BDNF is required for the induction of a presynaptic component of the functional conversion of silent synapses. *Hippocampus*

Cai C, Li H, Rivera C, Keinanen K (2006) Interaction between SAP97 and PSD-95, two Maguk proteins involved in synaptic trafficking of AMPA receptors. *J Biol Chem* 281(7): 4267-4273

Carrel D, Du Y, Komlos D, Hadzimichalis NM, Kwon M, Wang B, Brzustowicz LM, Firestein BL (2009) NOS1AP regulates dendrite patterning of hippocampal neurons through a carboxypeptidase E-mediated pathway. *J Neurosci* 29(25): 8248-8258

Chen H, Firestein BL (2007) RhoA regulates dendrite branching in hippocampal neurons by decreasing cypin protein levels. *J Neurosci* 27(31): 8378-8386

Chen L, Chetkovich DM, Petralia RS, Sweeney NT, Kawasaki Y, Wenthold RJ, Bredt DS, Nicoll RA (2000) Stargazin regulates synaptic targeting of AMPA receptors by two distinct mechanisms. *Nature* 408(6815): 936-943

Chih B, Engelman H, Scheiffele P (2005) Control of excitatory and inhibitory synapse formation by neuroligins. *Science* 307(5713): 1324-1328

Choi S, Klingauf J, Tsien RW (2000) Postfusional regulation of cleft glutamate concentration during LTP at 'silent synapses'. *Nat Neurosci* 3(4): 330-336

Choi S, Lovinger DM (1997) Decreased probability of neurotransmitter release underlies striatal long-term depression and postnatal development of corticostriatal synapses. *Proc Natl Acad Sci U S A* 94(6): 2665-2670

Coco S, Verderio C, De Camilli P, Matteoli M (1998) Calcium dependence of synaptic vesicle recycling before and after synaptogenesis. *J Neurochem* 71(5): 1987-1992

Craven SE, El-Husseini AE, Bredt DS (1999) Synaptic targeting of the postsynaptic density protein PSD-95 mediated by lipid and protein motifs. *Neuron* 22(3): 497-509

Dalva MB, McClelland AC, Kayser MS (2007) Cell adhesion molecules: signalling functions at the synapse. *Nat Rev Neurosci* 8(3): 206-220

Dalva MB, Takasu MA, Lin MZ, Shamah SM, Hu L, Gale NW, Greenberg ME (2000) EphB receptors interact with NMDA receptors and regulate excitatory synapse formation. *Cell* 103(6): 945-956

de Wit J, Sylwestrak E, O'Sullivan ML, Otto S, Tiglio K, Savas JN, Yates JR, 3rd, Comoletti D, Taylor P, Ghosh A (2009) LRRTM2 interacts with Neurexin1 and regulates excitatory synapse formation. *Neuron* 64(6): 799-806

Dean C, Scholl FG, Choih J, DeMaria S, Berger J, Isacoff E, Scheiffele P (2003) Neurexin mediates the assembly of presynaptic terminals. *Nat Neurosci* 6(7): 708-716

Dingledine R, Borges K, Bowie D, Traynelis SF (1999) The glutamate receptor ion channels. *Pharmacol Rev* 51(1): 7-61

Dobrunz LE, Stevens CF (1997) Heterogeneity of release probability, facilitation, and depletion at central synapses. *Neuron* 18(6): 995-1008

Dresbach T, Torres V, Wittenmayer N, Altrock WD, Zamorano P, Zuschratter W, Nawrotzki R, Ziv NE, Garner CC, Gundelfinger ED (2006) Assembly of active zone precursor vesicles: obligatory trafficking of presynaptic cytomatrix proteins Bassoon and Piccolo via a trans-Golgi compartment. *J Biol Chem* 281(9): 6038-6047

Dulubova I, Lou X, Lu J, Huryeva I, Alam A, Schneggenburger R, Sudhof TC, Rizo J (2005) A Munc13/RIM/Rab3 tripartite complex: from priming to plasticity? *EMBO J* 24(16): 2839-2850

Durand GM, Kovalchuk Y, Konnerth A (1996) Long-term potentiation and functional synapse induction in developing hippocampus. *Nature* 381(6577): 71-75

El-Husseini AE, Schnell E, Chetkovich DM, Nicoll RA, Bredt DS (2000) PSD-95 involvement in maturation of excitatory synapses. *Science* 290(5495): 1364-1368

El-Husseini Ael D, Schnell E, Dakoji S, Sweeney N, Zhou Q, Prange O, Gauthier-Campbell C, Aguilera-Moreno A, Nicoll RA, Bredt DS (2002) Synaptic strength regulated by palmitate cycling on PSD-95. *Cell* 108(6): 849-863

Eroglu C, Allen NJ, Susman MW, O'Rourke NA, Park CY, Ozkan E, Chakraborty C, Mulinyawe SB, Annis DS, Huberman AD, Green EM, Lawler J, Dolmetsch R, Garcia KC, Smith SJ, Luo ZD, Rosenthal A, Mosher DF, Barres BA (2009) Gabapentin receptor alpha2delta-1 is a neuronal thrombospondin receptor responsible for excitatory CNS synaptogenesis. *Cell* 139(2): 380-392

Erreger K, Dravid SM, Banke TG, Wyllie DJ, Traynelis SF (2005) Subunit-specific gating controls rat NR1/NR2A and NR1/NR2B NMDA channel kinetics and synaptic signalling profiles. *J Physiol* 563(Pt 2): 345-358

Ethell IM, Irie F, Kalo MS, Couchman JR, Pasquale EB, Yamaguchi Y (2001) EphB/syndecan-2 signaling in dendritic spine morphogenesis. *Neuron* 31(6): 1001-1013

Feil R, Kleppisch T (2008) NO/cGMP-dependent modulation of synaptic transmission. *Handb Exp Pharmacol*(184): 529-560

Fernandez-Chacon R, Konigstorfer A, Gerber SH, Garcia J, Matos MF, Stevens CF, Brose N, Rizo J, Rosenmund C, Sudhof TC (2001) Synaptotagmin I functions as a calcium regulator of release probability. *Nature* 410(6824): 41-49

Flint AC, Maisch US, Weishaupt JH, Kriegstein AR, Monyer H (1997) NR2A subunit expression shortens NMDA receptor synaptic currents in developing neocortex. *J Neurosci* 17(7): 2469-2476

Fogel AI, Akins MR, Krupp AJ, Stagi M, Stein V, Biederer T (2007) SynCAMs organize synapses through heterophilic adhesion. *J Neurosci* 27(46): 12516-12530

Friedman HV, Bresler T, Garner CC, Ziv NE (2000) Assembly of new individual excitatory synapses: time course and temporal order of synaptic molecule recruitment. *Neuron* 27(1): 57-69

Fu Z, Washbourne P, Ortinski P, Vicini S (2003) Functional excitatory synapses in HEK293 cells expressing neuroligin and glutamate receptors. *J Neurophysiol* 90(6): 3950-3957

Gasparini S, Saviane C, Voronin LL, Cherubini E (2000) Silent synapses in the developing hippocampus: lack of functional AMPA receptors or low probability of glutamate release? *Proc Natl Acad Sci U S A* 97(17): 9741-9746

Gomperts SN, Carroll R, Malenka RC, Nicoll RA (2000) Distinct roles for ionotropic and metabotropic glutamate receptors in the maturation of excitatory synapses. *J Neurosci* 20(6): 2229-2237

Gomperts SN, Rao A, Craig AM, Malenka RC, Nicoll RA (1998) Postsynaptically silent synapses in single neuron cultures. *Neuron* 21(6): 1443-1451

Grabrucker A, Vaida B, Bockmann J, Boeckers TM (2009) Synaptogenesis of hippocampal neurons in primary cell culture. *Cell Tissue Res* 338(3): 333-341

Graf ER, Zhang X, Jin SX, Linhoff MW, Craig AM (2004) Neurexins induce differentiation of GABA and glutamate postsynaptic specializations via neuroligins. *Cell* 119(7): 1013-1026

Guan R, Dai H, Rizo J (2008) Binding of the Munc13-1 MUN domain to membrane-anchored SNARE complexes. *Biochemistry* 47(6): 1474-1481

Harms KJ, Craig AM (2005) Synapse composition and organization following chronic activity blockade in cultured hippocampal neurons. *J Comp Neurol* 490(1): 72-84

Hata Y, Butz S, Sudhof TC (1996) CASK: a novel dlg/PSD95 homolog with an N-terminal calmodulin-dependent protein kinase domain identified by interaction with neurexins. *J Neurosci* 16(8): 2488-2494

Hata Y, Slaughter CA, Sudhof TC (1993) Synaptic vesicle fusion complex contains unc-18 homologue bound to syntaxin. *Nature* 366(6453): 347-351

Henkemeyer M, Itkis OS, Ngo M, Hickmott PW, Ethell IM (2003) Multiple EphB receptor tyrosine kinases shape dendritic spines in the hippocampus. *J Cell Biol* 163(6): 1313-1326

Hessler NA, Shirke AM, Malinow R (1993) The probability of transmitter release at a mammalian central synapse. *Nature* 366(6455): 569-572

Hestrin S (1992) Developmental regulation of NMDA receptor-mediated synaptic currents at a central synapse. *Nature* 357(6380): 686-689

Isaac JT, Nicoll RA, Malenka RC (1995) Evidence for silent synapses: implications for the expression of LTP. *Neuron* 15(2): 427-434

Iwasaki S, Takahashi T (2001) Developmental regulation of transmitter release at the calyx of Held in rat auditory brainstem. *J Physiol* 534(Pt 3): 861-871

Jia Z, Agopyan N, Miu P, Xiong Z, Henderson J, Gerlai R, Taverna FA, Velumian A, MacDonald J, Carlen P, Abramow-Newerly W, Roder J (1996) Enhanced LTP in mice deficient in the AMPA receptor GluR2. *Neuron* 17(5): 945-956

Jin Y, Garner CC (2008) Molecular mechanisms of presynaptic differentiation. *Annu Rev Cell Dev Biol* 24: 237-262

Kalashnikova E, Lorca RA, Kaur I, Barisone GA, Li B, Ishimaru T, Trimmer JS, Mohapatra DP, Diaz E SynDIG1: an activity-regulated, AMPA- receptor-interacting transmembrane protein that regulates excitatory synapse development. *Neuron* 65(1): 80-93

Katz B, Miledi R (1968) The role of calcium in neuromuscular facilitation. *J Physiol* 195(2): 481-492

Kavalali ET (2007) Multiple vesicle recycling pathways in central synapses and their impact on neurotransmission. *J Physiol* 585(Pt 3): 669-679

Kayser MS, McClelland AC, Hughes EG, Dalva MB (2006) Intracellular and trans-synaptic regulation of glutamatergic synaptogenesis by EphB receptors. *J Neurosci* 26(47): 12152-12164

Kim E, Sheng M (2004) PDZ domain proteins of synapses. *Nat Rev Neurosci* 5(10): 771-781

Ko J, Fuccillo MV, Malenka RC, Sudhof TC (2009) LRRTM2 functions as a neurexin ligand in promoting excitatory synapse formation. *Neuron* 64(6): 791-798

Koushika SP, Richmond JE, Hadwiger G, Weimer RM, Jorgensen EM, Nonet ML (2001) A post-docking role for active zone protein Rim. *Nat Neurosci* 4(10): 997-1005

Kraszewski K, Mundigl O, Daniell L, Verderio C, Matteoli M, De Camilli P (1995) Synaptic vesicle dynamics in living cultured hippocampal neurons visualized with CY3-conjugated antibodies directed against the lumenal domain of synaptotagmin. *J Neurosci* 15(6): 4328-4342

Krueger SR, Kolar A, Fitzsimonds RM (2003) The presynaptic release apparatus is functional in the absence of dendritic contact and highly mobile within isolated axons. *Neuron* 40(5): 945-957

Kullmann DM, Asztely F (1998) Extrasynaptic glutamate spillover in the hippocampus: evidence and implications. *Trends Neurosci* 21(1): 8-14

Kullmann DM, Erdemli G, Asztely F (1996) LTP of AMPA and NMDA receptor-mediated signals: evidence for presynaptic expression and extrasynaptic glutamate spill-over. *Neuron* 17(3): 461-474

Lessmann V (1998) Neurotrophin-dependent modulation of glutamatergic synaptic transmission in the mammalian CNS. *Gen Pharmacol* 31(5): 667-674

Li B, Woo RS, Mei L, Malinow R (2007) The neuregulin-1 receptor erbB4 controls glutamatergic synapse maturation and plasticity. *Neuron* 54(4): 583-597

Liao D, Hessler NA, Malinow R (1995) Activation of postsynaptically silent synapses during pairing-induced LTP in CA1 region of hippocampal slice. *Nature* 375(6530): 400-404

Lu W, Shi Y, Jackson AC, Bjorgan K, During MJ, Sprengel R, Seeburg PH, Nicoll RA (2009) Subunit composition of synaptic AMPA receptors revealed by a single-cell genetic approach. *Neuron* 62(2): 254-268

Mah W, Ko J, Nam J, Han K, Chung WS, Kim E Selected SALM (synaptic adhesion-like molecule) family proteins regulate synapse formation. *J Neurosci* 30(16): 5559-5568

Malgaroli A, Ting AE, Wendland B, Bergamaschi A, Villa A, Tsien RW, Scheller RH (1995) Presynaptic component of long-term potentiation visualized at individual hippocampal synapses. *Science* 268(5217): 1624-1628

Matteoli M, Takei K, Perin MS, Sudhof TC, De Camilli P (1992) Exo-endocytotic recycling of synaptic vesicles in developing processes of cultured hippocampal neurons. *J Cell Biol* 117(4): 849-861

Matteoli M, Verderio C, Krawzeski K, Mundigl O, Coco S, Fumagalli G, De Camilli P (1995) Mechanisms of synaptogenesis in hippocampal neurons in primary culture. *J Physiol Paris* 89(1): 51-55

Maximov A, Pang ZP, Tervo DG, Sudhof TC (2007) Monitoring synaptic transmission in primary neuronal cultures using local extracellular stimulation. *J Neurosci Methods* 161(1): 75-87

Meng Y, Zhang Y, Jia Z (2003) Synaptic transmission and plasticity in the absence of AMPA glutamate receptor GluR2 and GluR3. *Neuron* 39(1): 163-176

Meyer G, Varoqueaux F, Neeb A, Oschlies M, Brose N (2004) The complexity of PDZ domain-mediated interactions at glutamatergic synapses: a case study on neuroligin. *Neuropharmacology* 47(5): 724-733

Monyer H, Burnashev N, Laurie DJ, Sakmann B, Seeburg PH (1994) Developmental and regional expression in the rat brain and functional properties of four NMDA receptors. *Neuron* 12(3): 529-540

Mori-Kawakami F, Kobayashi K, Takahashi T (2003) Developmental decrease in synaptic facilitation at the mouse hippocampal mossy fibre synapse. *J Physiol* 553(Pt 1): 37-48

Moulder KL, Jiang X, Taylor AA, Shin W, Gillis KD, Mennerick S (2007) Vesicle pool heterogeneity at hippocampal glutamate and GABA synapses. *J Neurosci* 27(37): 9846-9854

Mozhayeva MG, Sara Y, Liu X, Kavalali ET (2002) Development of vesicle pools during maturation of hippocampal synapses. *J Neurosci* 22(3): 654-665

Murthy VN, Sejnowski TJ, Stevens CF (1997) Heterogeneous release properties of visualized individual hippocampal synapses. *Neuron* 18(4): 599-612

Naisbitt S, Kim E, Tu JC, Xiao B, Sala C, Valtschanoff J, Weinberg RJ, Worley PF, Sheng M (1999) Shank, a novel family of postsynaptic density proteins that binds to the NMDA receptor/PSD-95/GKAP complex and cortactin. *Neuron* 23(3): 569-582

Nam CI, Chen L (2005) Postsynaptic assembly induced by neurexin-neuroligin interaction and neurotransmitter. *Proc Natl Acad Sci U S A* 102(17): 6137-6142

O'Brien R, Xu D, Mi R, Tang X, Hopf C, Worley P (2002) Synaptically targeted narp plays an essential role in the aggregation of AMPA receptors at excitatory synapses in cultured spinal neurons. *J Neurosci* 22(11): 4487-4498

Passafaro M, Nakagawa T, Sala C, Sheng M (2003) Induction of dendritic spines by an extracellular domain of AMPA receptor subunit GluR2. *Nature* 424(6949): 677-681

Penzes P, Beeser A, Chernoff J, Schiller MR, Eipper BA, Mains RE, Huganir RL (2003) Rapid induction of dendritic spine morphogenesis by trans-synaptic ephrinB-EphB receptor activation of the Rho-GEF kalirin. *Neuron* 37(2): 263-274

Petralia RS, Esteban JA, Wang YX, Partridge JG, Zhao HM, Wenthold RJ, Malinow R (1999) Selective acquisition of AMPA receptors over postnatal development suggests a molecular basis for silent synapses. *Nat Neurosci* 2(1): 31-36

Pickard L, Noel J, Henley JM, Collingridge GL, Molnar E (2000) Developmental changes in synaptic AMPA and NMDA receptor distribution and AMPA receptor subunit composition in living hippocampal neurons. *J Neurosci* 20(21): 7922-7931

Prange O, Wong TP, Gerrow K, Wang YT, El-Husseini A (2004) A balance between excitatory and inhibitory synapses is controlled by PSD-95 and neuroligin. *Proc Natl Acad Sci U S A* 101(38): 13915-13920

Pravettoni E, Bacci A, Coco S, Forbicini P, Matteoli M, Verderio C (2000) Different localizations and functions of L-type and N-type calcium channels during development of hippocampal neurons. *Dev Biol* 227(2): 581-594

Regalado MP, Terry-Lorenzo RT, Waites CL, Garner CC, Malenka RC (2006) Transsynaptic signaling by postsynaptic synapse-associated protein 97. *J Neurosci* 26(8): 2343-2357

Reid CA, Clements JD, Bekkers JM (1997) Nonuniform distribution of Ca2+ channel subtypes on presynaptic terminals of excitatory synapses in hippocampal cultures. *J Neurosci* 17(8): 2738-2745

Renger JJ, Egles C, Liu G (2001) A developmental switch in neurotransmitter flux enhances synaptic efficacy by affecting AMPA receptor activation. *Neuron* 29(2): 469-484

Richmond JE, Weimer RM, Jorgensen EM (2001) An open form of syntaxin bypasses the requirement for UNC-13 in vesicle priming. *Nature* 412(6844): 338-341

Rizo J, Rosenmund C (2008) Synaptic vesicle fusion. *Nat Struct Mol Biol* 15(7): 665-674

Rosenmund C, Clements JD, Westbrook GL (1993) Nonuniform probability of glutamate release at a hippocampal synapse. *Science* 262(5134): 754-757

Rosenmund C, Feltz A, Westbrook GL (1995) Synaptic NMDA receptor channels have a low open probability. *J Neurosci* 15(4): 2788-2795

Rosenmund C, Sigler A, Augustin I, Reim K, Brose N, Rhee JS (2002) Differential control of vesicle priming and short-term plasticity by Munc13 isoforms. *Neuron* 33(3): 411-424

Rosenmund C, Stevens CF (1996) Definition of the readily releasable pool of vesicles at hippocampal synapses. *Neuron* 16(6): 1197-1207

Roussignol G, Ango F, Romorini S, Tu JC, Sala C, Worley PF, Bockaert J, Fagni L (2005) Shank expression is sufficient to induce functional dendritic spine synapses in aspiny neurons. *J Neurosci* 25(14): 3560-3570

Rumbaugh G, Sia GM, Garner CC, Huganir RL (2003) Synapse-associated protein-97 isoform-specific regulation of surface AMPA receptors and synaptic function in cultured neurons. *J Neurosci* 23(11): 4567-4576

Saglietti L, Dequidt C, Kamieniarz K, Rousset MC, Valnegri P, Thoumine O, Beretta F, Fagni L, Choquet D, Sala C, Sheng M, Passafaro M (2007) Extracellular interactions between GluR2 and N-cadherin in spine regulation. *Neuron* 54(3): 461-477

Sala C, Piech V, Wilson NR, Passafaro M, Liu G, Sheng M (2001) Regulation of dendritic spine morphology and synaptic function by Shank and Homer. *Neuron* 31(1): 115-130

Sara Y, Biederer T, Atasoy D, Chubykin A, Mozhayeva MG, Sudhof TC, Kavalali ET (2005) Selective capability of SynCAM and neuroligin for functional synapse assembly. *J Neurosci* 25(1): 260-270

Scheiffele P, Fan J, Choih J, Fetter R, Serafini T (2000) Neuroligin expressed in nonneuronal cells triggers presynaptic development in contacting axons. *Cell* 101(6): 657-669

Schikorski T, Stevens CF (1997) Quantitative ultrastructural analysis of hippocampal excitatory synapses. *J Neurosci* 17(15): 5858-5867

Schnell E, Sizemore M, Karimzadegan S, Chen L, Bredt DS, Nicoll RA (2002) Direct interactions between PSD-95 and stargazin control synaptic AMPA receptor number. *Proc Natl Acad Sci U S A* 99(21): 13902-13907

Schoch S, Castillo PE, Jo T, Mukherjee K, Geppert M, Wang Y, Schmitz F, Malenka RC, Sudhof TC (2002) RIM1alpha forms a protein scaffold for regulating neurotransmitter release at the active zone. *Nature* 415(6869): 321-326

Scholz KP, Miller RJ (1995) Developmental changes in presynaptic calcium channels coupled to glutamate release in cultured rat hippocampal neurons. *J Neurosci* 15(6): 4612-4617

Shen W, Wu B, Zhang Z, Dou Y, Rao ZR, Chen YR, Duan S (2006) Activity-induced rapid synaptic maturation mediated by presynaptic cdc42 signaling. *Neuron* 50(3): 401-414

Sia GM, Beique JC, Rumbaugh G, Cho R, Worley PF, Huganir RL (2007) Interaction of the N-terminal domain of the AMPA receptor GluR4 subunit with the neuronal pentraxin NP1 mediates GluR4 synaptic recruitment. *Neuron* 55(1): 87-102

Song I, Huganir RL (2002) Regulation of AMPA receptors during synaptic plasticity. *Trends Neurosci* 25(11): 578-588

Standley S, Roche KW, McCallum J, Sans N, Wenthold RJ (2000) PDZ domain suppression of an ER retention signal in NMDA receptor NR1 splice variants. *Neuron* 28(3): 887-898

Sudhof TC (2000) The synaptic vesicle cycle revisited. *Neuron* 28(2): 317-320

Sudhof TC (2004) The synaptic vesicle cycle. *Annu Rev Neurosci* 27: 509-547

Thomas CG, Miller AJ, Westbrook GL (2006) Synaptic and extrasynaptic NMDA receptor NR2 subunits in cultured hippocampal neurons. *J Neurophysiol* 95(3): 1727-1734

Varoqueaux F, Aramuni G, Rawson RL, Mohrmann R, Missler M, Gottmann K, Zhang W, Sudhof TC, Brose N (2006) Neuroligins determine synapse maturation and function. *Neuron* 51(6): 741-754

Varoqueaux F, Sigler A, Rhee JS, Brose N, Enk C, Reim K, Rosenmund C (2002) Total arrest of spontaneous and evoked synaptic transmission but normal synaptogenesis in the absence of Munc13-mediated vesicle priming. *Proc Natl Acad Sci U S A* 99(13): 9037-9042

Verderio C, Coco S, Bacci A, Rossetto O, De Camilli P, Montecucco C, Matteoli M (1999) Tetanus toxin blocks the exocytosis of synaptic vesicles clustered at synapses but not of synaptic vesicles in isolated axons. *J Neurosci* 19(16): 6723-6732

Verderio C, Coco S, Fumagalli G, Matteoli M (1995) Calcium-dependent glutamate release during neuronal development and synaptogenesis: different involvement of omega-agatoxin IVA- and omega-conotoxin GVIA-sensitive channels. *Proc Natl Acad Sci U S A* 92(14): 6449-6453

Verhage M, Maia AS, Plomp JJ, Brussaard AB, Heeroma JH, Vermeer H, Toonen RF, Hammer RE, van den Berg TK, Missler M, Geuze HJ, Sudhof TC (2000) Synaptic assembly of the brain in the absence of neurotransmitter secretion. *Science* 287(5454): 864-869

Voronin LL, Cherubini E (2003) "Presynaptic silence" may be golden. *Neuropharmacology* 45(4): 439-449

Washbourne P, Dityatev A, Scheiffele P, Biederer T, Weiner JA, Christopherson KS, El-Husseini A (2004) Cell adhesion molecules in synapse formation. *J Neurosci* 24(42): 9244-9249

Wasling P, Hanse E, Gustafsson B (2004) Developmental changes in release properties of the CA3-CA1 glutamate synapse in rat hippocampus. *J Neurophysiol* 92(5): 2714-2724

Wenthold RJ, Petralia RS, Blahos J, II, Niedzielski AS (1996) Evidence for multiple AMPA receptor complexes in hippocampal CA1/CA2 neurons. *J Neurosci* 16(6): 1982-1989

Wilson RI, Nicoll RA (2001) Endogenous cannabinoids mediate retrograde signalling at hippocampal synapses. *Nature* 410(6828): 588-592

Woo J, Kwon SK, Choi S, Kim S, Lee JR, Dunah AW, Sheng M, Kim E (2009) Trans-synaptic adhesion between NGL-3 and LAR regulates the formation of excitatory synapses. *Nat Neurosci* 12(4): 428-437

Wu LG, Borst JG (1999) The reduced release probability of releasable vesicles during recovery from short-term synaptic depression. *Neuron* 23(4): 821-832

Xu D, Hopf C, Reddy R, Cho RW, Guo L, Lanahan A, Petralia RS, Wenthold RJ, O'Brien RJ, Worley P (2003) Narp and NP1 form heterocomplexes that function in developmental and activity-dependent synaptic plasticity. *Neuron* 39(3): 513-528

Yoshihara Y, De Roo M, Muller D (2009) Dendritic spine formation and stabilization. *Curr Opin Neurobiol* 19(2): 146-153

Young SH, Poo MM (1983) Spontaneous release of transmitter from growth cones of embryonic neurones. *Nature* 305(5935): 634-637

Zamanillo D, Sprengel R, Hvalby O, Jensen V, Burnashev N, Rozov A, Kaiser KM, Koster HJ, Borchardt T, Worley P, Lubke J, Frotscher M, Kelly PH, Sommer B, Andersen P, Seeburg PH, Sakmann B (1999) Importance of AMPA receptors for hippocampal synaptic plasticity but not for spatial learning. *Science* 284(5421): 1805-1811

Zhai RG, Vardinon-Friedman H, Cases-Langhoff C, Becker B, Gundelfinger ED, Ziv NE, Garner CC (2001) Assembling the presynaptic active zone: a characterization of an active one precursor vesicle. *Neuron* 29(1): 131-143

Zhang W, Benson DL (2001) Stages of synapse development defined by dependence on F-actin. *J Neurosci* 21(14): 5169-5181

Zhou Q, Petersen CC, Nicoll RA (2000) Effects of reduced vesicular filling on synaptic transmission in rat hippocampal neurones. *J Physiol* 525 Pt 1: 195-206

Ziff EB (2007) TARPs and the AMPA receptor trafficking paradox. *Neuron* 53(5): 627-633

Ziv NE, Garner CC (2001) Principles of glutamatergic synapse formation: seeing the forest for the trees. *Curr Opin Neurobiol* 11(5): 536-543

Ziv NE, Garner CC (2004) Cellular and molecular mechanisms of presynaptic assembly. *Nat Rev Neurosci* 5(5): 385-399

Zucker RS, Regehr WG (2002) Short-term synaptic plasticity. *Annu Rev Physiol* 64: 355-405